Study of angular correlations in the ortho-positronium annihilation with the J-PET detector for the search of CPT symmetry violation

Muhsin Mohammed

On behalf of J-PET collaboration

Jagiellonian University
Krakow, Poland

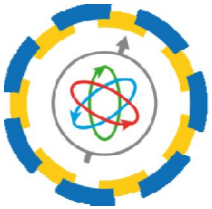

26.09.2019

Outline

1.The J-PET data analysis.

2.The Imaging of the cylindrical annihilation chambers.

3.Determination the annihilation points of 2-gamma decay.

4. Reconstruction the annihilation points of 3-gamma decay.

5. Test results of the CPT symmetry violation.

The J-PET data analysis

The large annihilation chamber measurements were performed for 57 days, resulting in a total of 260 TB of collected raw data.

The J-PET data analysis was performed using the J-PET Framework Analysis software.

In this analysis only the candidates with 2 and 3 hits in the event within 20 ns were accepted for further analysis, which allowed for a reduction of the raw data volume by a factor of about 99.8%.

The J-PET data analysis

Diagram of data processing by the J-PET Framework Analysis software. The input data (TDC times) were recorded and delivered by the data acquisition system (DAQ) as HLD (raw data) files shown in the blue rectangle.

The green rectangles represent the computational tasks responsible for some reconstruction algorithm or time calibration etc.,

The yellow rectangles represent the reconstructed physical quantities e.g. signals, hits (photon interaction points) at the scintillator strip and events, which leads to the output in the purple rectangle.

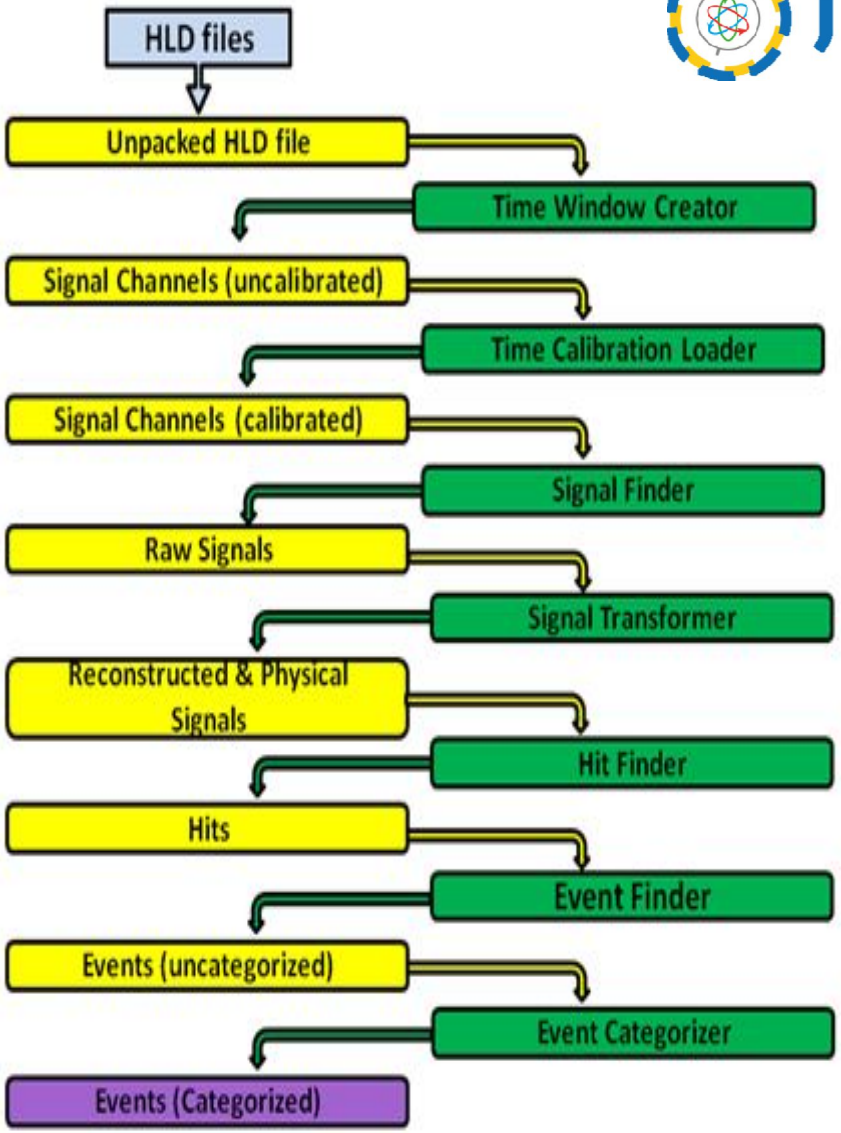

Run-6D and Run-7

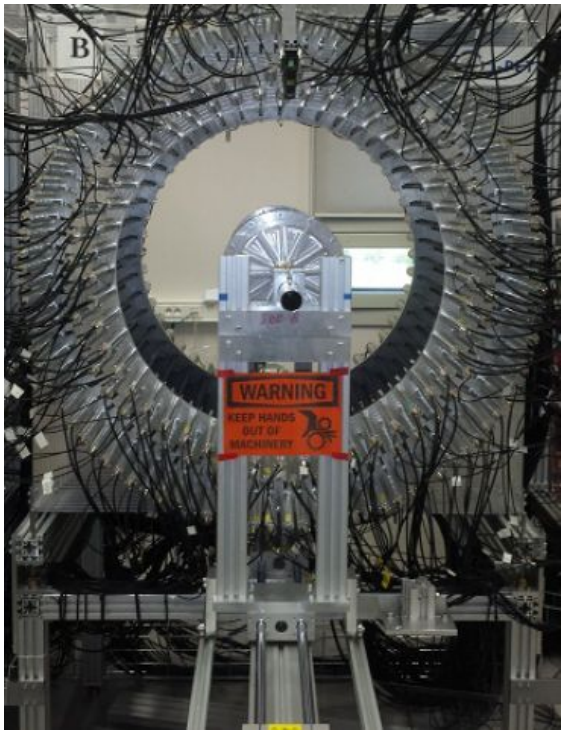

Run-6 D data, 3000 hld files

Run-7 data, 10500 hld files

The pre-selection criteria:

Number of Hits in an Event: 2Hits

2-hits must have |z-pos| <= 23 cm

2-hits must happened in 2-different scintillator strips.

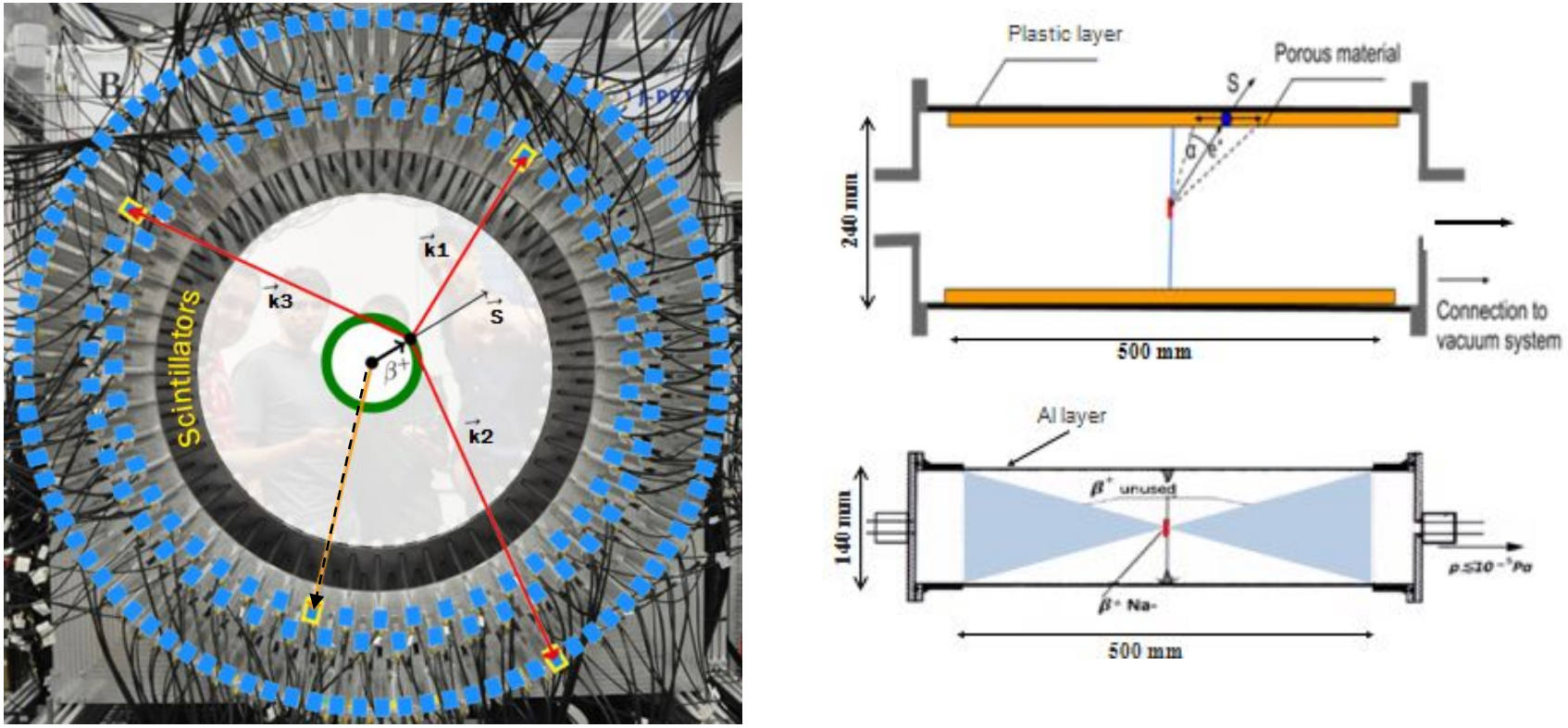

Fig.1. (Left) Photo of the Jagiellonian positron emission tomograph (J-PET). J-PET is made of 3 cylindrical layers of EJ-230 plastic scintillator strips (black) with a dimension of 7 × 19 × 500 mm^3 and Hamamatsu R9800 photomultipliers (gray). The superimposed rectangles indicate positions of photomultipliers. (Right-top) Scheme of large annihilation chamber. (Right-bottom) Scheme of small annihilation chamber.

The 2 gamma back to back analysis

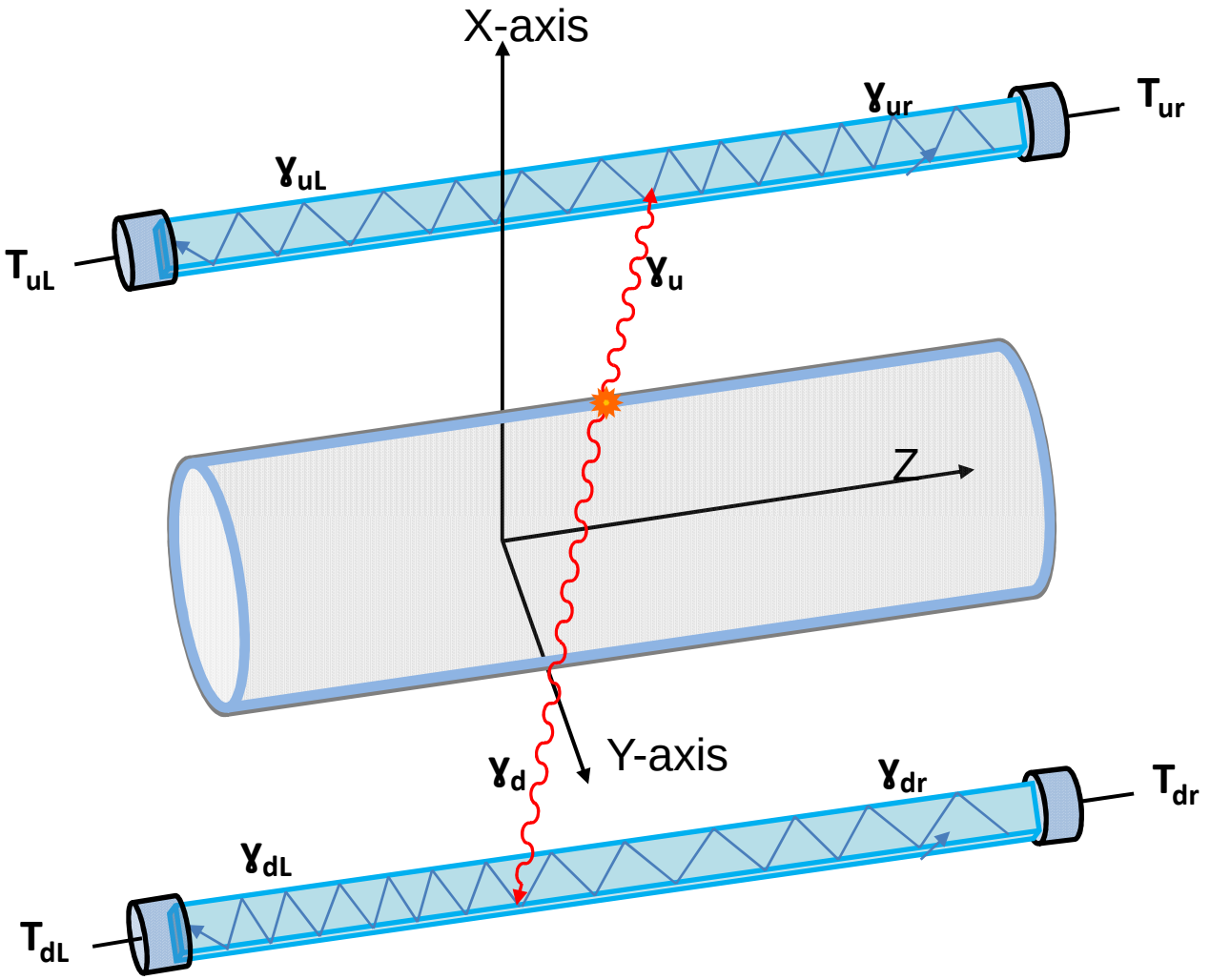

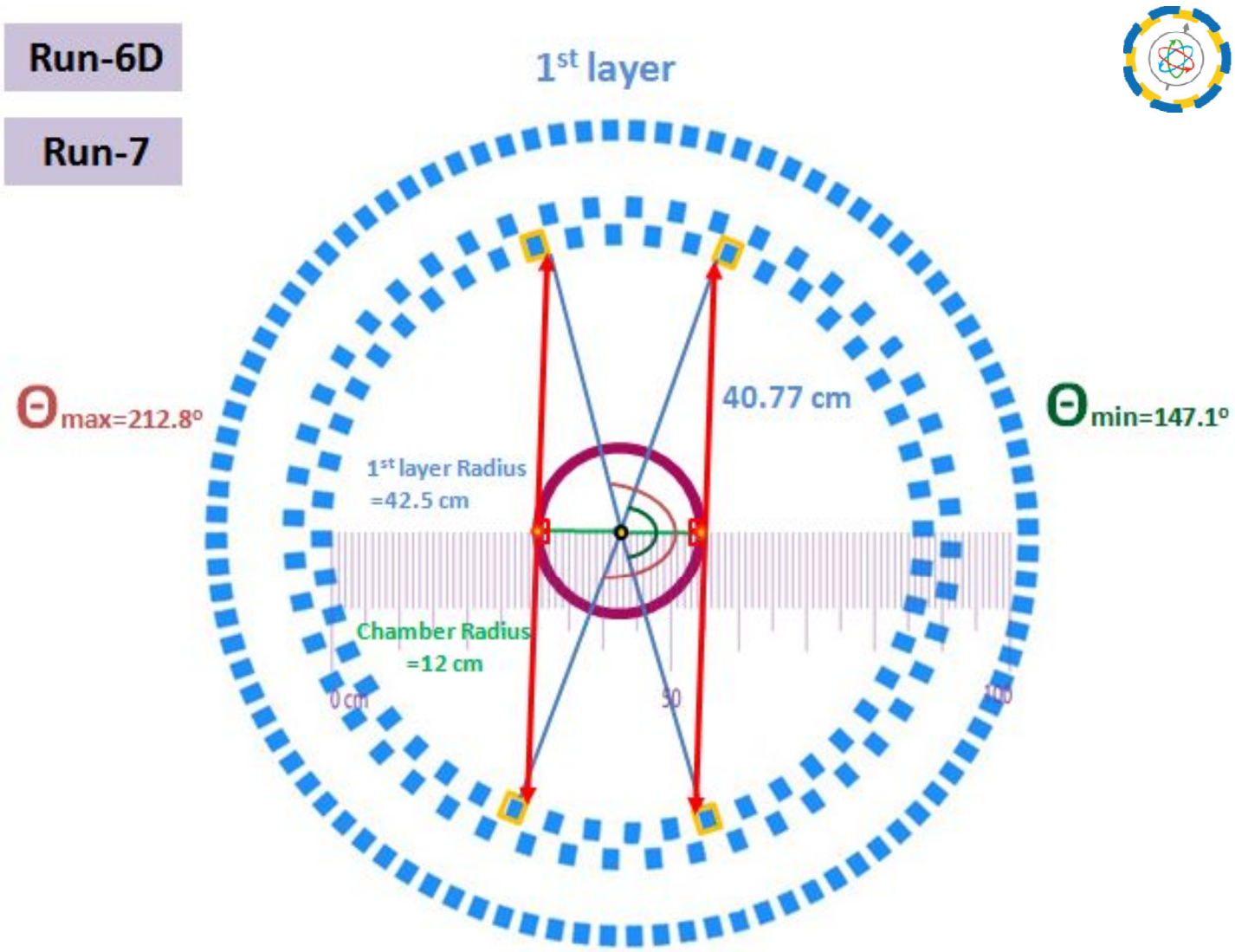

Figure: The view of the J-PET detector showing the maximum and minimum values of angles between two gamma back to back decay at the wall of the large cylindrical annihilation chamber with 12 cm radius, measured with respect to the center of the detector.

The dimensions of Run-6 D, 7 annihilation chamber

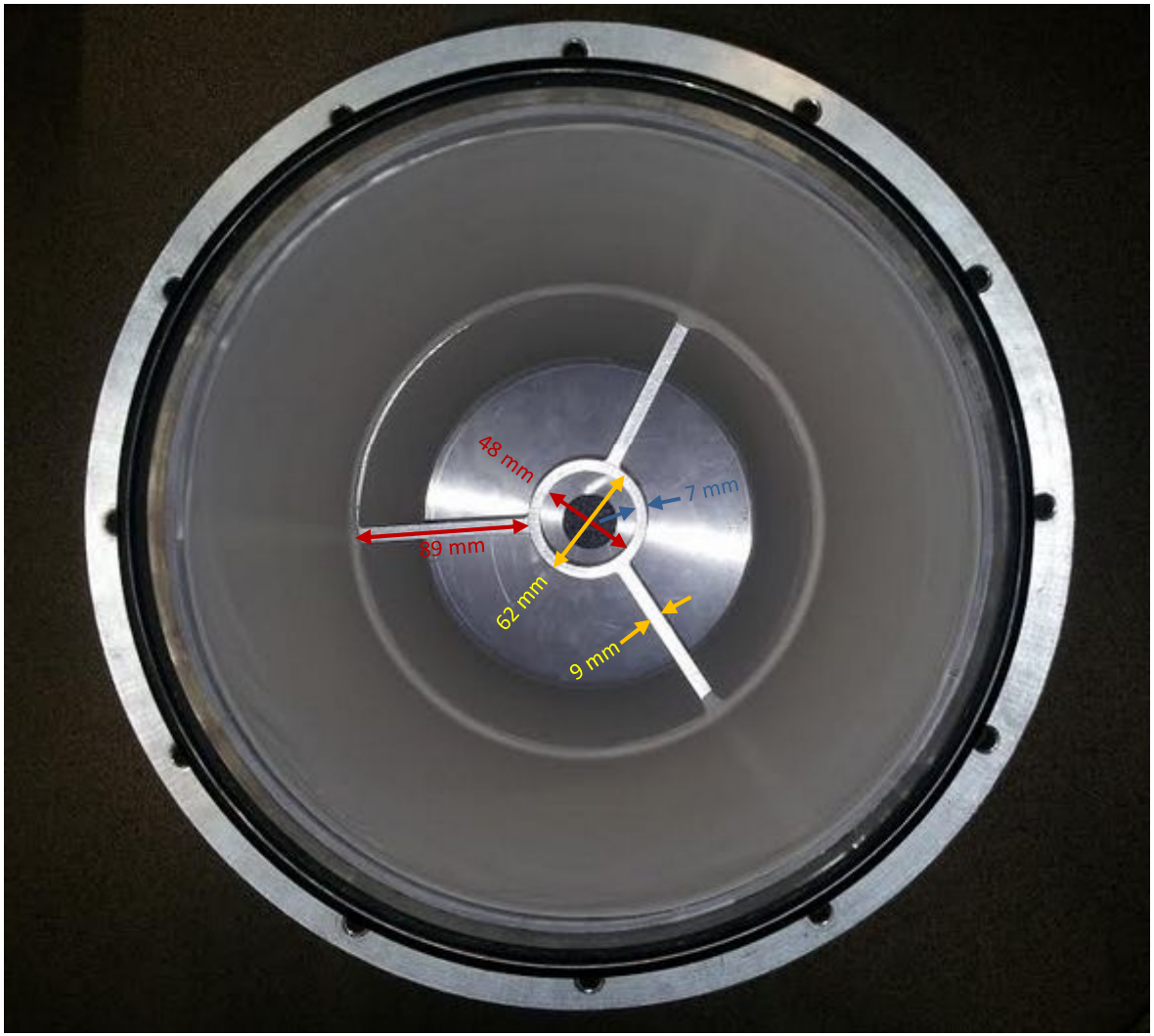

The dimensions of Run-6 D, 7 annihilation chamber

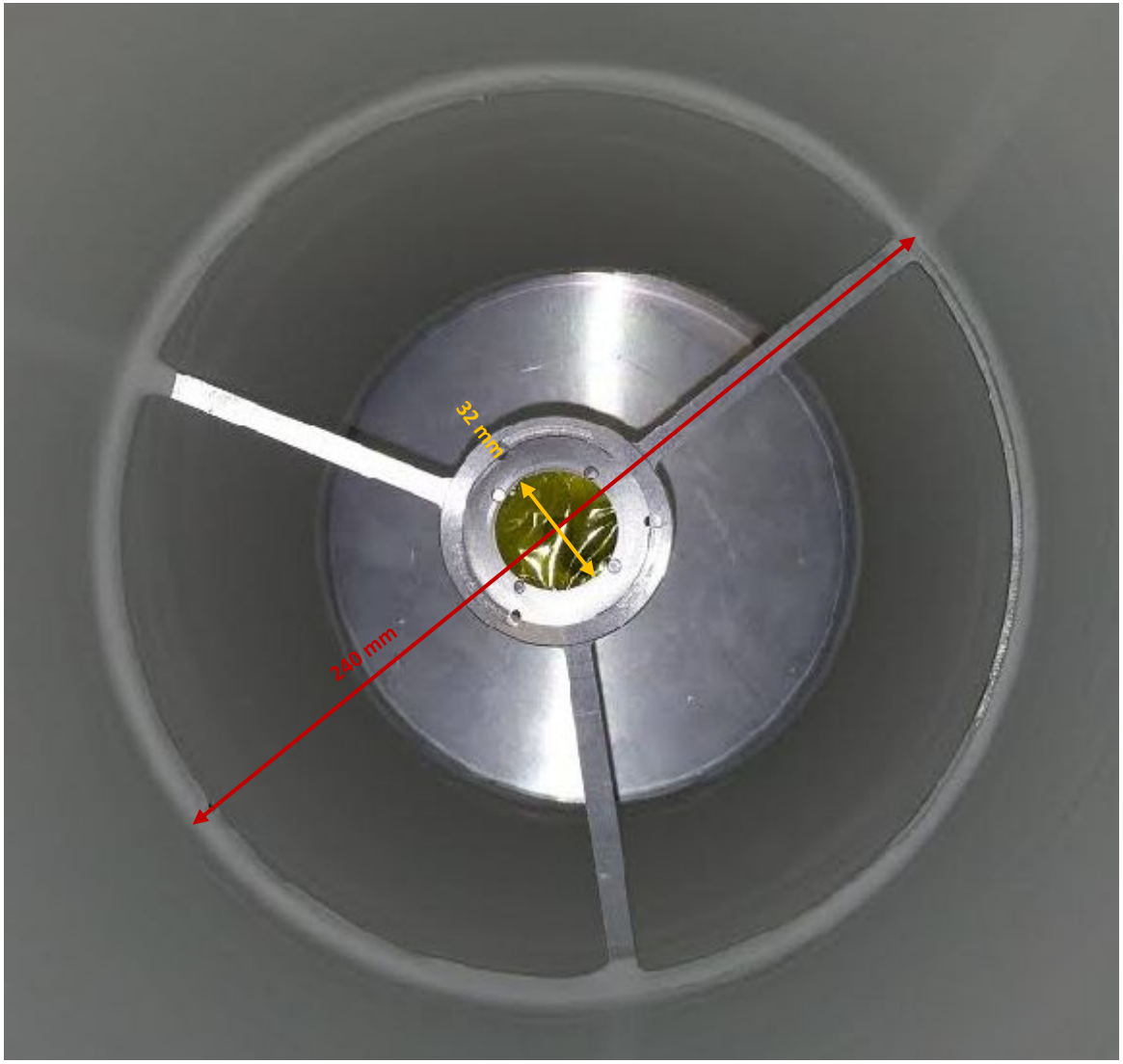

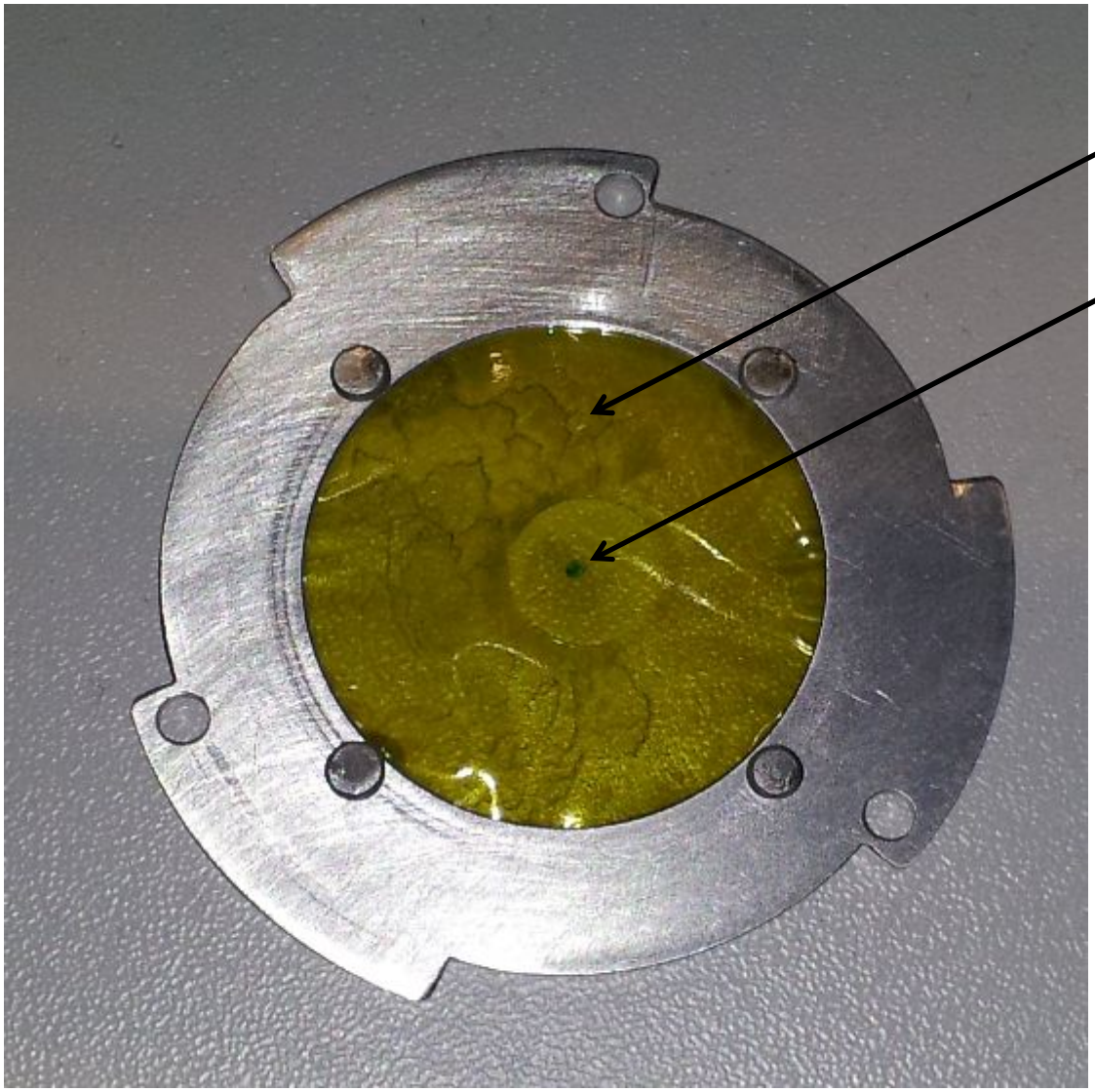
kapton foil
Sodium-22
Radioactive
source

Run-6D Data:

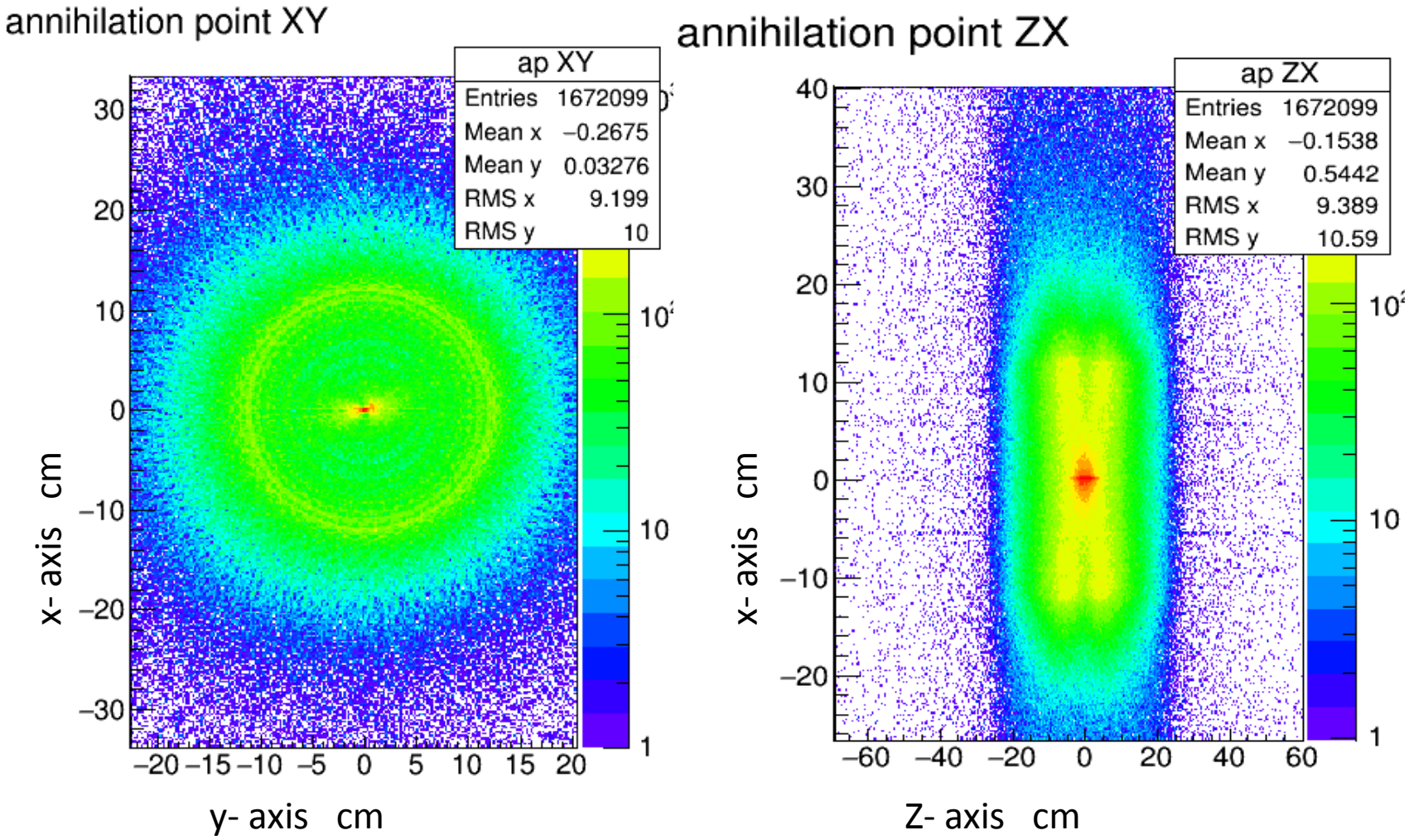

The tomographic image of the annihilation target cylinder obtained using Ps →2ɣ annihilations (left) xy view, (right) xz view.

Run-6D

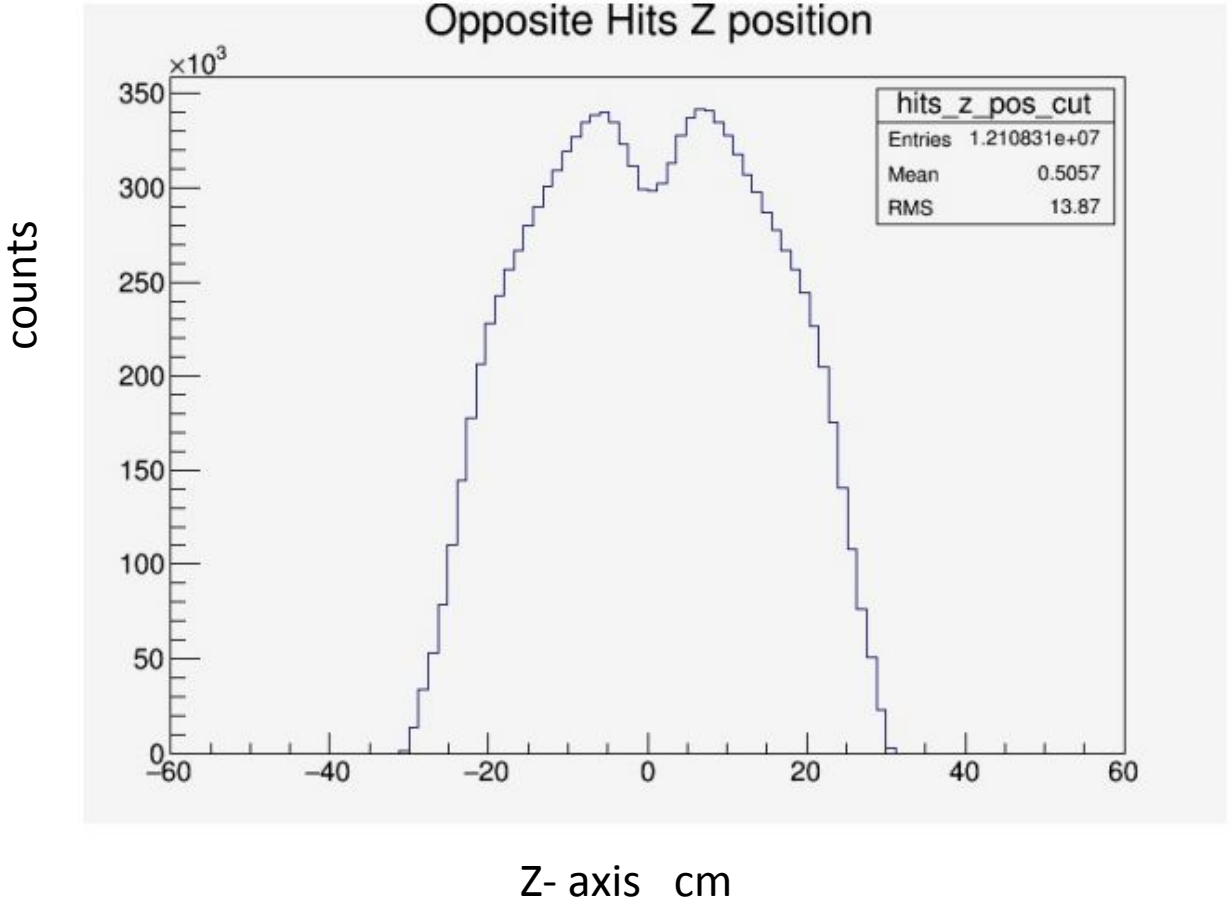

Figure : The hits distribution along z-axis shows a gap by the effect of the aluminum source holder. As we will see later.

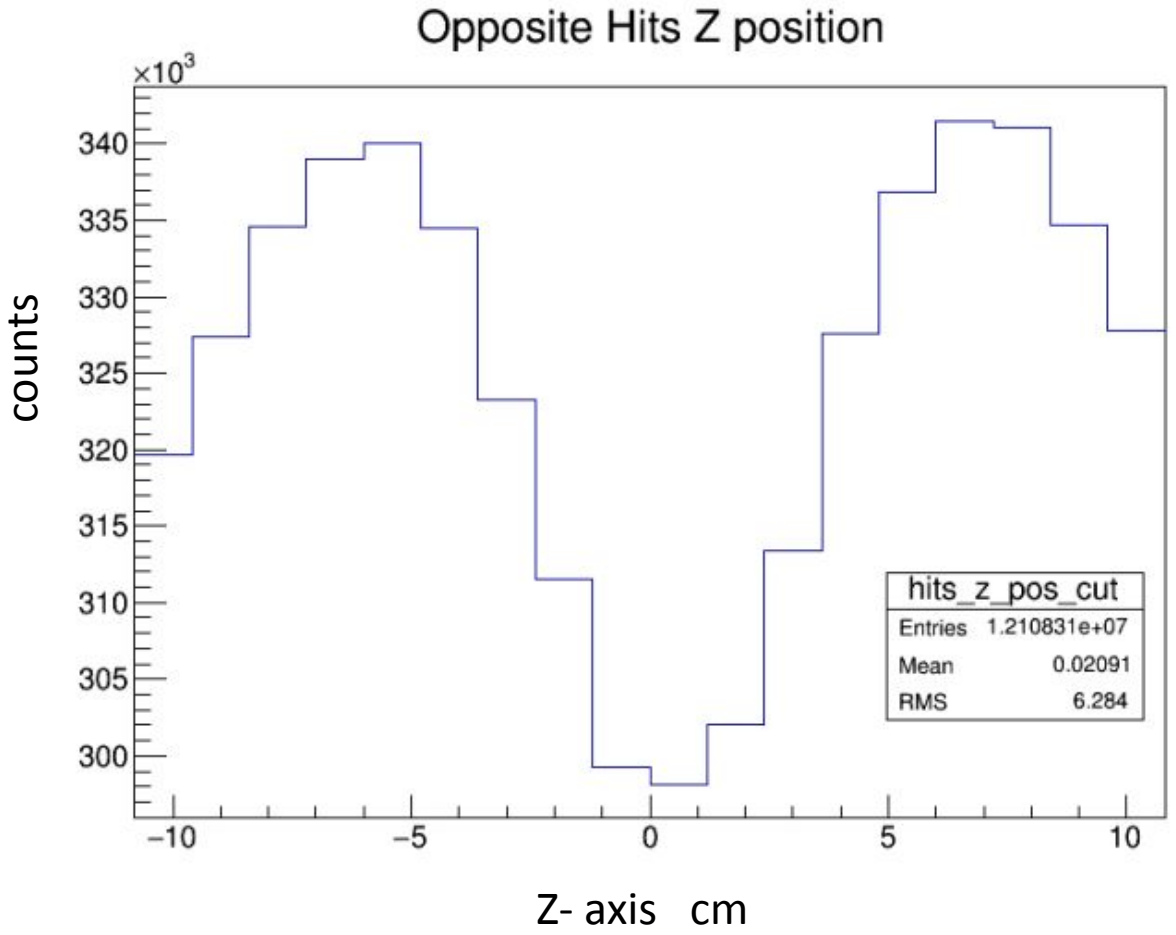
Opposite Hits Z position
×10^3
340
335
330
325
320
315
310
305
300
counts
hits_z_pos_cut
Entries 1.210831e+07
Mean 0.02091
RMS 6.284
−10
−5
0
5
10
Z- axis cm

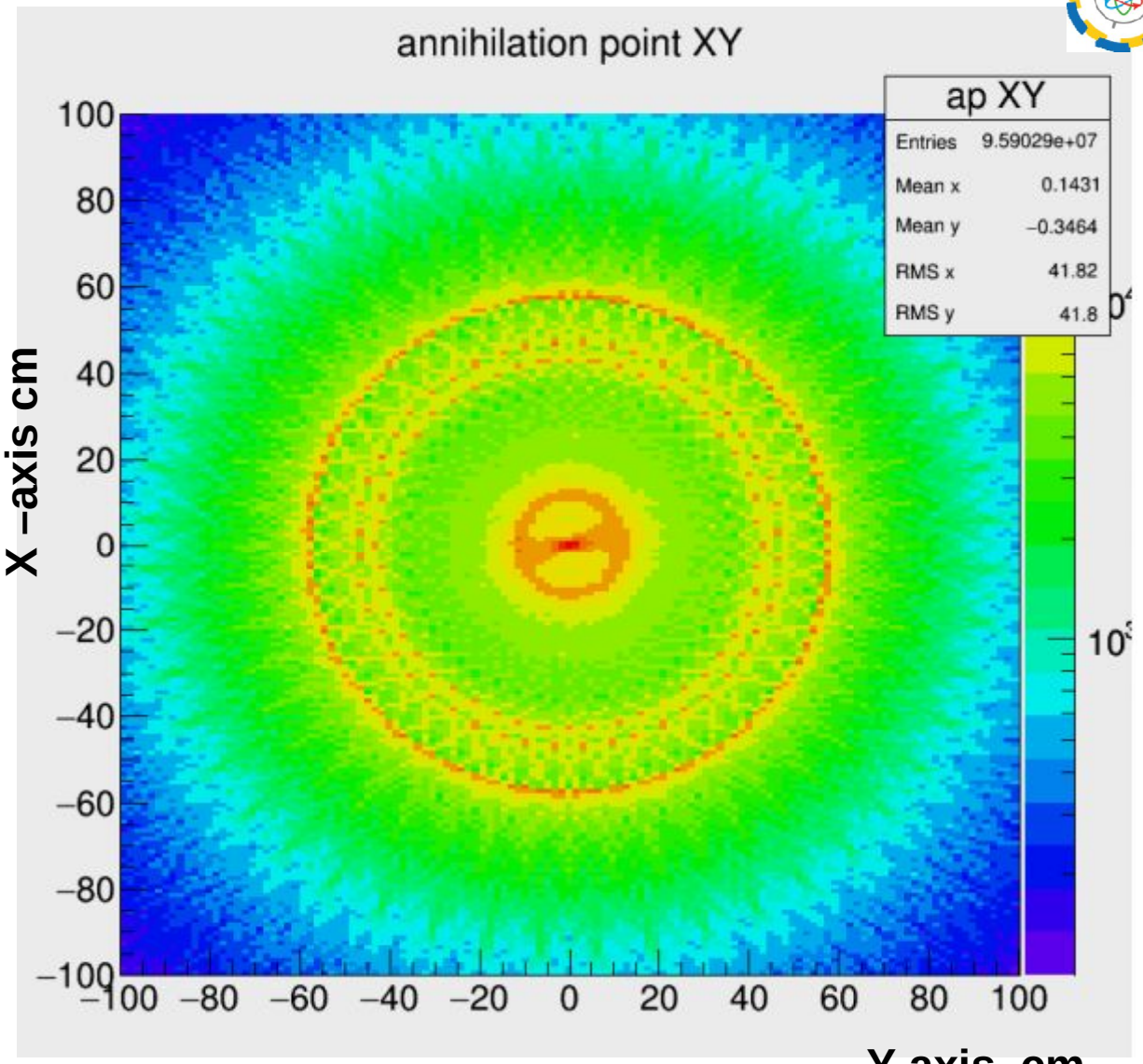
annihilation point XY
ap XY
Entries 9.59029e+07
Mean x 0.1431
Mean y −0.3464
RMS x 41.82
RMS y 41.8
X –axis cm
Y-axis cm
100
80
60
40
20
0
−20
−40
−60
−80
−100
−100 −80 −60 −40 −20 0 20 40 60 80 100

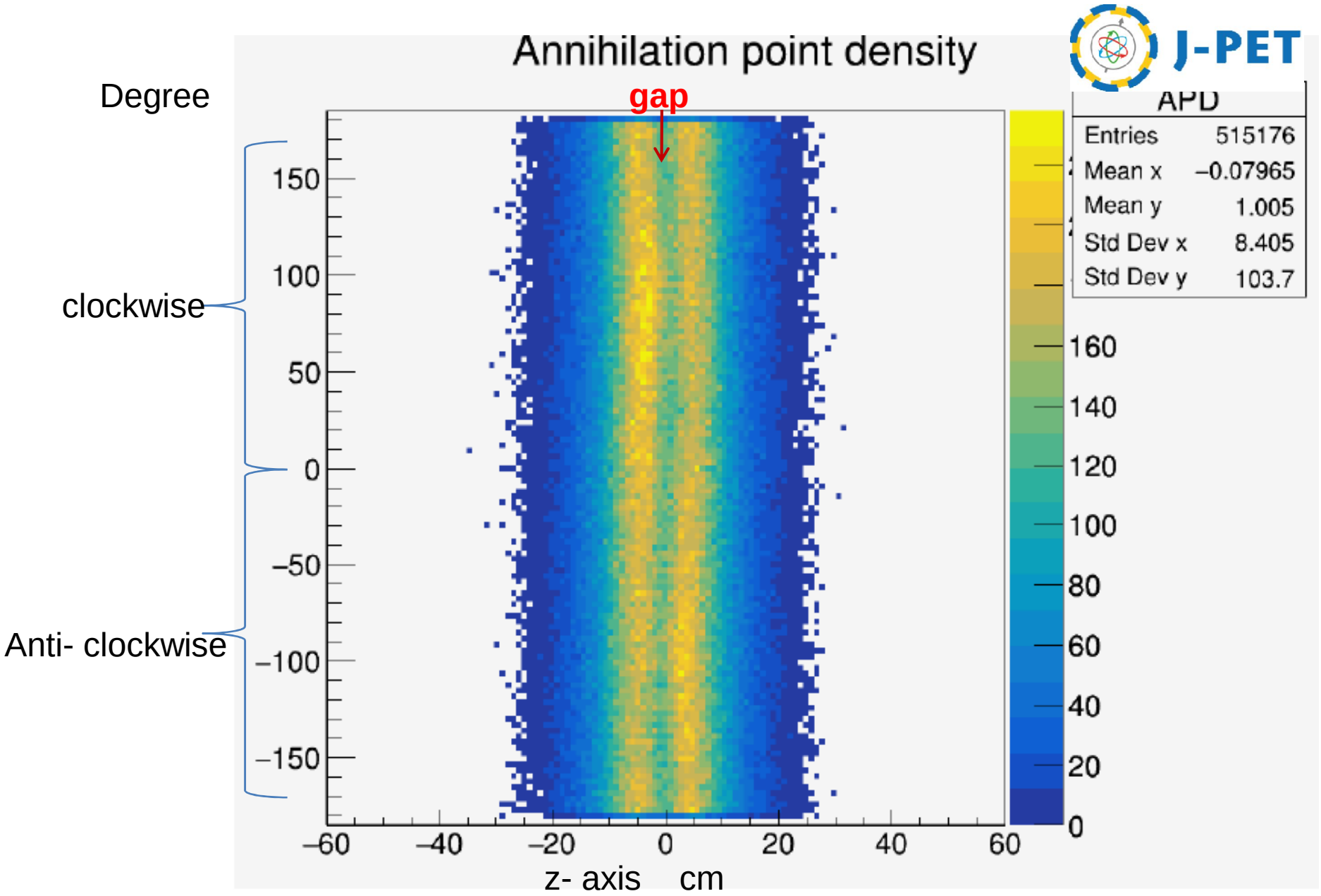
Annihilation point density
gap
APD
Entries 515176
Mean x −0.07965
Mean y 1.005
Std Dev x 8.405
Std Dev y 103.7
Degree
clockwise
Anti- clockwise
150
100
50
0
−50
−100
−150
−60
−40
−20
0
20
40
60
160
140
120
100
80
60
40
20
0
z- axis cm

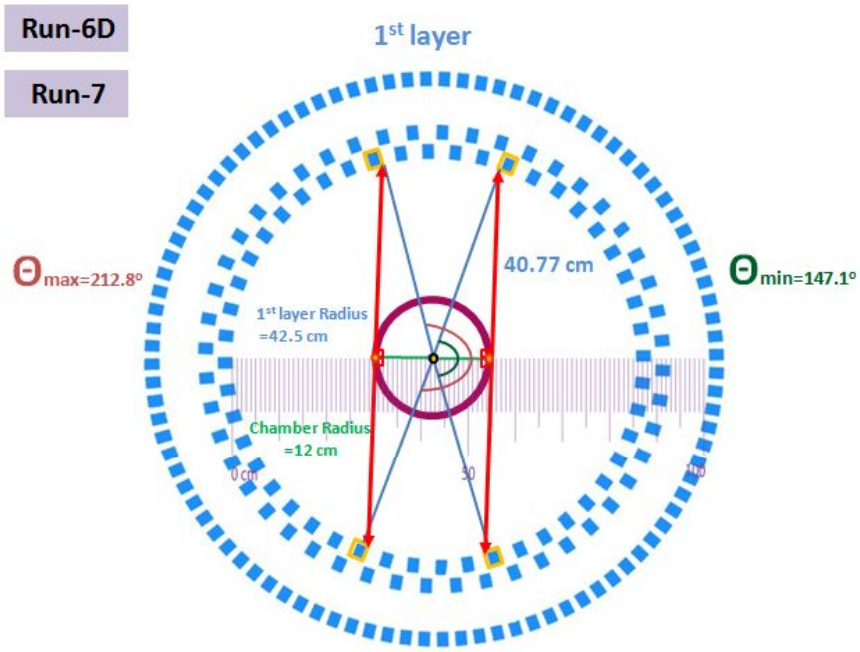

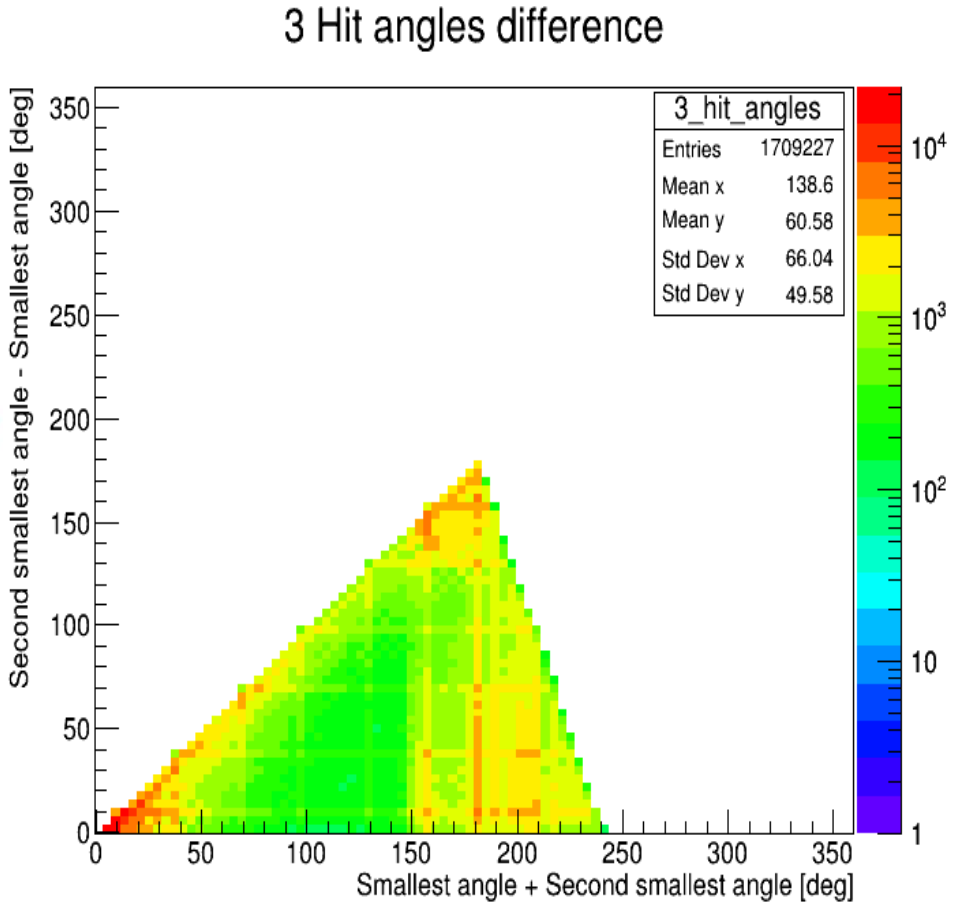

The distribution of the difference versus the sum of the two smallest angles with respect to the geometrical center of the detector for the case of large chamber experiment. which contain two photons with opposite momenta, which are together in a vertical band symmetrically around 180^{o}. This band is wider comparing to the band in the case of the small chamber, also it's unsymmetrical, where there are more counts on the right of 180^{o} because the of the contamination as results of o-Ps which is overlapping in this region.

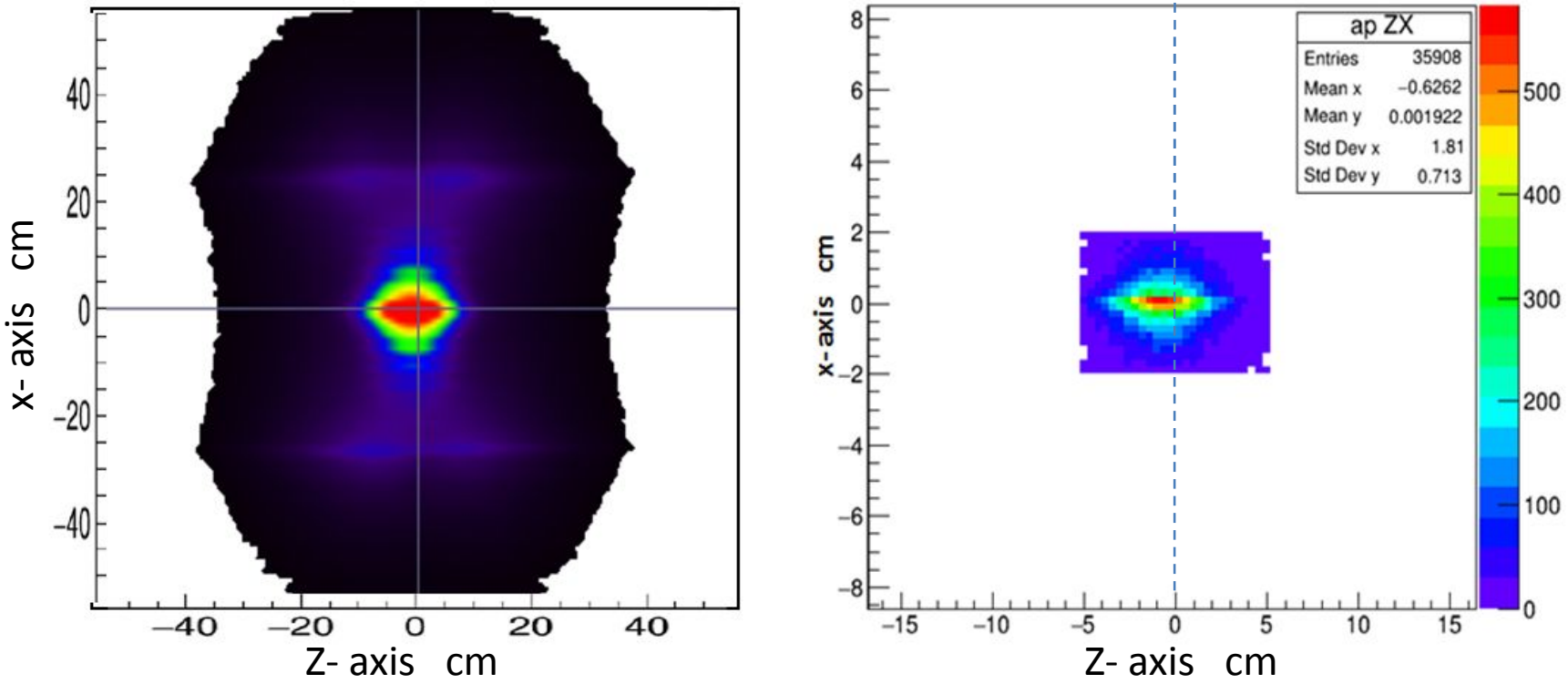

Figure : Left: The tomographic image of the annihilation points in (xz view) at the large decay chamber using 10Mb source, obtained using MLEM (Maximum Likelihood Estimation algorithm method). Right: The reconstruction of the annihilation points at the center (source region) with 2 cm radius and $\pm$ 5 a long z-axis, obtained using $e^+e^- \rightarrow 2\gamma$ annihilations (xz view).

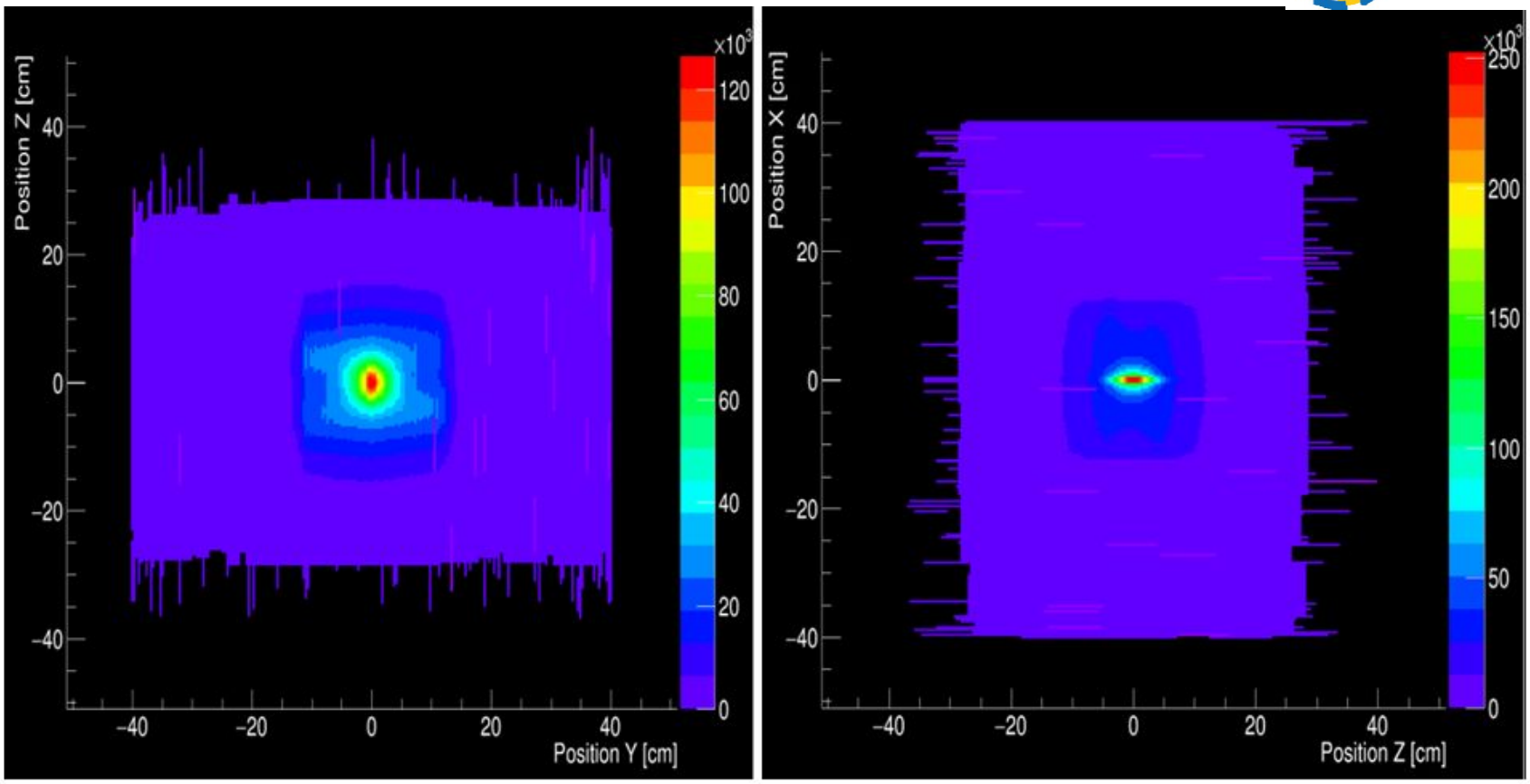

Figure : Left: The tomographic image of the annihilation points in YZ plane (longitudinal image or top view) at the large decay chamber using 10Mb source. Right: The tomographic image of the annihilation points in (xz view) at the large decay chamber using 10Mb source, obtained using MLEM method.

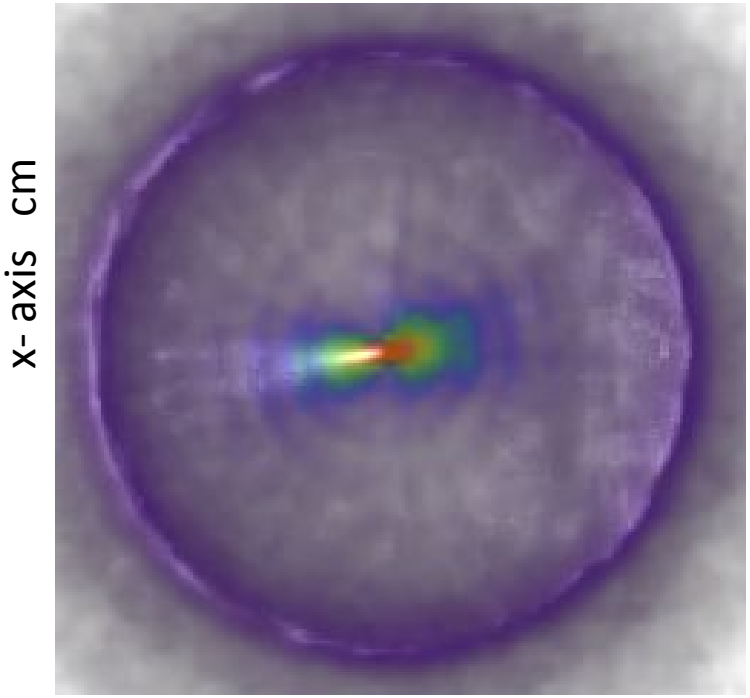

Run-6D for 1 file
20 sec of measurements

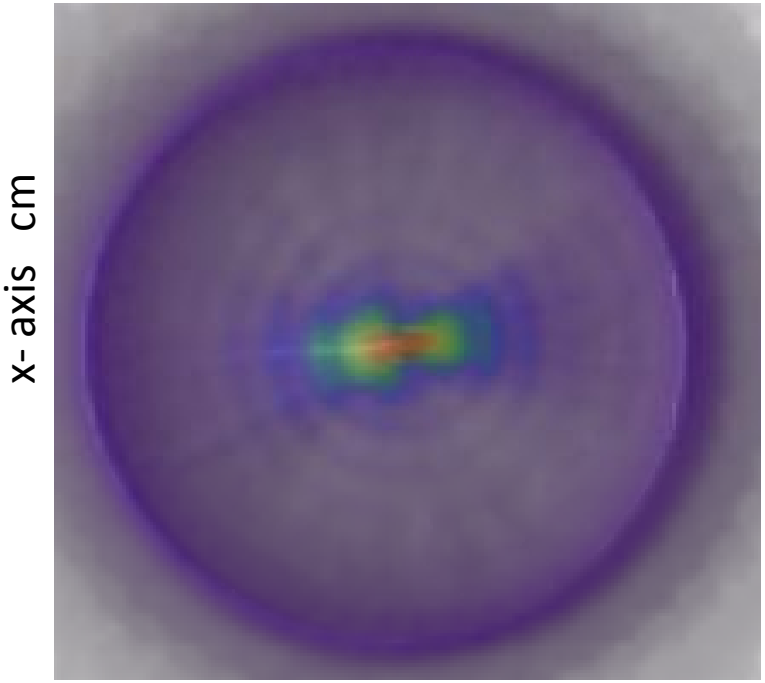

Run-6 for 100 files
33 min of measurements

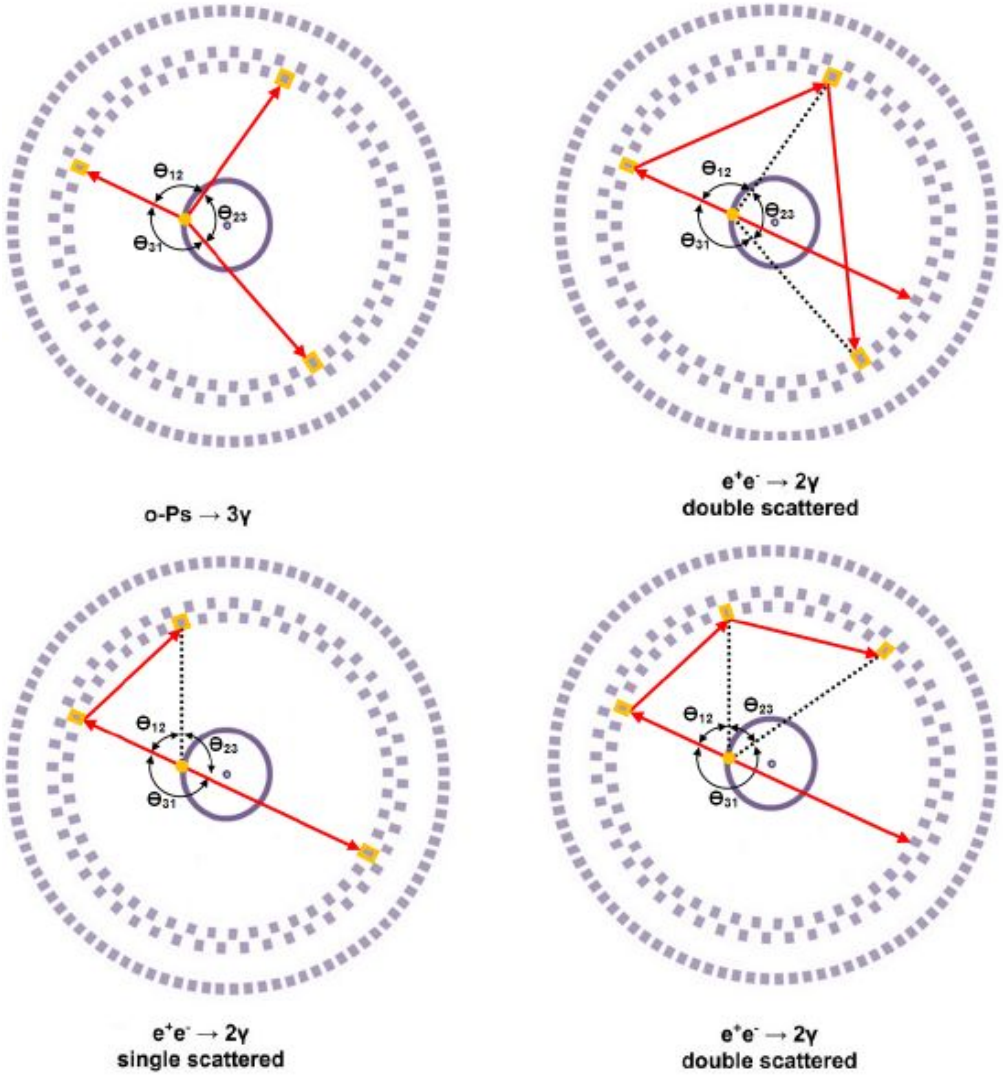

Fig:The four possible responses of the J-PET detector to three (decay) gamma quanta annihilation o-Ps → 3γ (upper-left) and e+e− annihilation into 3γ. Circularly arranged purple rectangles represent scintillator strips, purple and orange colors indicate strips where the gamma quanta were registered. **The solid red arrows represent gamma quanta occurring in the events, while dashed black lines indicate the artificially identified primary photons.** Single or double scattering gamma quanta. Also Θ_{ij} are the ordered angles between registered gammas.

LOR (line of response between any two hits)

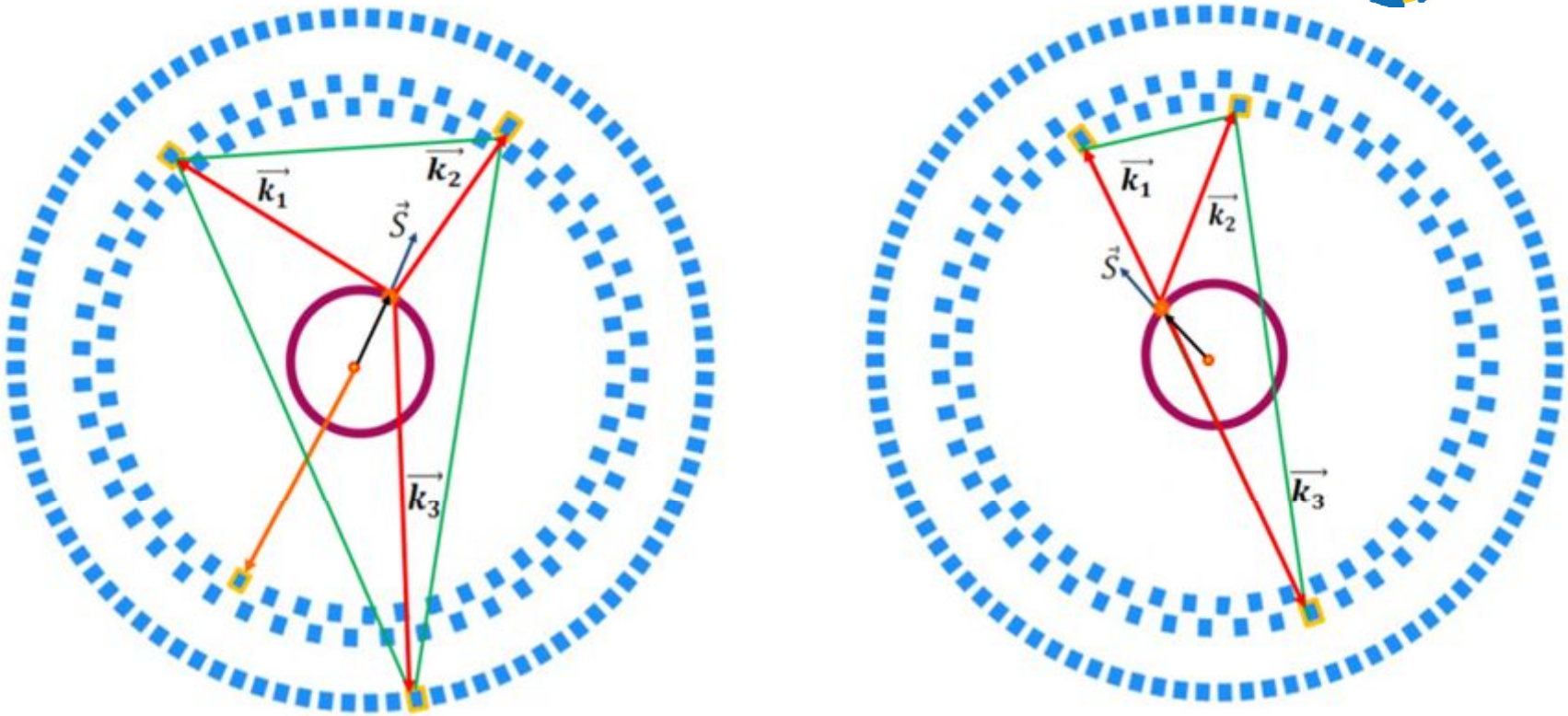

Figure : Schematic view of the J-PET detector showing the shortest distances (dmin) between the point on each LOR and the annihilation point on the wall of the large annihilation chamber, for the case of o-Ps annihilate into 3ɣ (left), and 2ɣ back to back annihilation and one scattering photon (right).

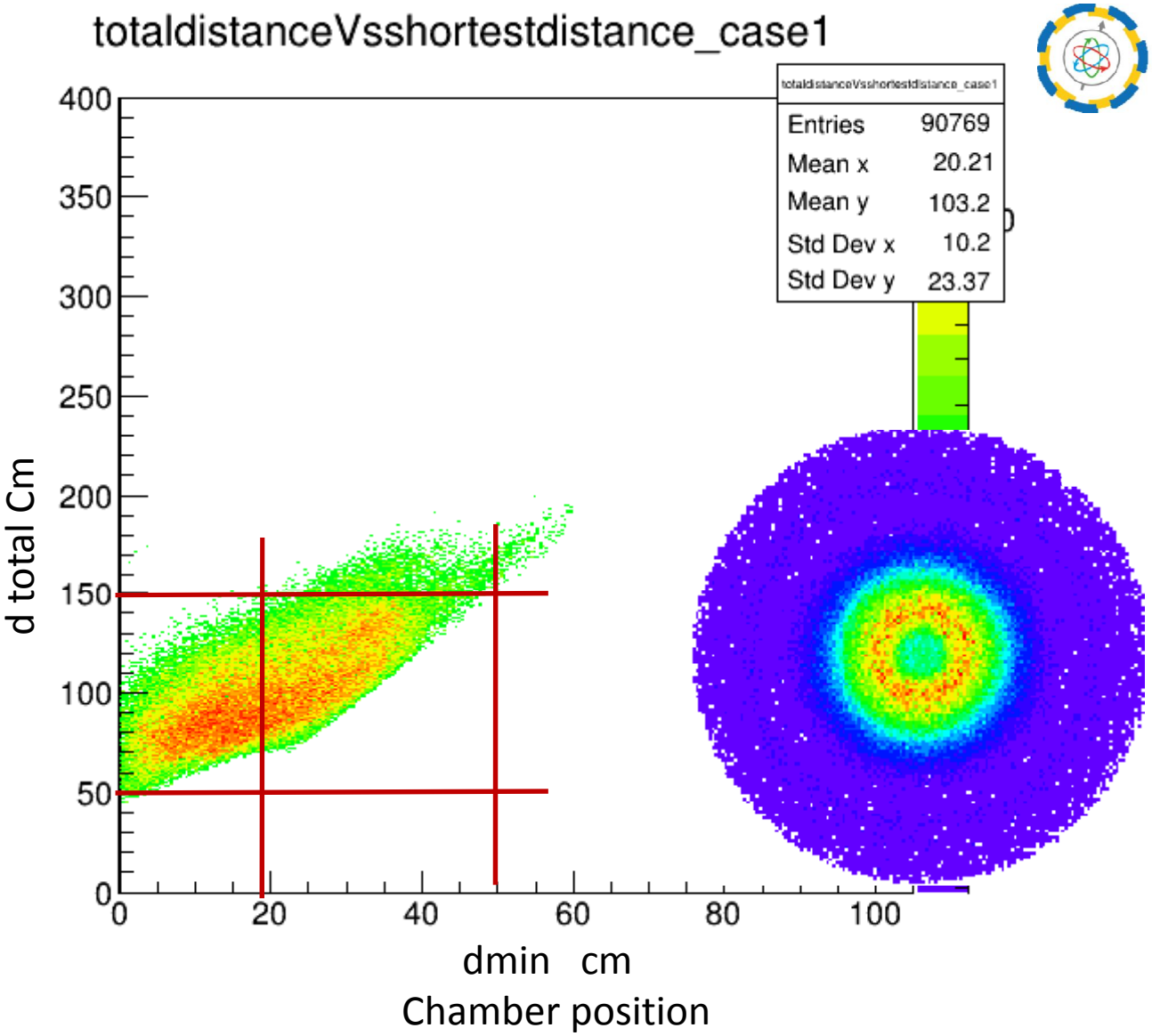

Additional criteria has been applied !!

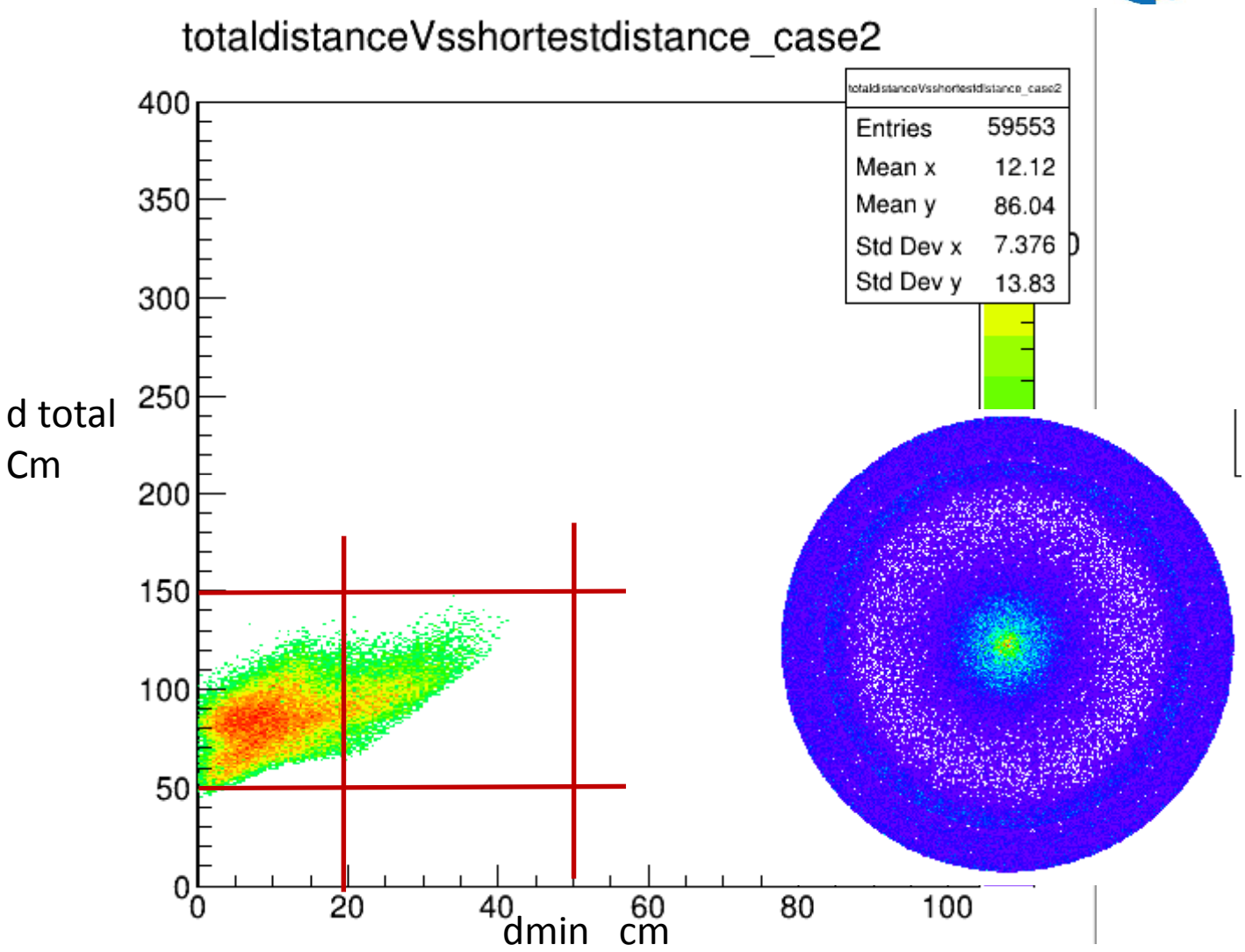

Source position

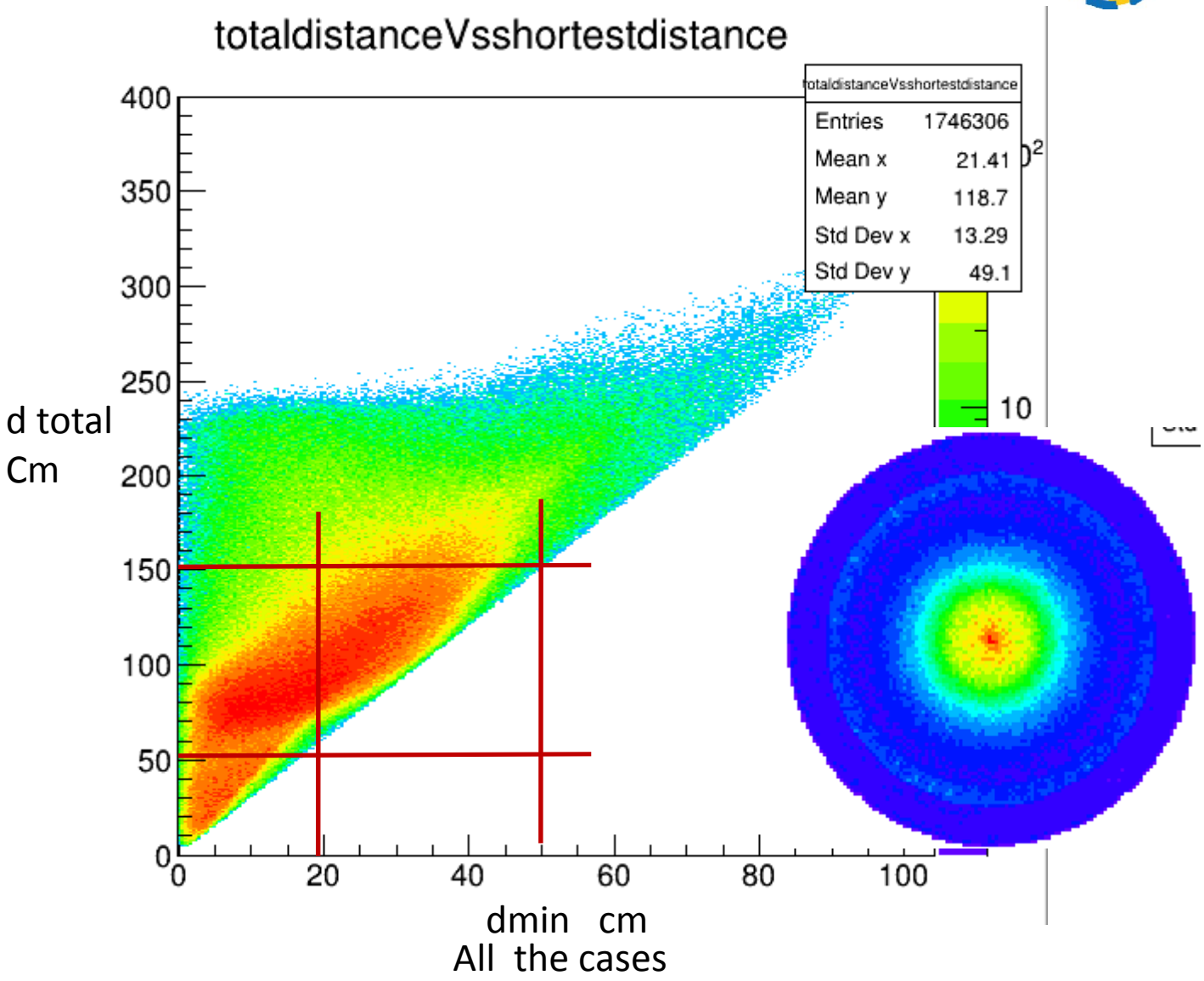
totaldistanceVsshortestdistance
totaldistanceVsshortestdistance
Entries 1746306
Mean x 21.41
Mean y 118.7
Std Dev x 13.29
Std Dev y 49.1
d total
Cm
dmin cm
All the cases
0
20
40
60
80
100
50
150
200
250
300
350
400
10

The summary of distances cuts.

Range of distances cut for chamber r=12 cm

Shortest distance range : $19.5 < (d_{min}) < 50$ cm

Longest distance range: $25 < (d_{max}) < 79$ cm

Total distance range: $50 < (d_{total}) < 175$ cm

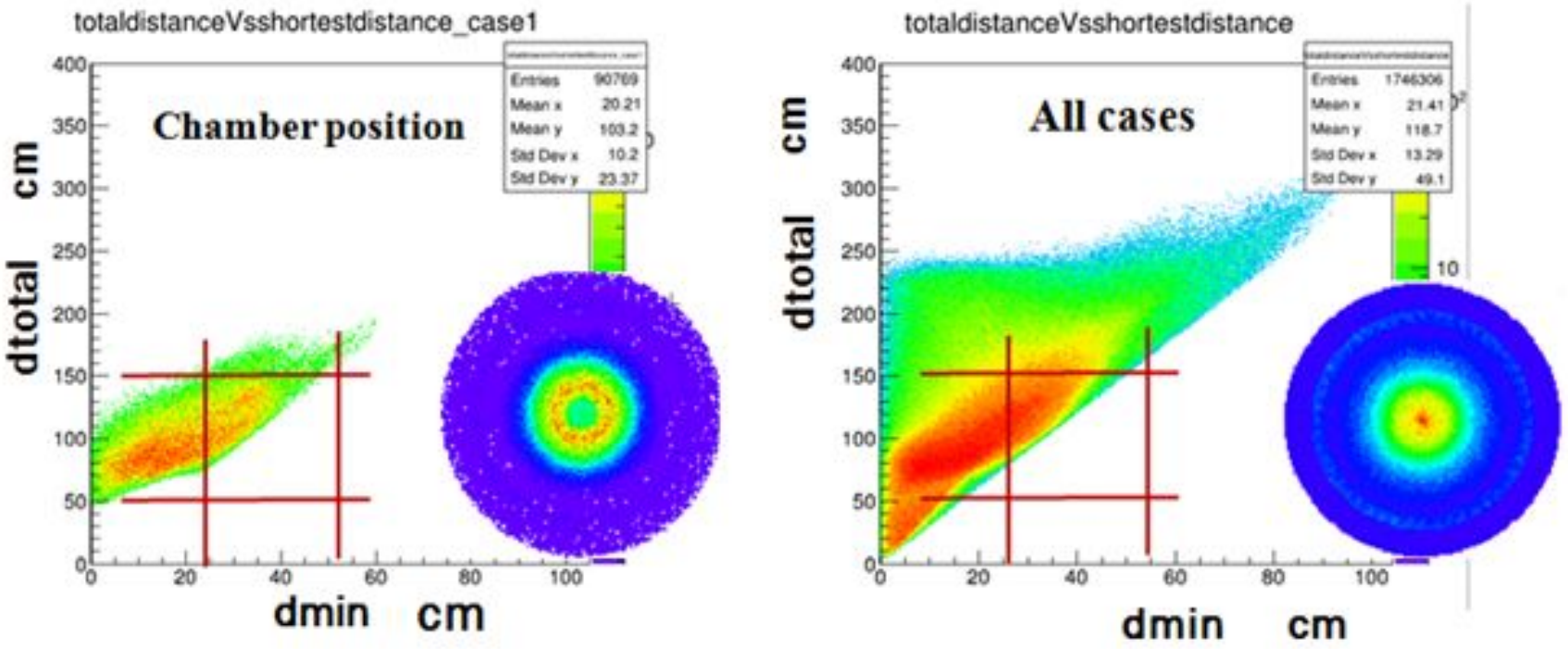

Figure : The shortest distances (dmin) Vs the total distances (dtotal) between the point on each LOR and the annihilation point. (Left): the decay points on the chamber walls only, (Right): the case of all the decay points. The red lines indicate the ranges of dmin and dtotal for the corresponding to the annihilation chamber location.

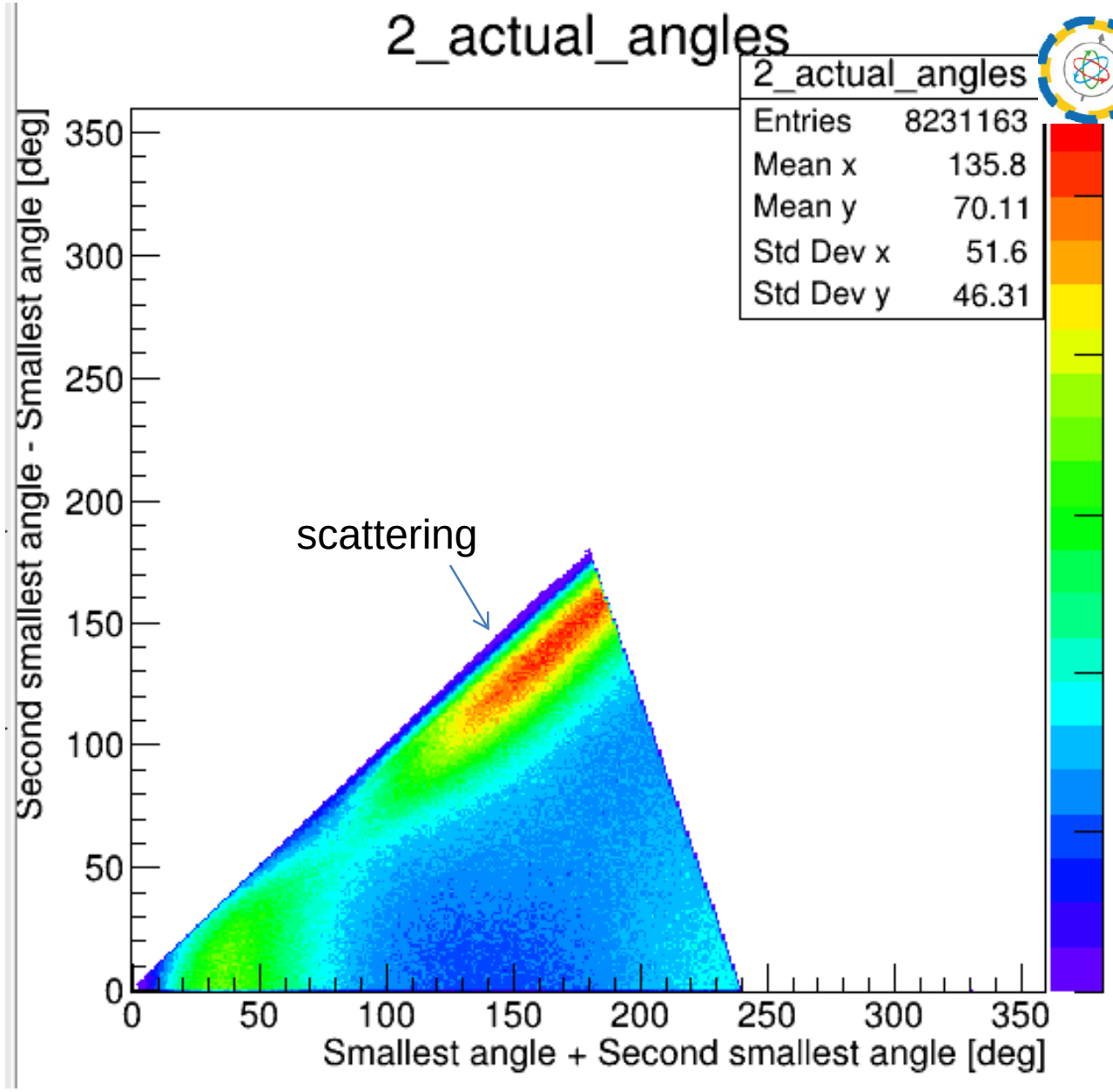

The sum of the1st and 2nd smallest angles versus the difference between them.

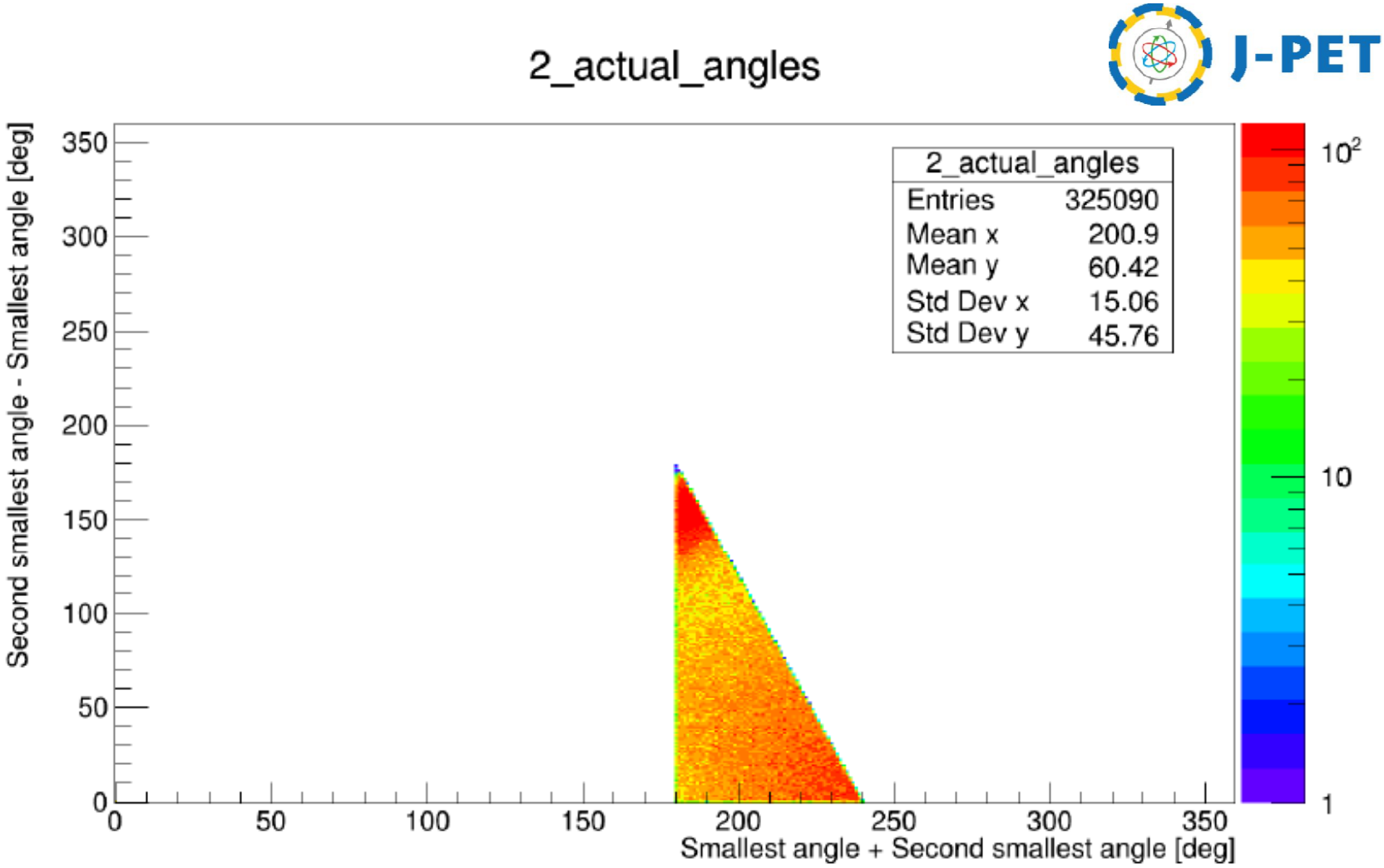

Figure: The sum of the1st and 2nd smallest angles > 180^o

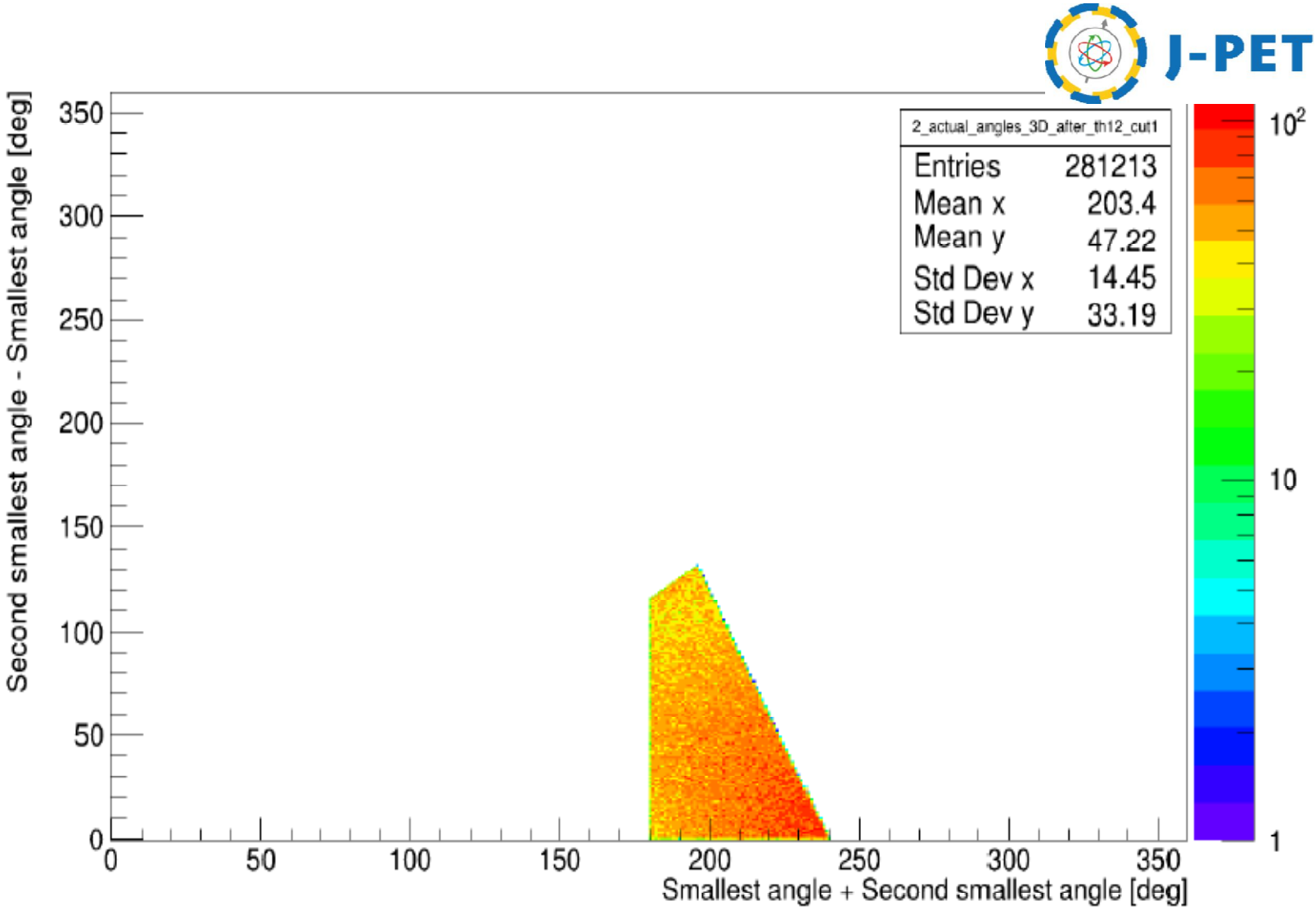

The sum of the1st and 2nd smallest angles versus the difference after cut out the angles <20^{o}.

The scatter test

- The shortest distance between two hits: (d_{min}) = |d-c*dt|

- Where dt =|t_i-t_j|
- d = |r_i-r_j|

- Where ti and ri denote to the recording time and position vector of i-th photon interaction in an event respectively, and c is the velocity of light in ns.

- A value of dt close to zero corresponds to a pair of hits created by subsequent Compton scatterings of the same photon in different detection modules. Distribution of d_{min}, defined as the smallest (in terms of absolute value) of three possible d12, d23 and d31 values for each event is displayed in Figure 7.7.
- In order to avoid any possible contamination of the 3-hits event sample with secondary scatterings of the primary photons, a three-hit event was rejected if its d_{min} was less than 17 cm.

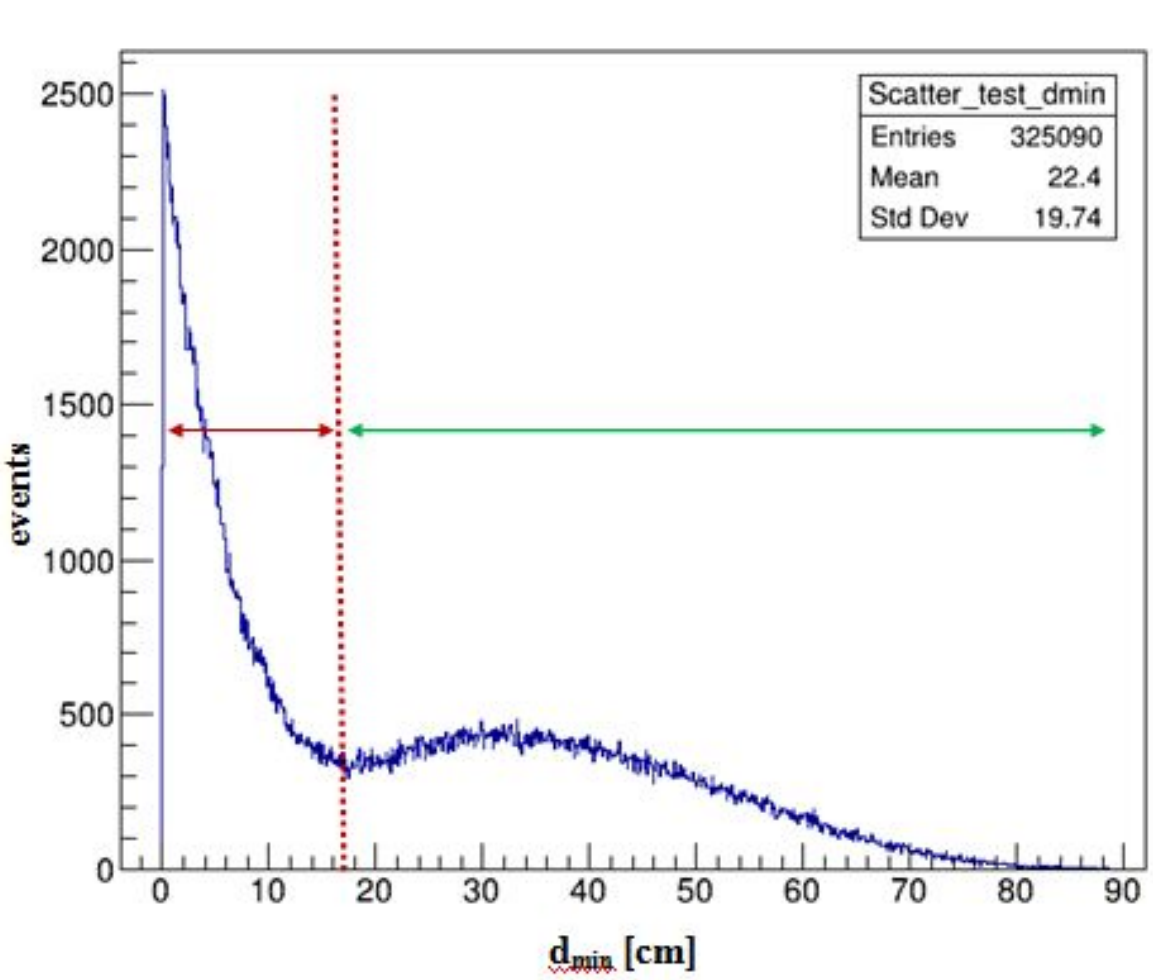

Figure : Distribution of the minimal discrepancy between inter-hit distance and hypothetical TOF times the velocity of light among all hit pairs in a 3-hits event shows 2 structures . The events with dmin > 17 cm are considered in the further analysis as marked with the dashed line and green arrow.

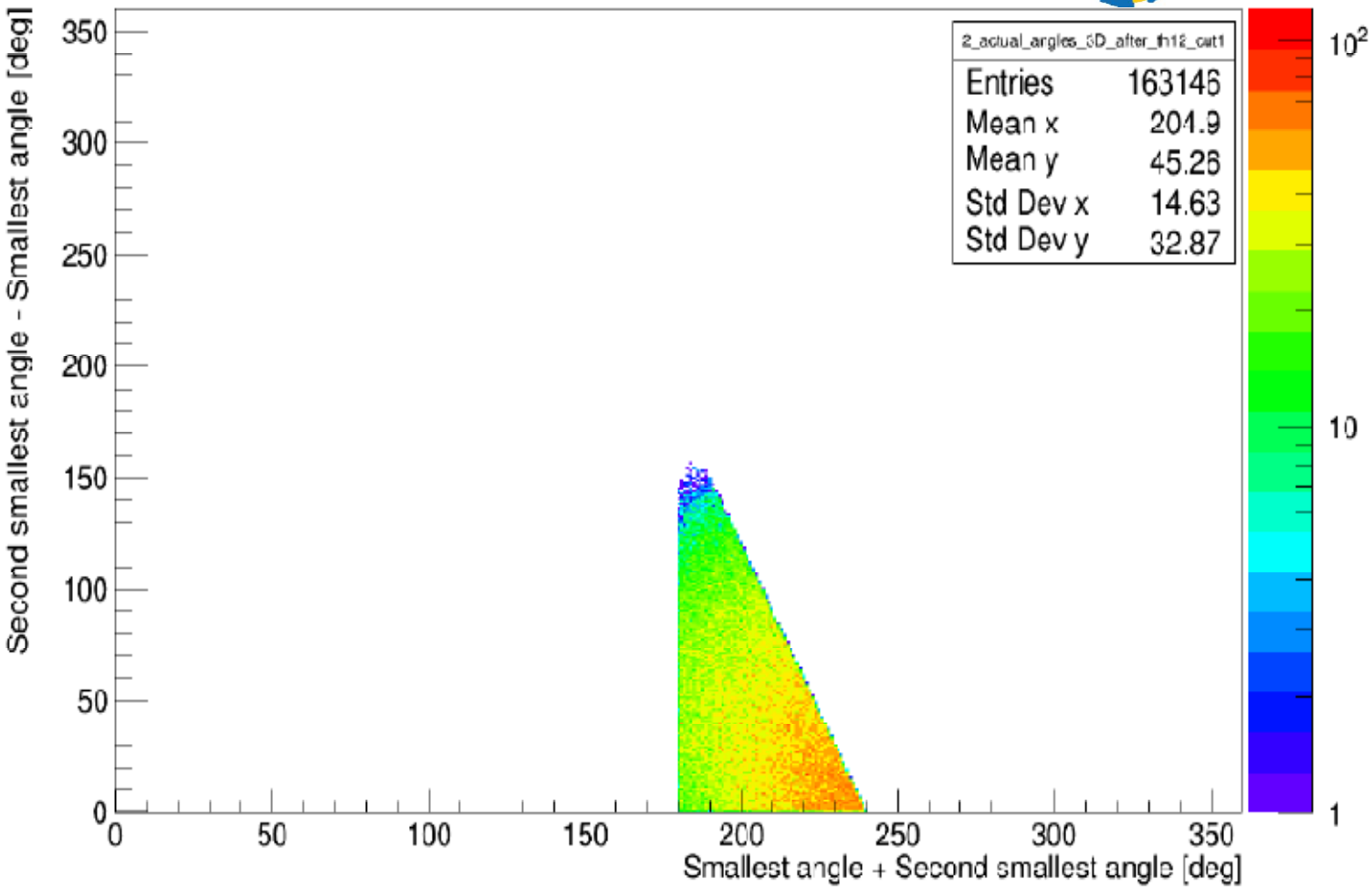

The sum of the1st and 2nd smallest angles versus the difference after applied the scatter test (17 cm cut).

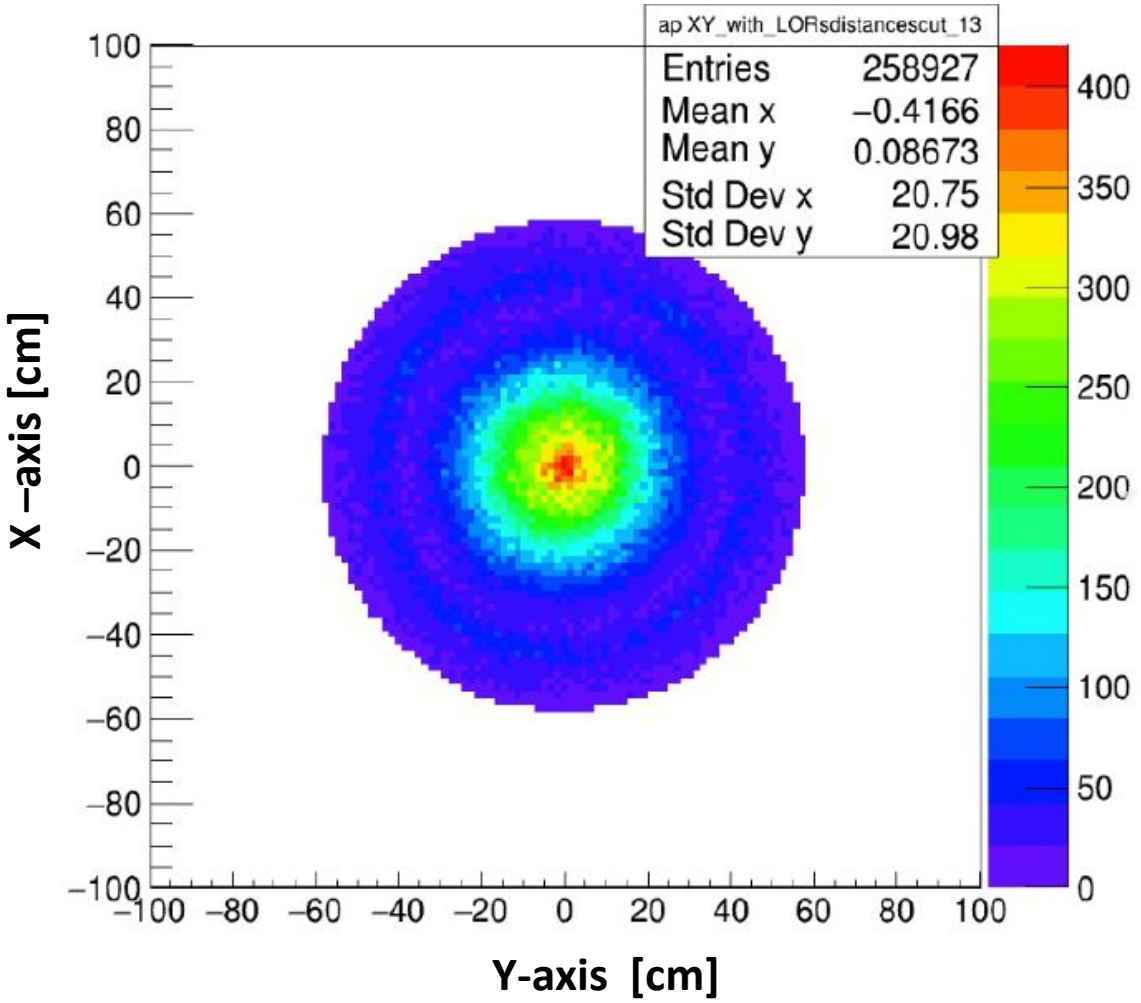

Figure : The tomographic image for all the annihilation points.

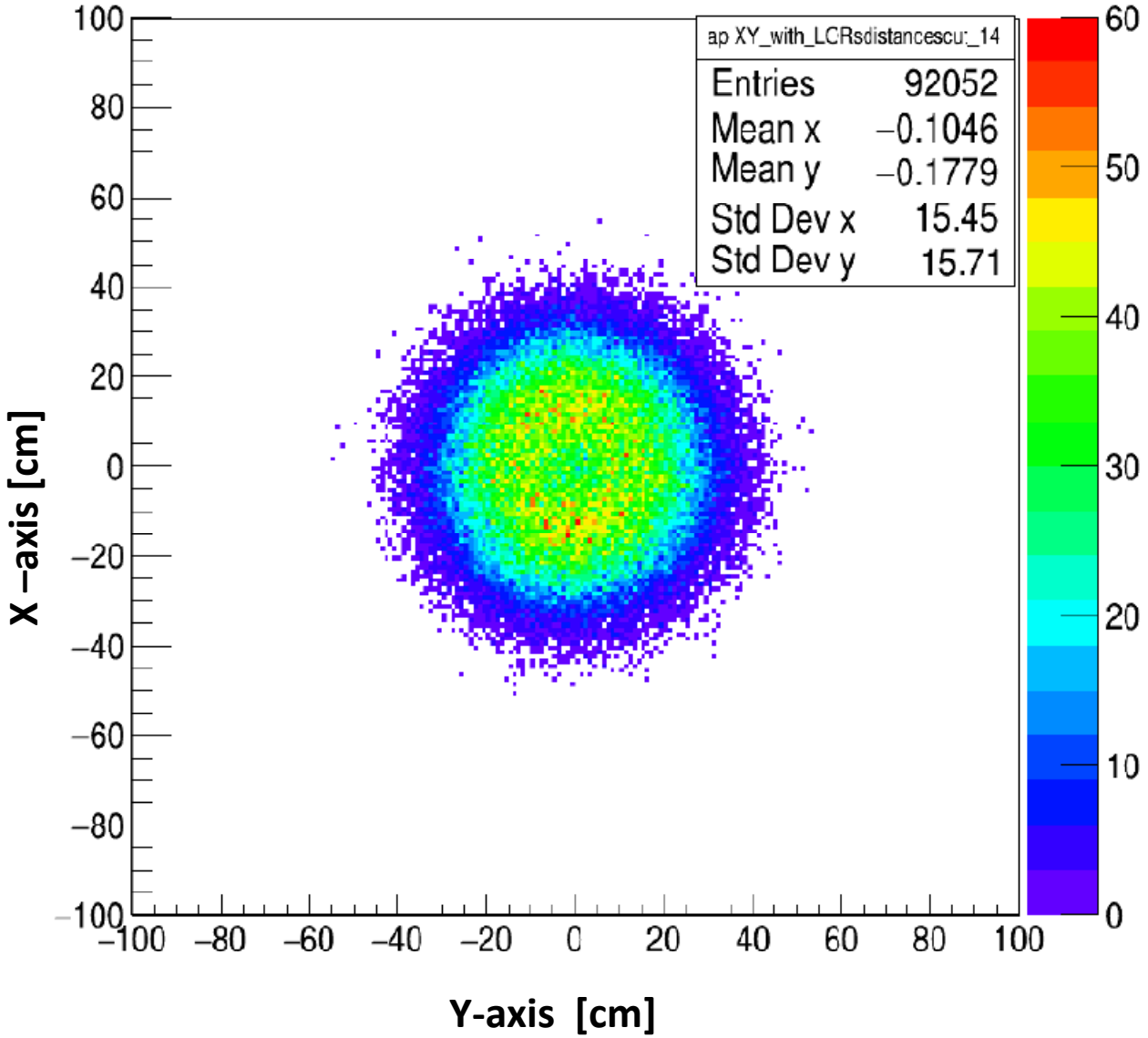

Figure : The decay points on the chamber after applied the scatter test.

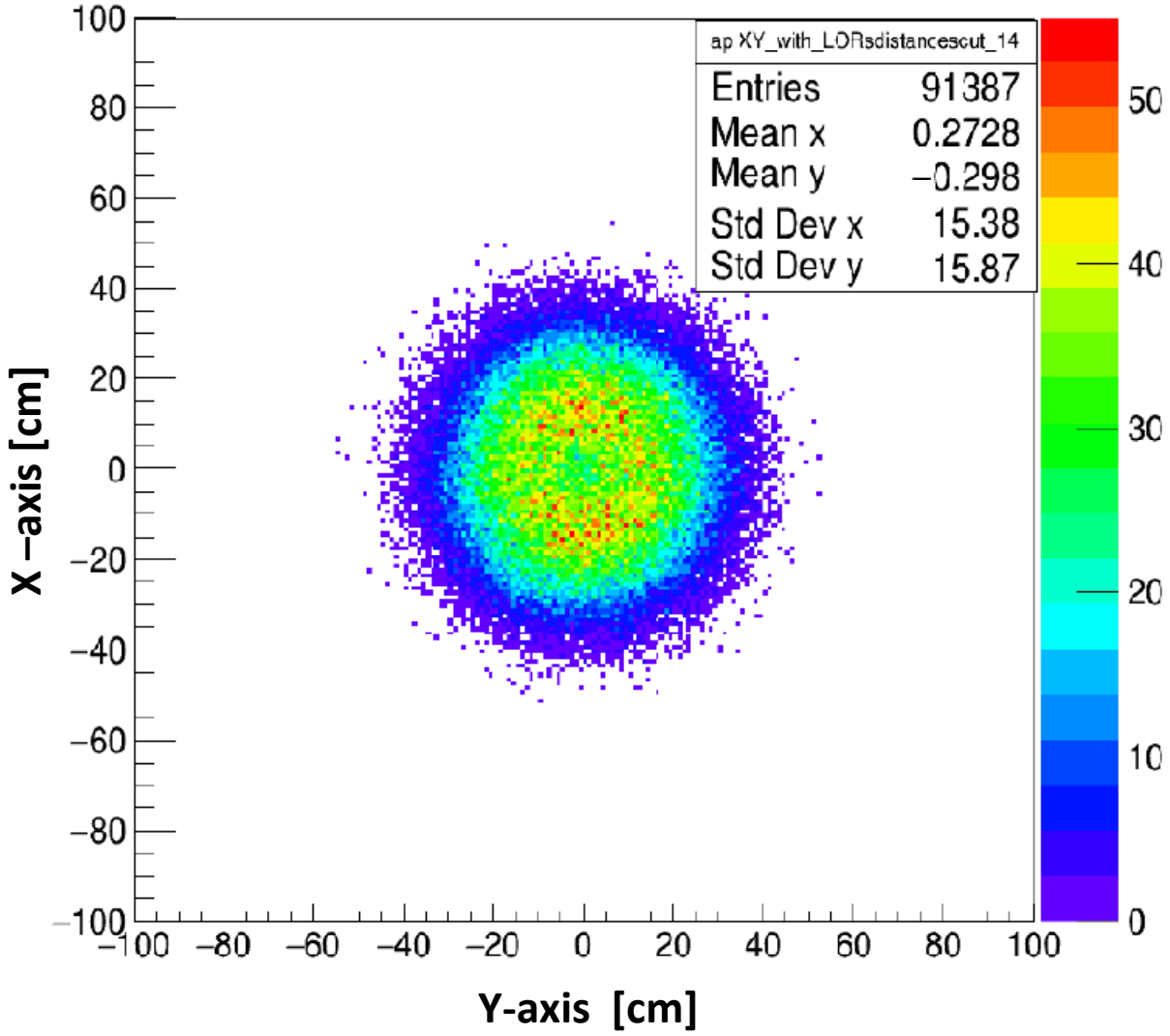

Figure : The decay points of the chamber after applied the scatter test and the time calibration.

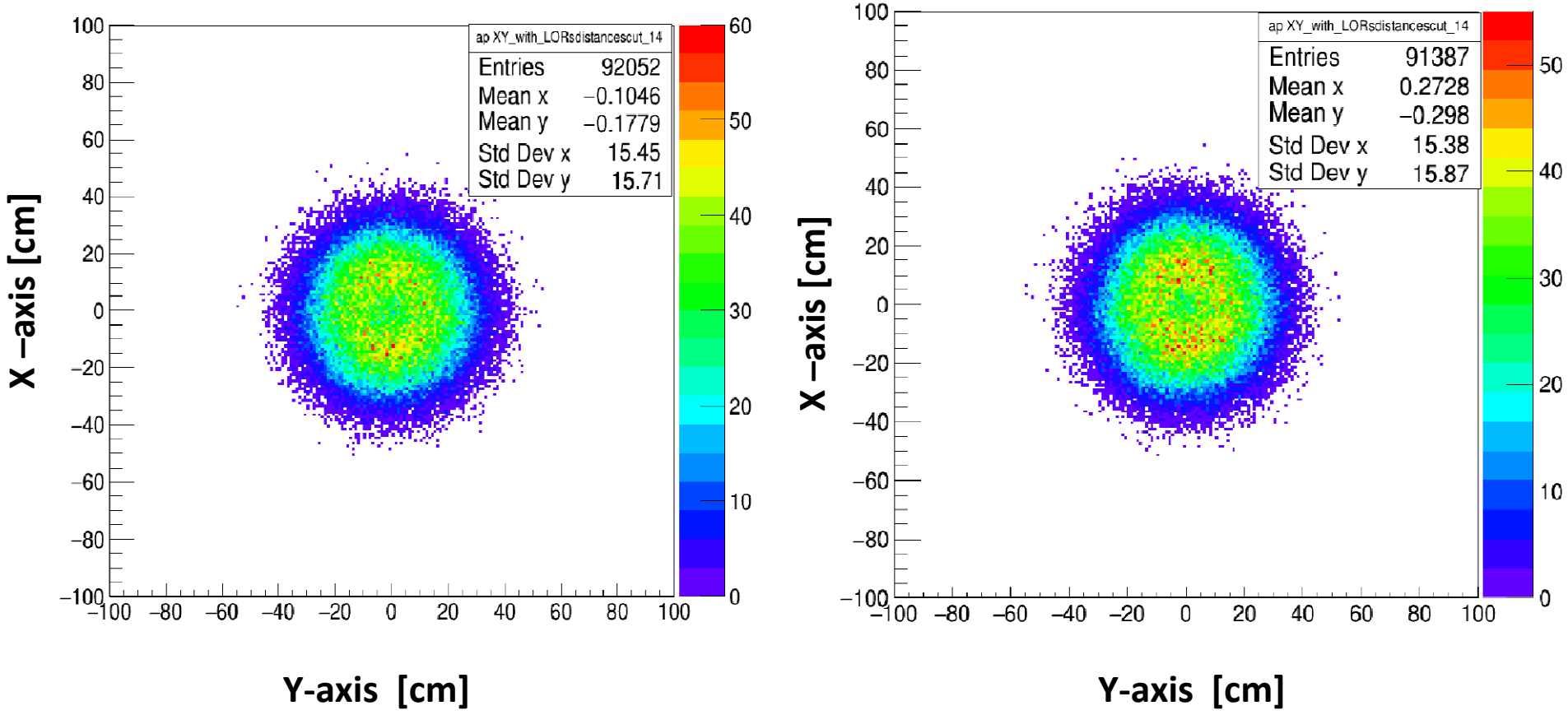

Figure : The decay points of the decay chamber after applied the scatter test ,(left) before time calibration, (right) after time calibration .

Run-7 Data analysis:

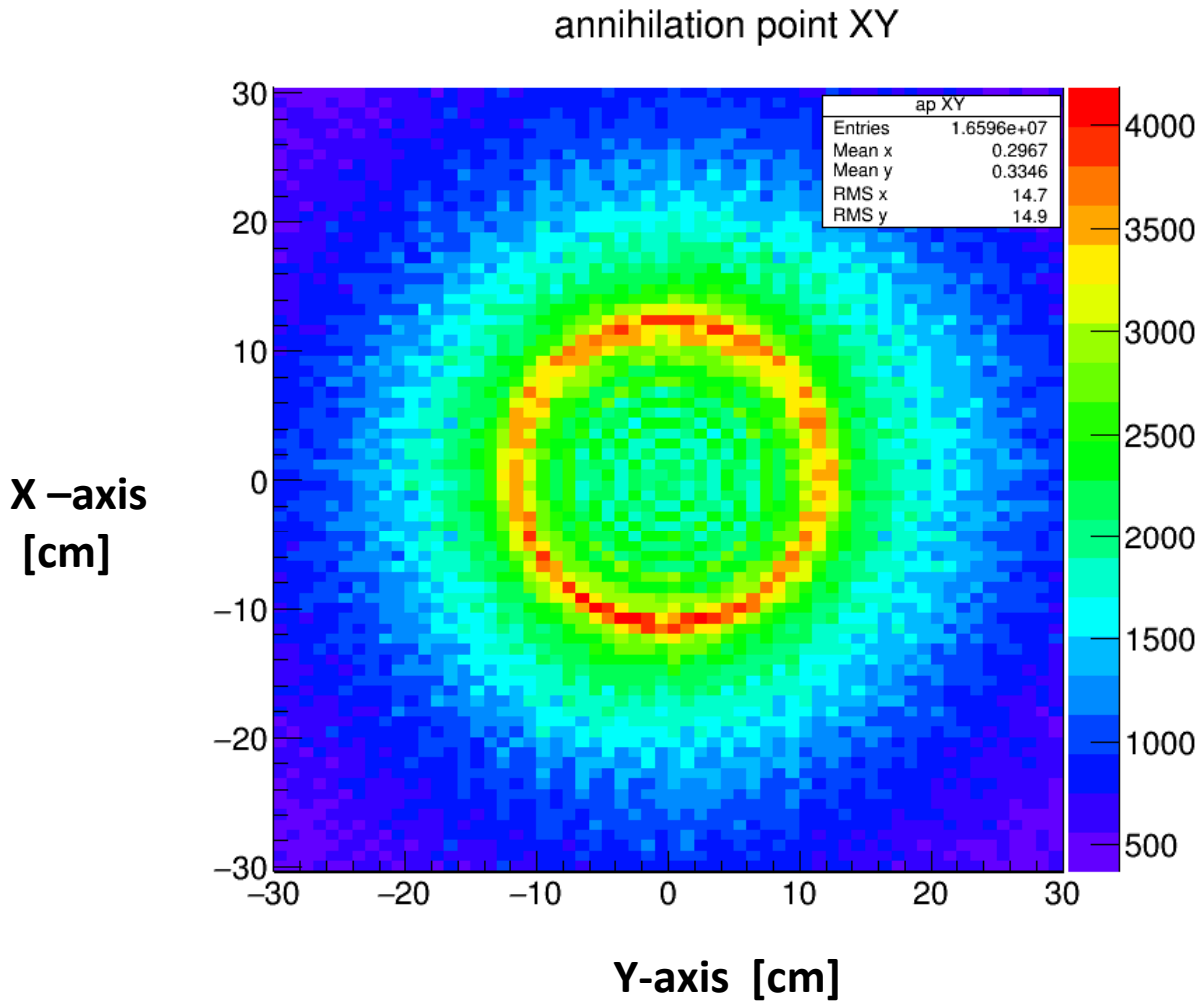

The tomographic image of the annihilation target cylinder (Run-7) obtained using Ps →2ɣ annihilations (xy view) transverse view, |z| > 5 cm

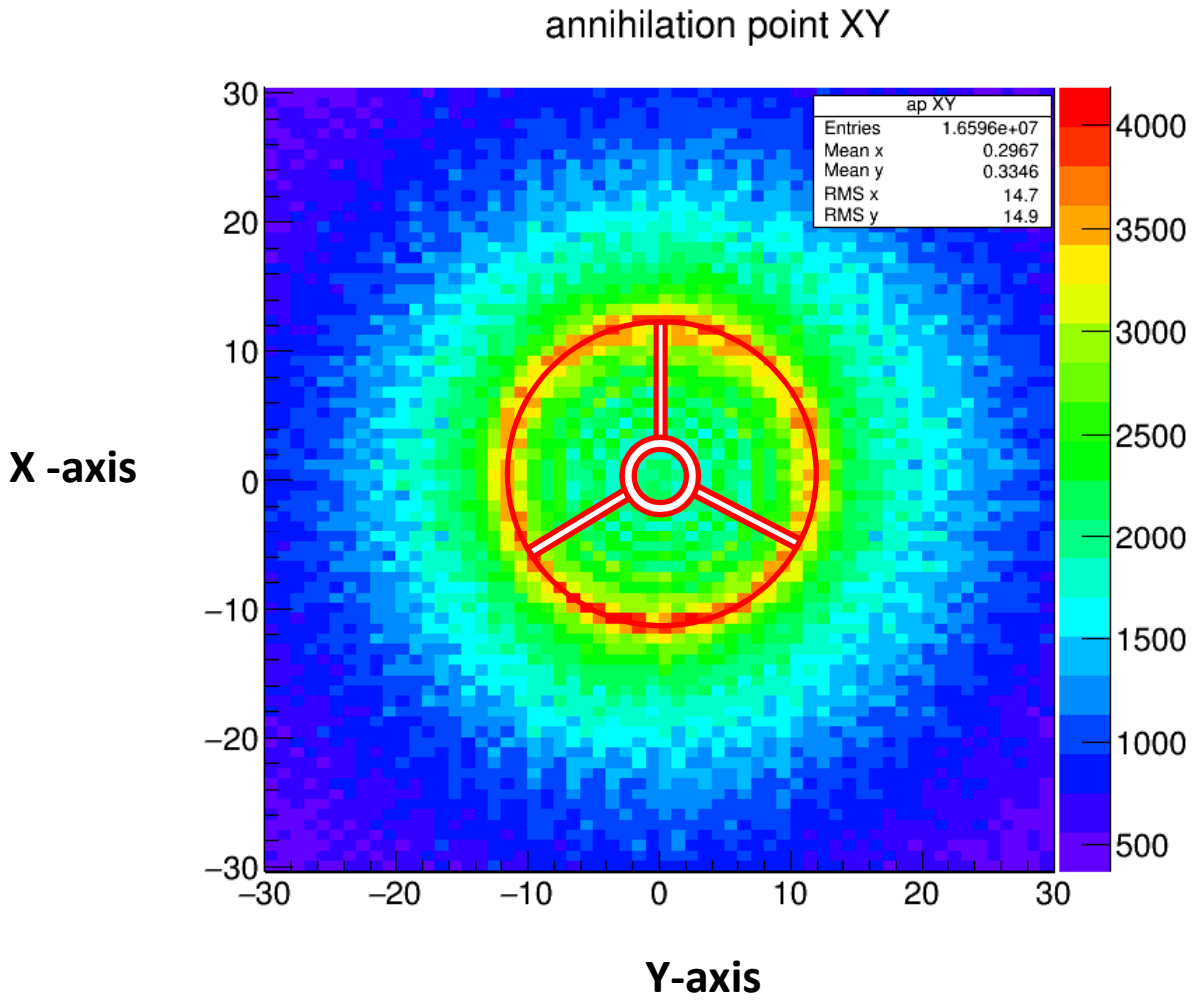

The tomographic image of the annihilation target cylinder obtained using Ps →2ɣ annihilations (xy view) transverse view, |z| > 5 cm

Run-7 for 20 files

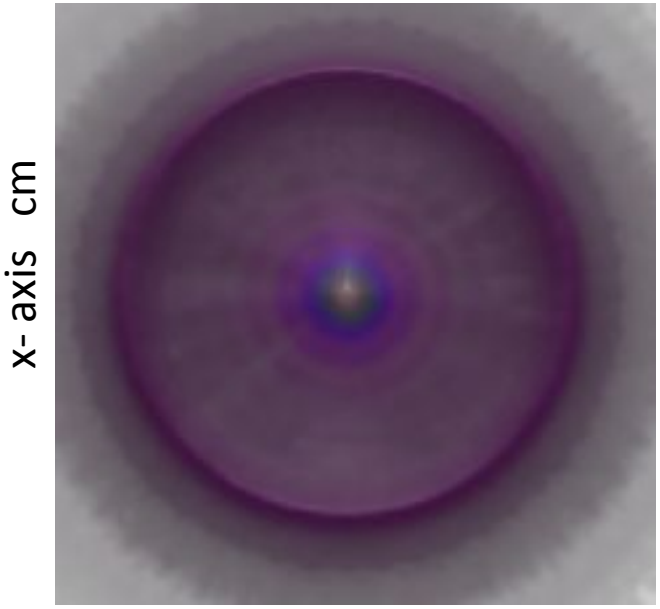

Run-7 for 100 files

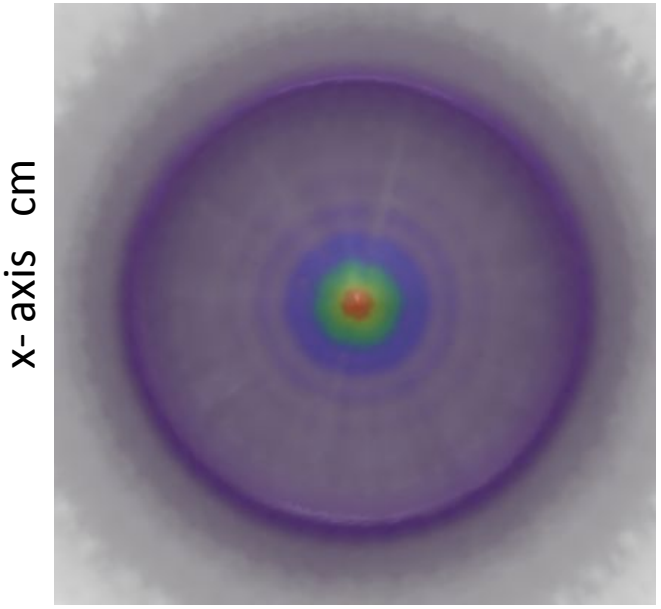

Run-7 Data:

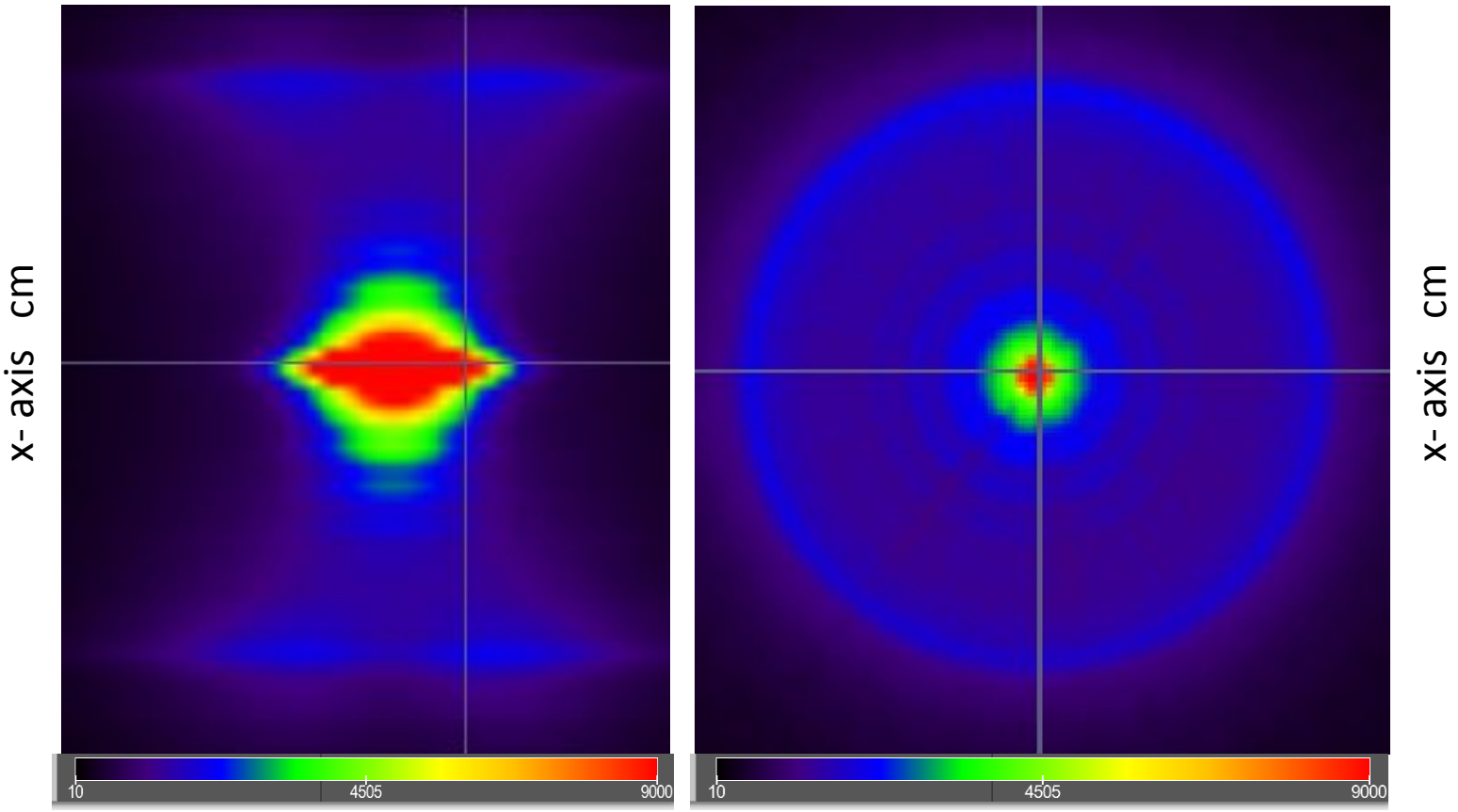

Run-6D and Run-7 Data analysis:

Number of Hits in an Event: 3Hits

3-hits must have |z-pos| <= 23 cm

3-hits must happened in 3-different scintillator strips.

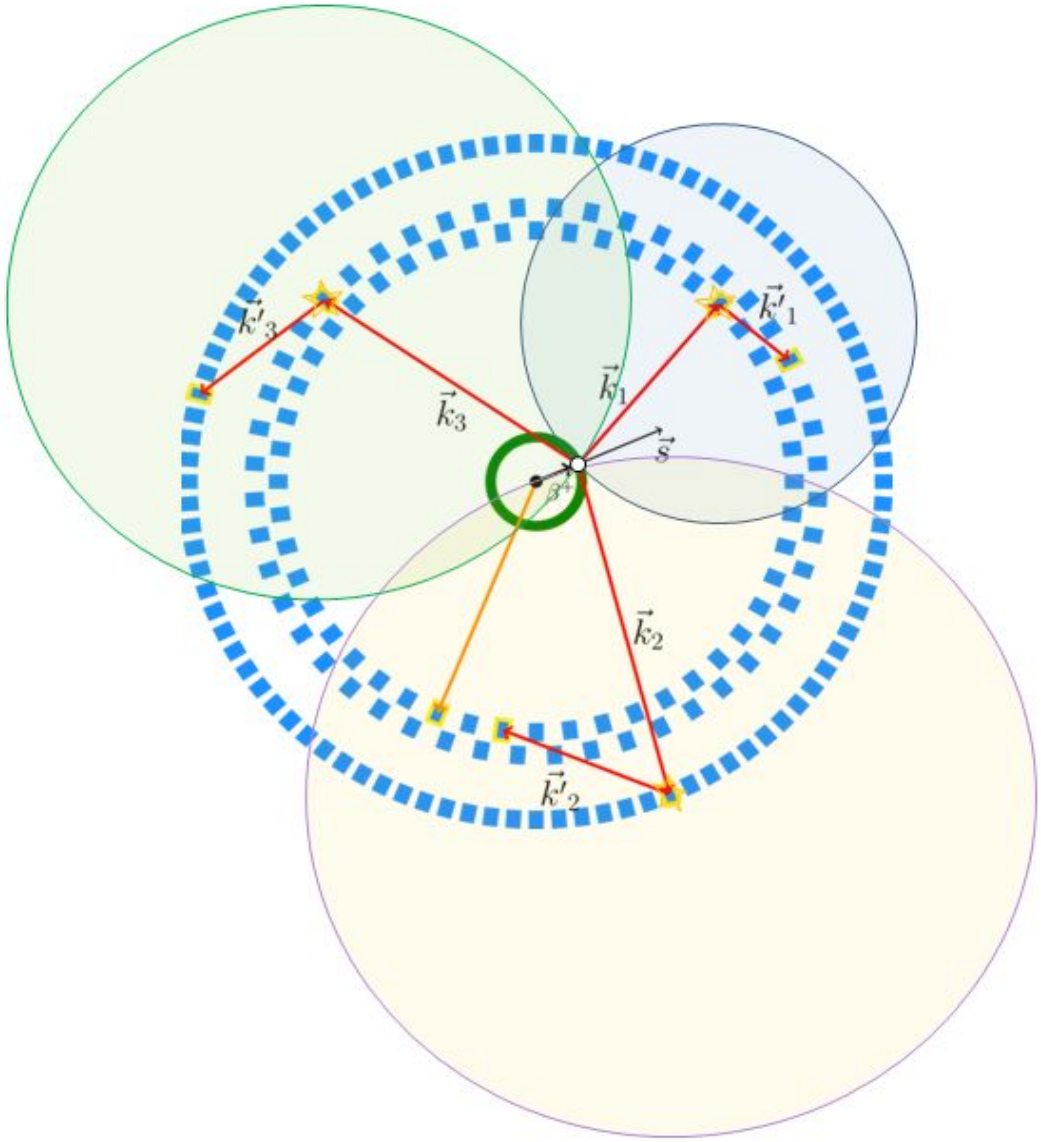

Figure: Scheme of the ortho-positronium decay, GPS based reconstruction method.

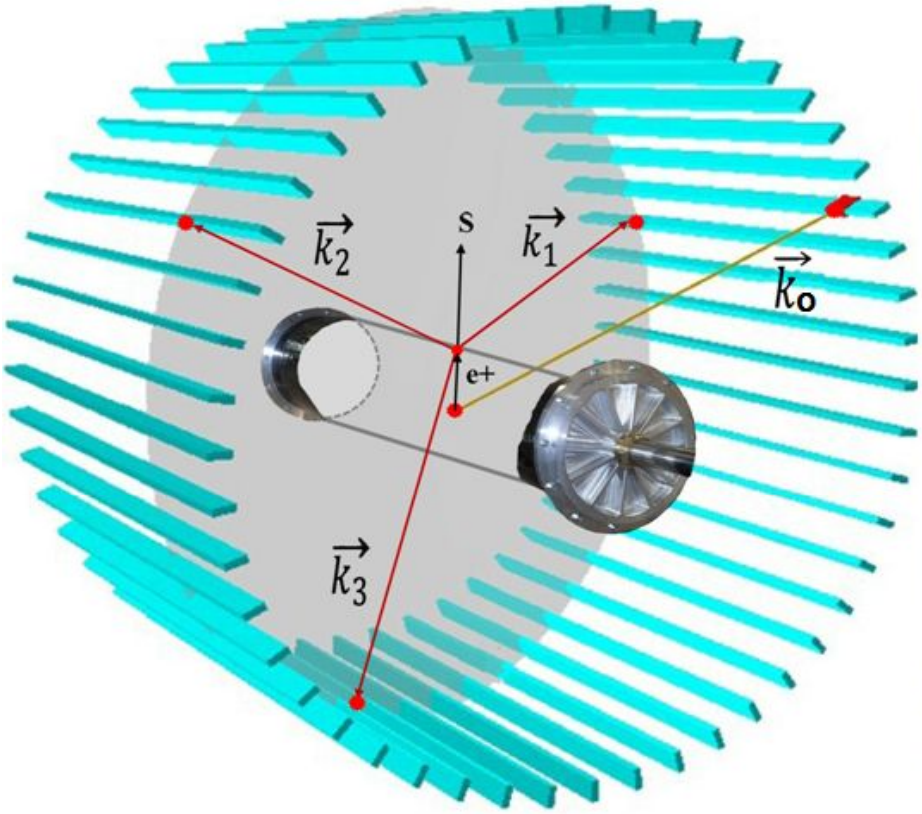

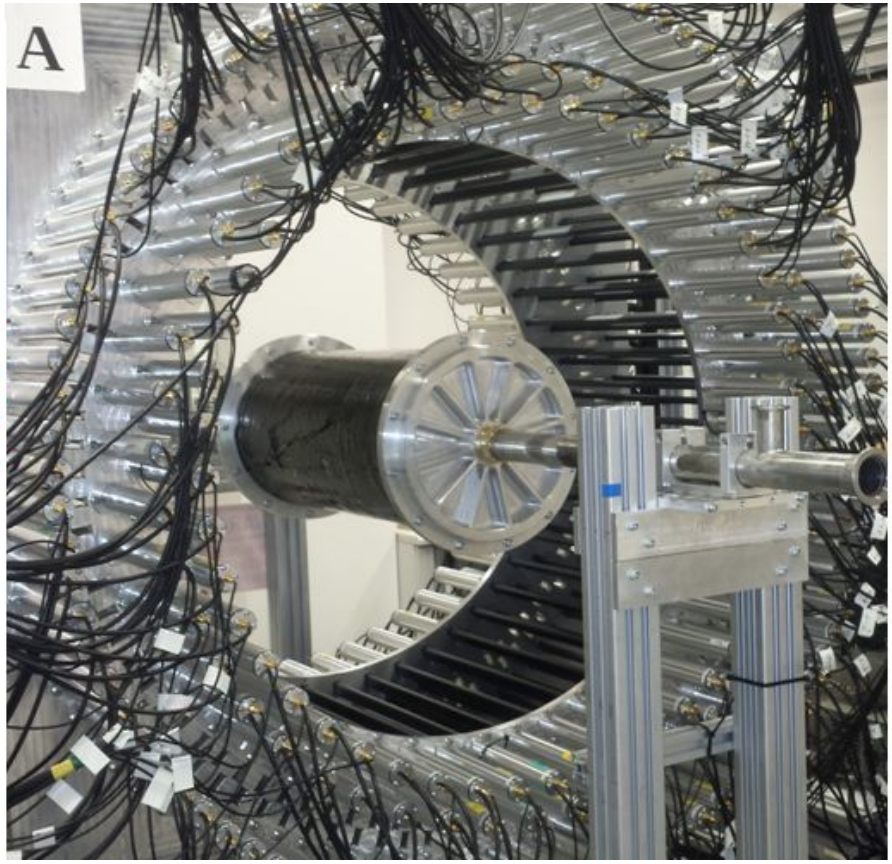

Determination the distribution of the reconstructed origin decay points of 3 annihilation events & the distance between the iso center of J-PET and the 3ɣ decay planes

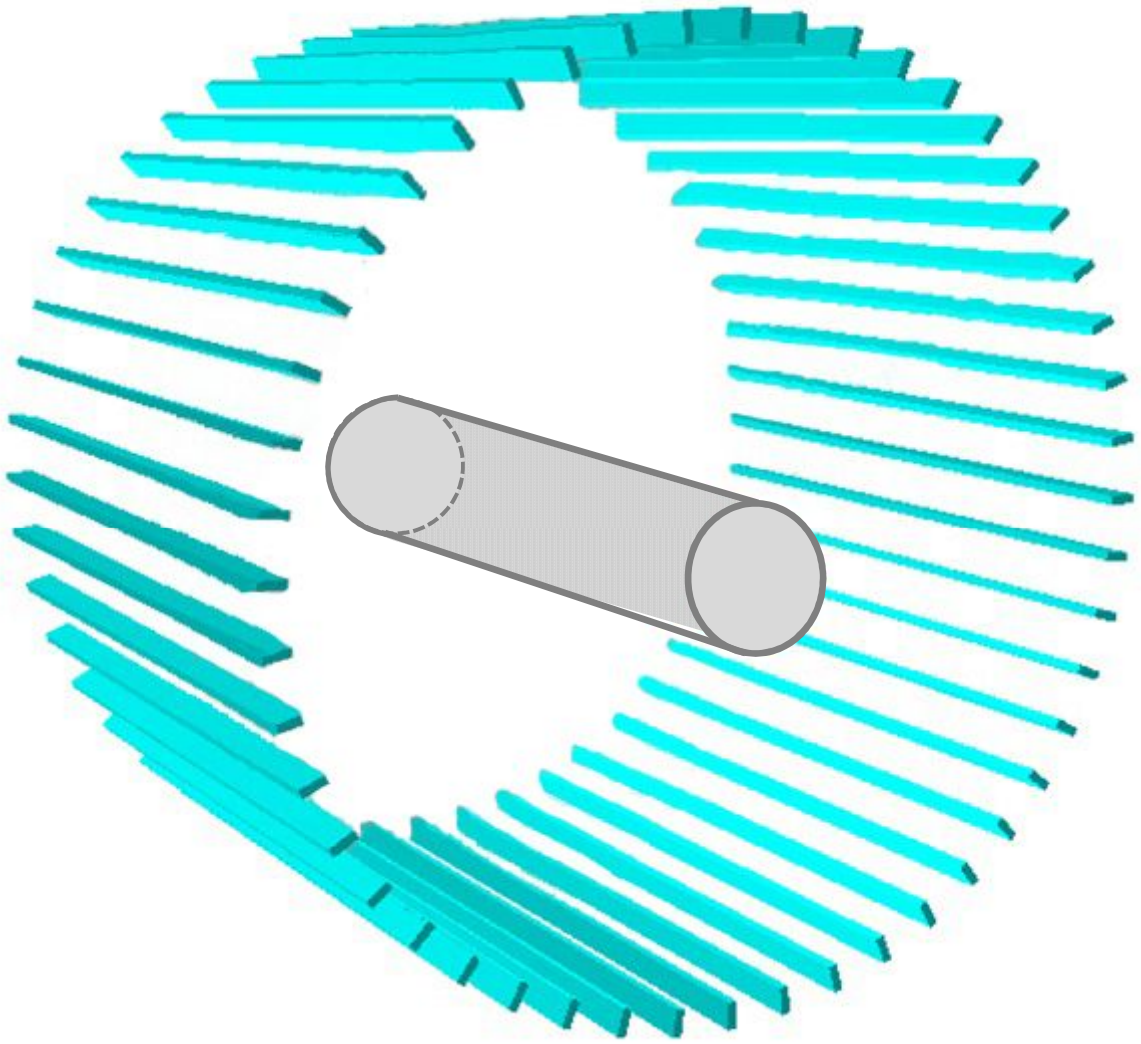

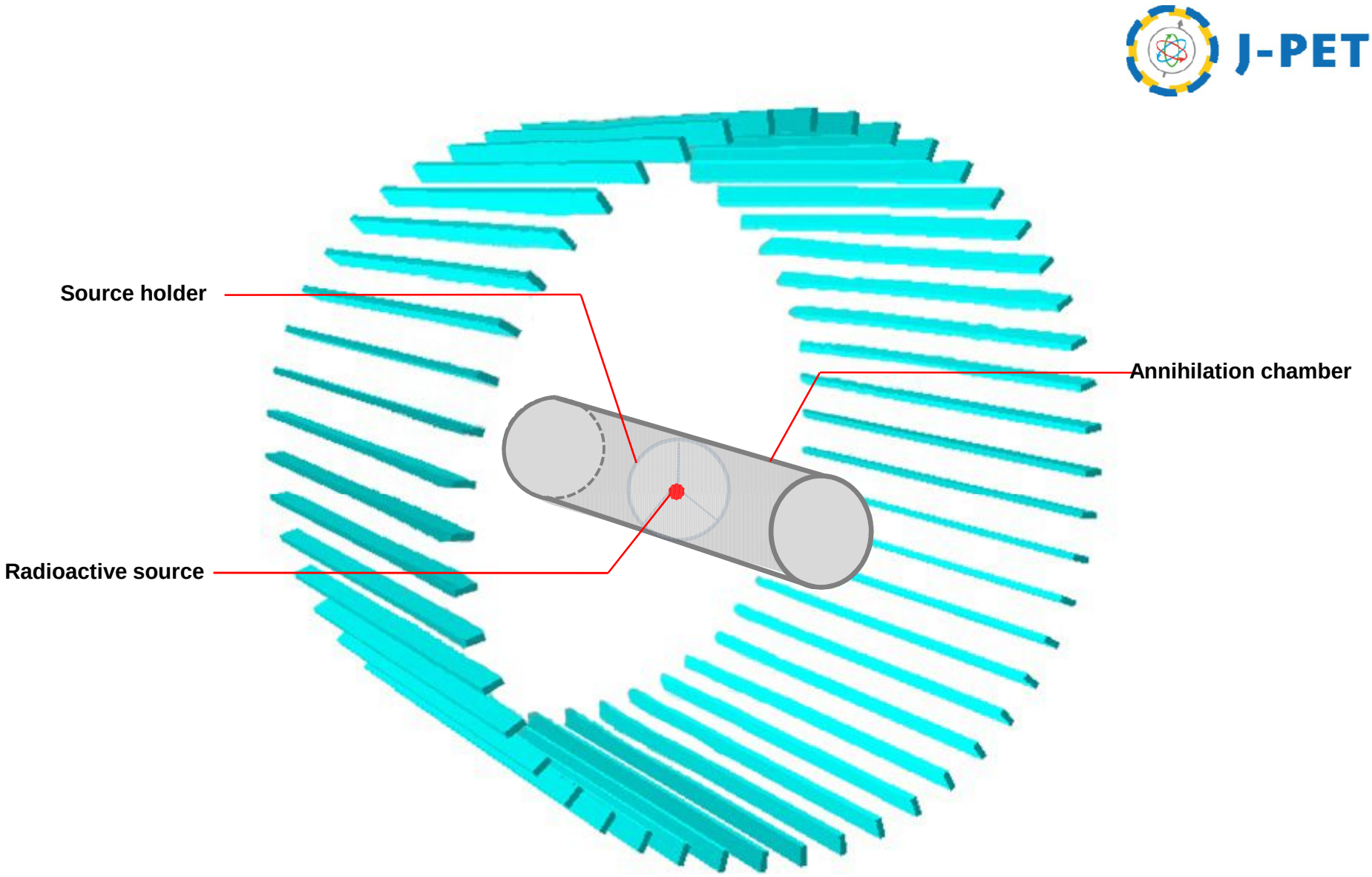
Source holder
Annihilation chamber
Radioactive source

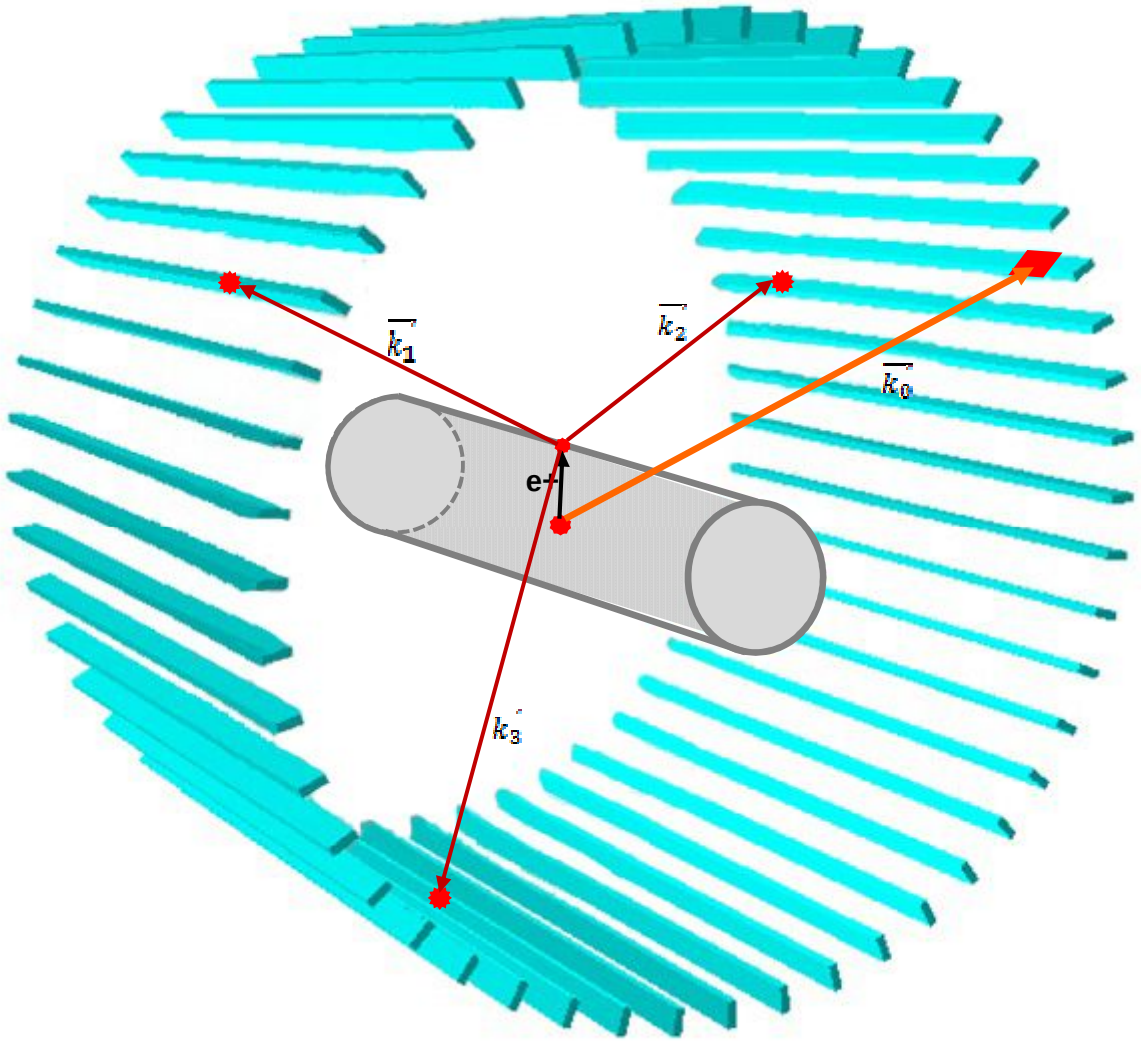
$\overrightarrow{k_1}$
$\overrightarrow{k_2}$
$\overrightarrow{k_0}$
e+
$\overrightarrow{k_3}$

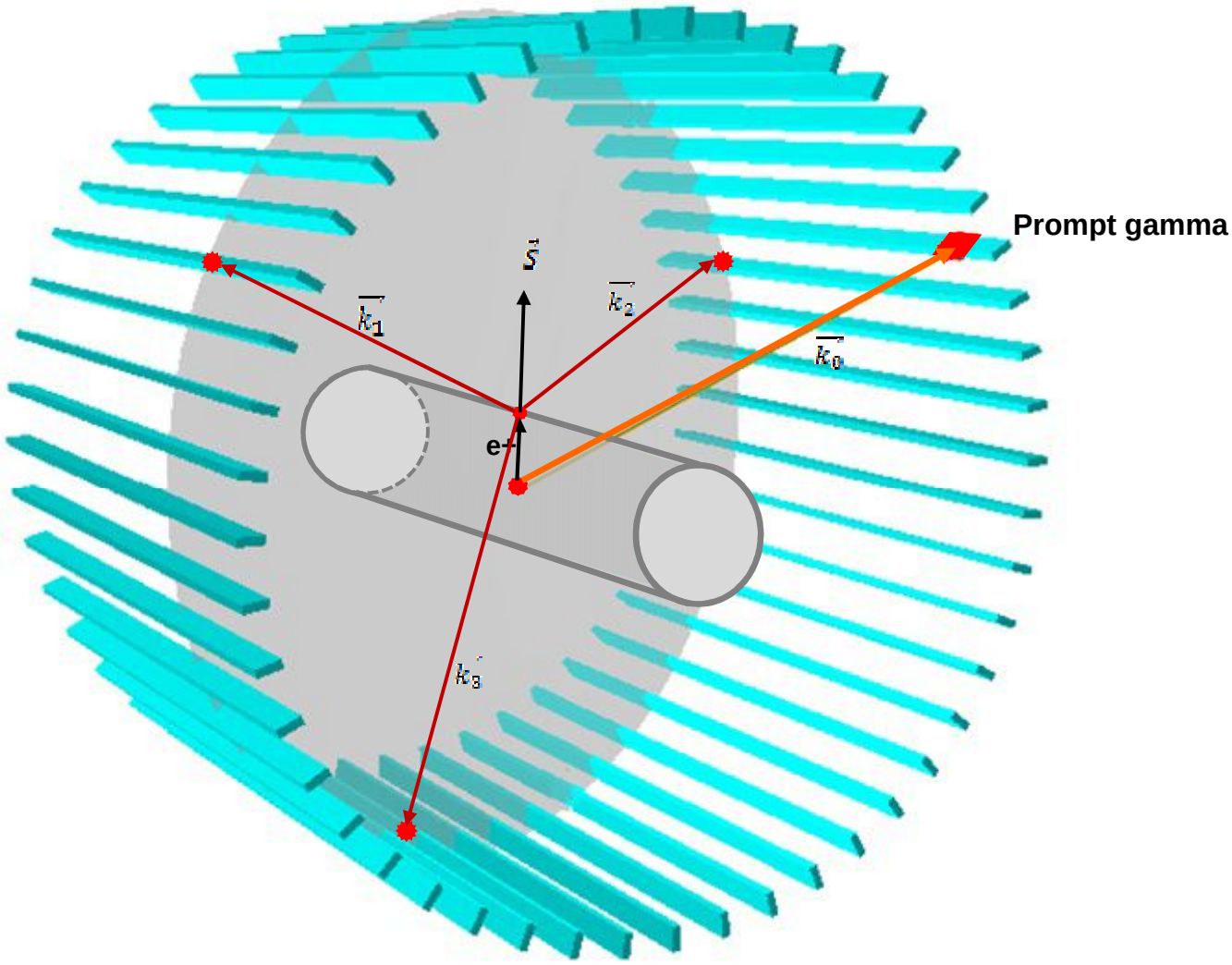
Prompt gamma
$\vec{S}$
$\vec{k_1}$
$\vec{k_2}$
$\vec{k_0}$
e+
$\vec{k_3}$

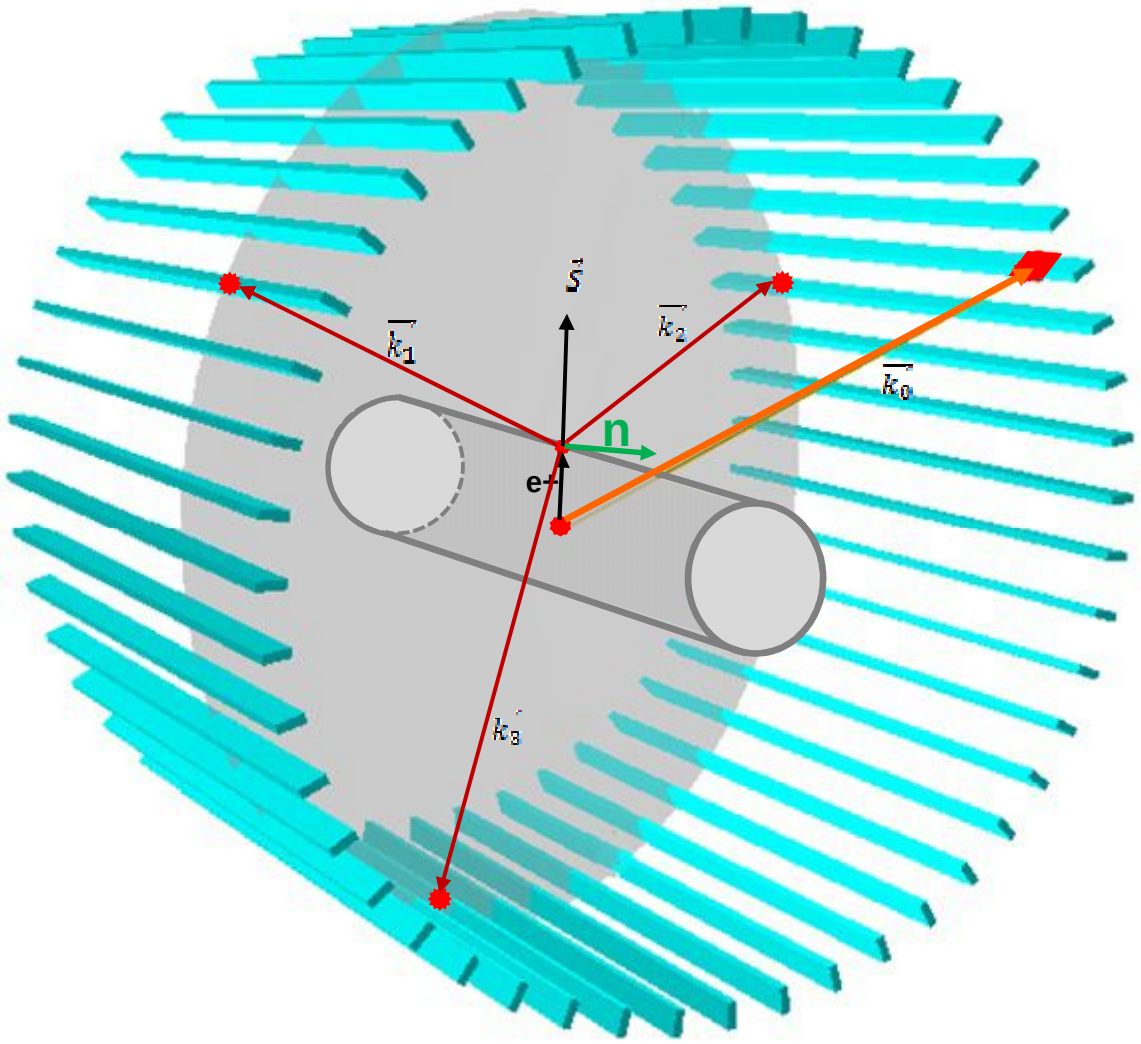

1- The pre-selection criteria of data required the presence of at least three gamma photons interactions (3-hits) within a 20 ns of the time window.
2- The second criterion is the calibrated time over threshold (TOT) values which is able for restricting further considerations to the hits whose deposited energy in the scintillator, measured as TOT values, could correspond to a photon from 3γ photons annihilation.

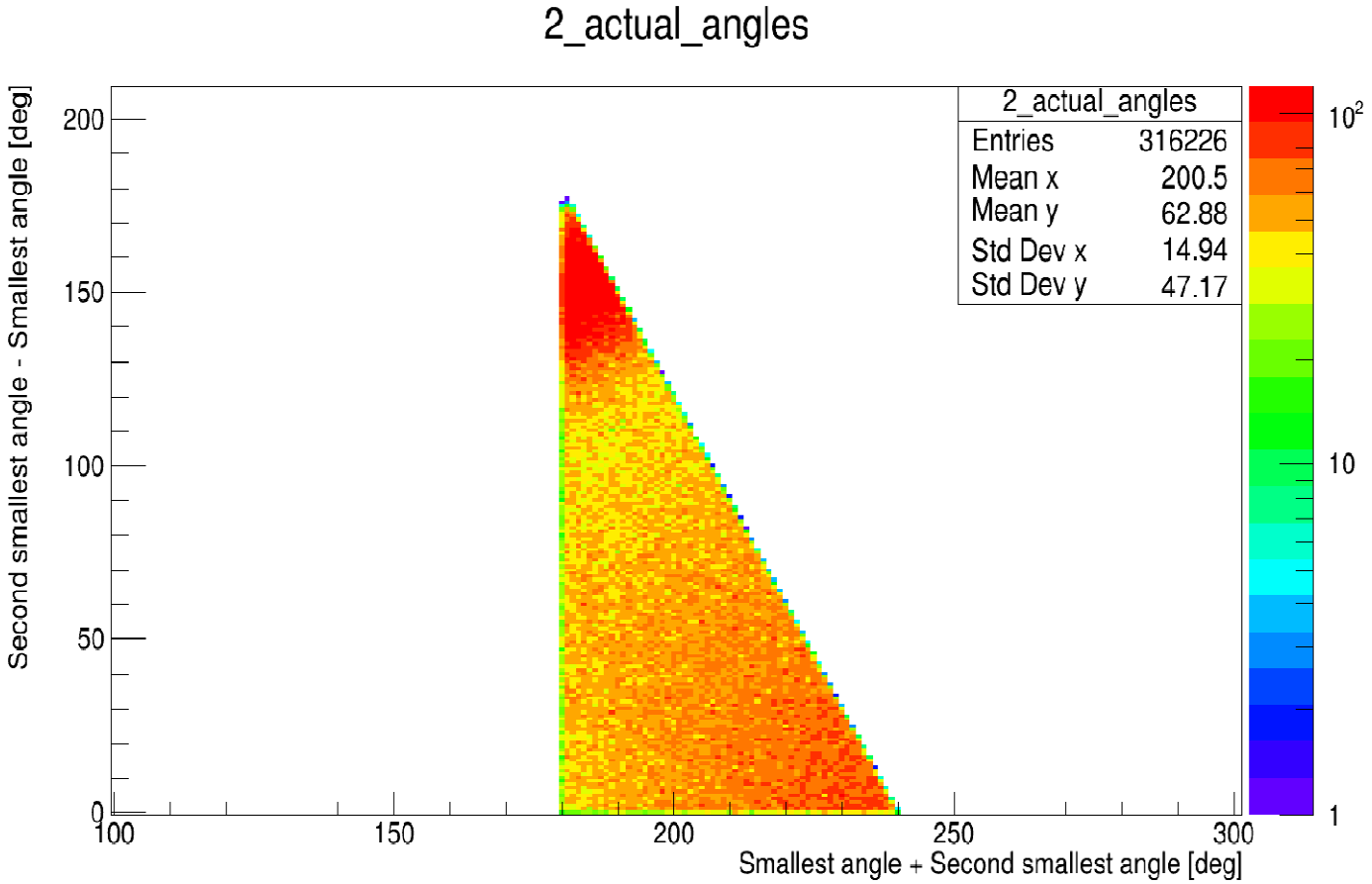

Figure: The sum of the1st and 2nd smallest angles versus the difference between them in the case of large annihilation chamber with a layer of porous material.

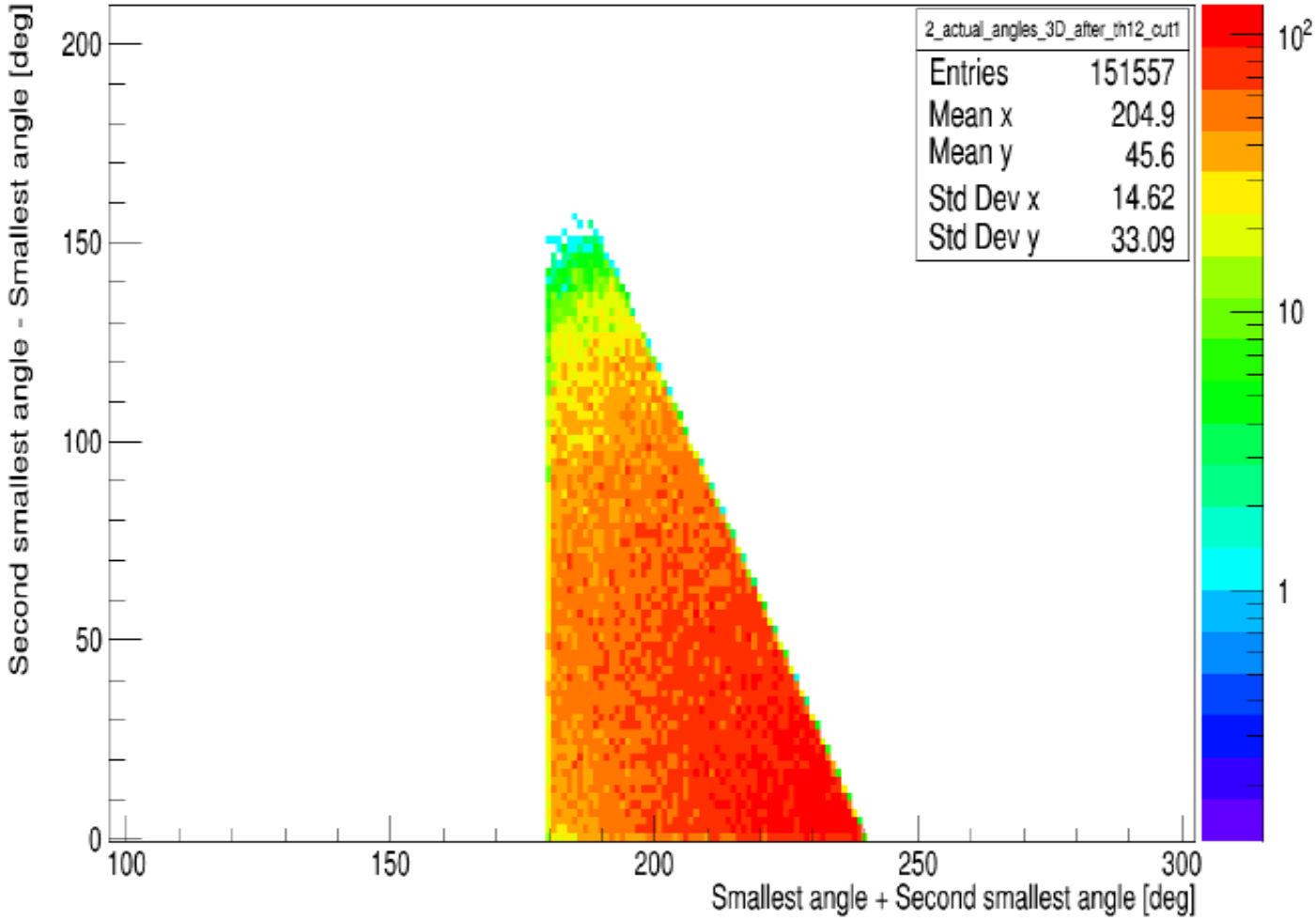

The sum of the1st and 2nd smallest angles versus the difference after applied the scatter test (17 cm cut).

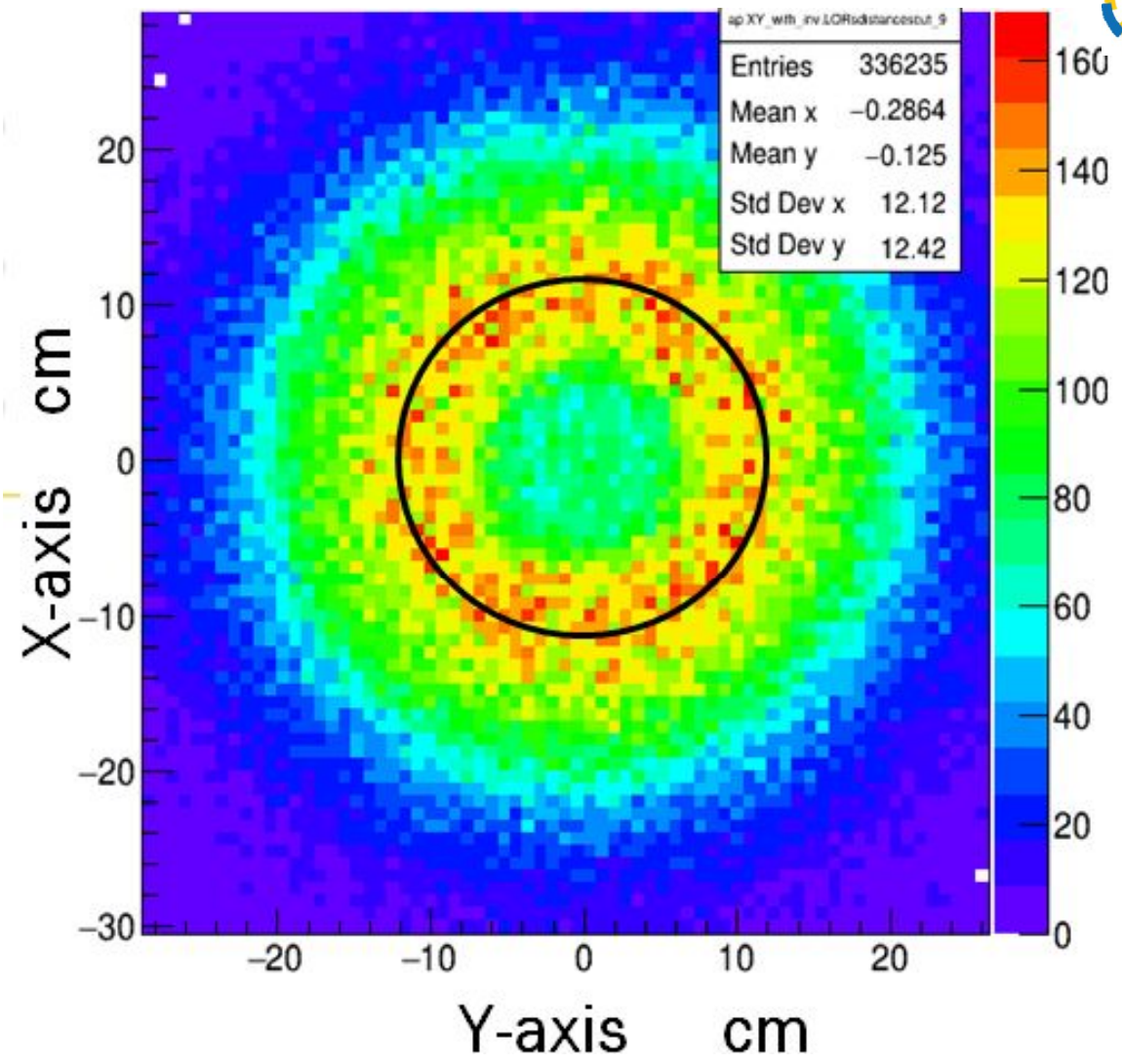

The distribution of the reconstructed annihilation points for events which were identified as o-Ps→3ɣ in the data of large chamber measurement in Run-7. The black circle indicates the wall location of the large cylindrical chamber used in the measurements.

Run-3 decay chamber reconstruction:

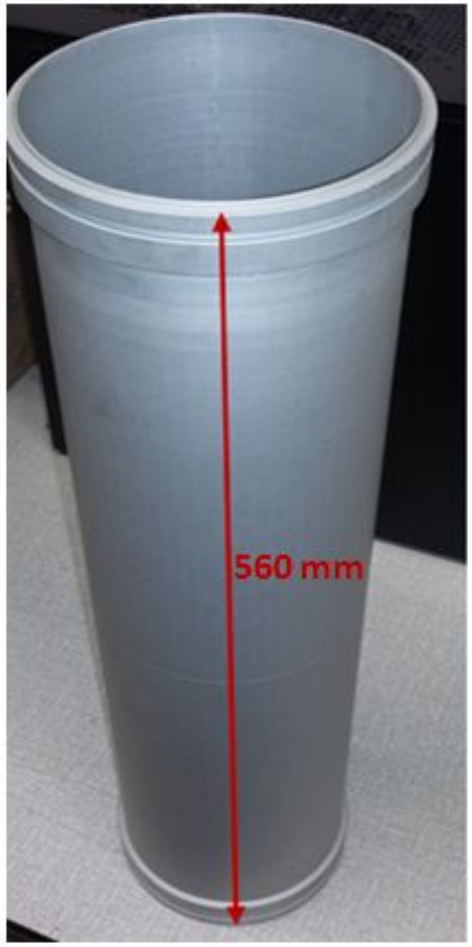

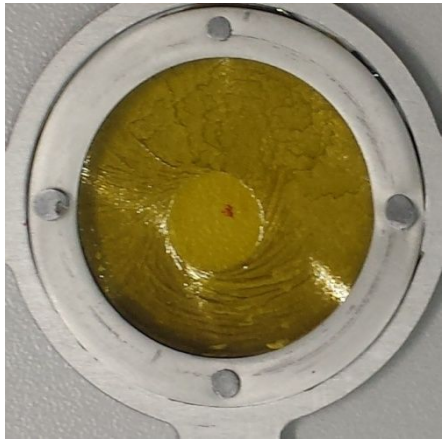

Run-3 Data analysis:

Number of Hits in an Event: 2Hits

2-hits must have |z-pos| <= 23 cm

2-hits must happened in 2-different scintillator strips.

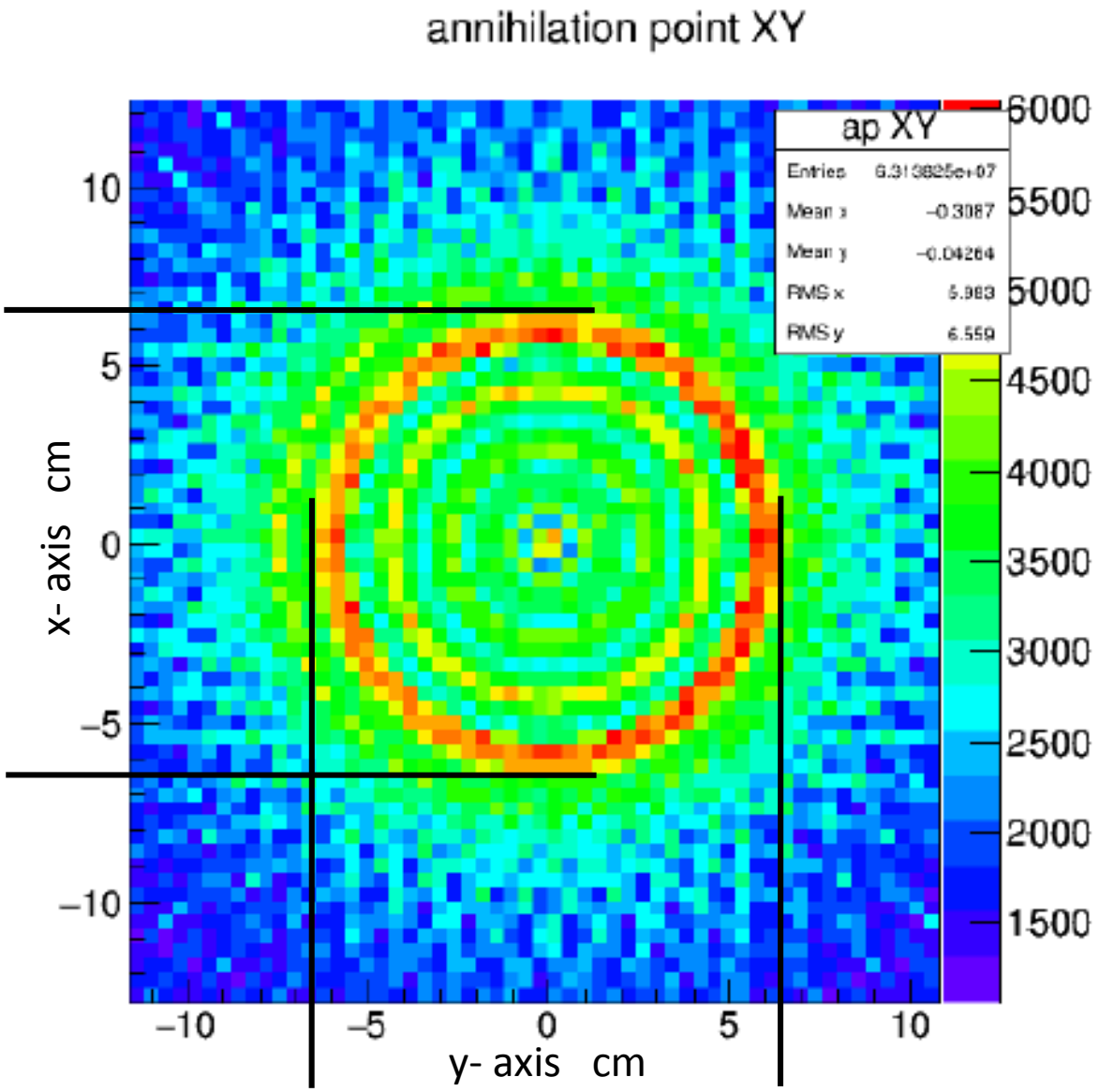

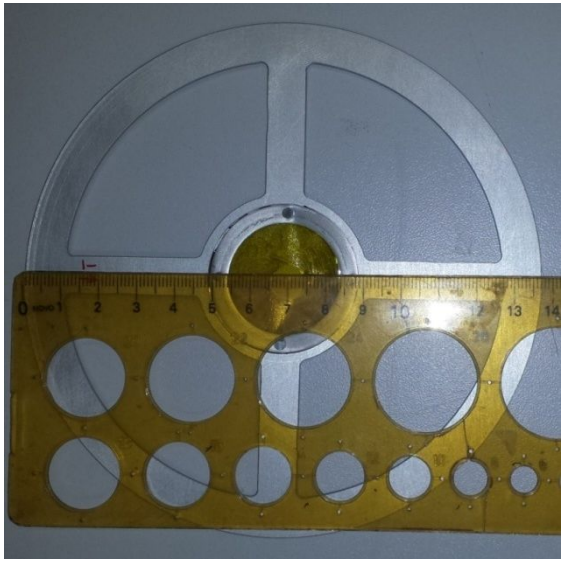

Diameter =13.6 cm

The case of 2 gamma +scattering and 3 gammas

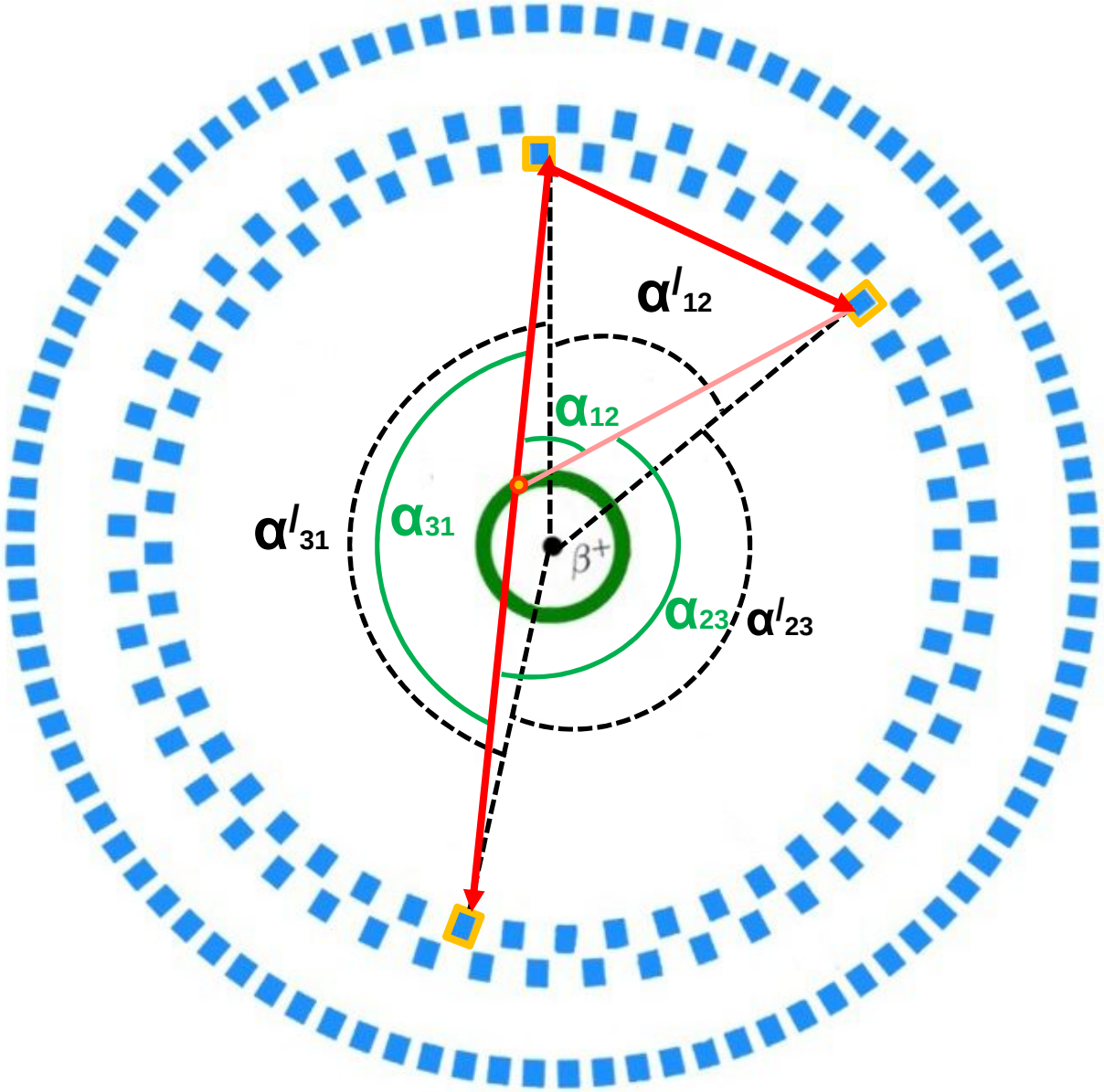

The pre selection criteria for Run-3 Data analysis:

Number of Hits in an Event: 2Hits

2-hits must have |z-pos| <= 23 cm

2-hits must happened in 2-different scintillator strips.

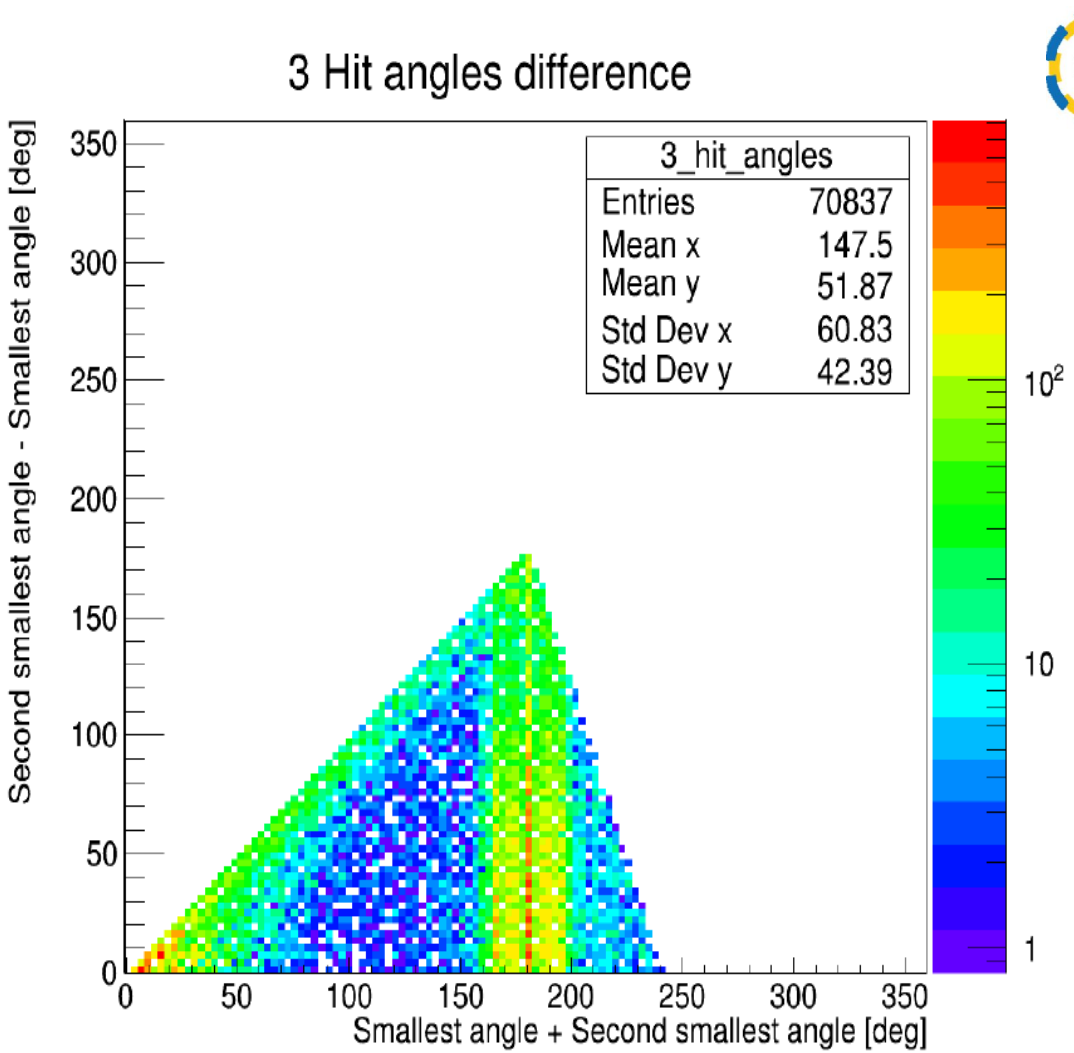

The distribution of the difference versus the sum of the two smallest angles. With such a choice of variables on the x, y axes, events from two gamma photons annihilations, which contain the two photons with opposite momenta, are collected together in a vertical band symmetrically around 180^{o}.

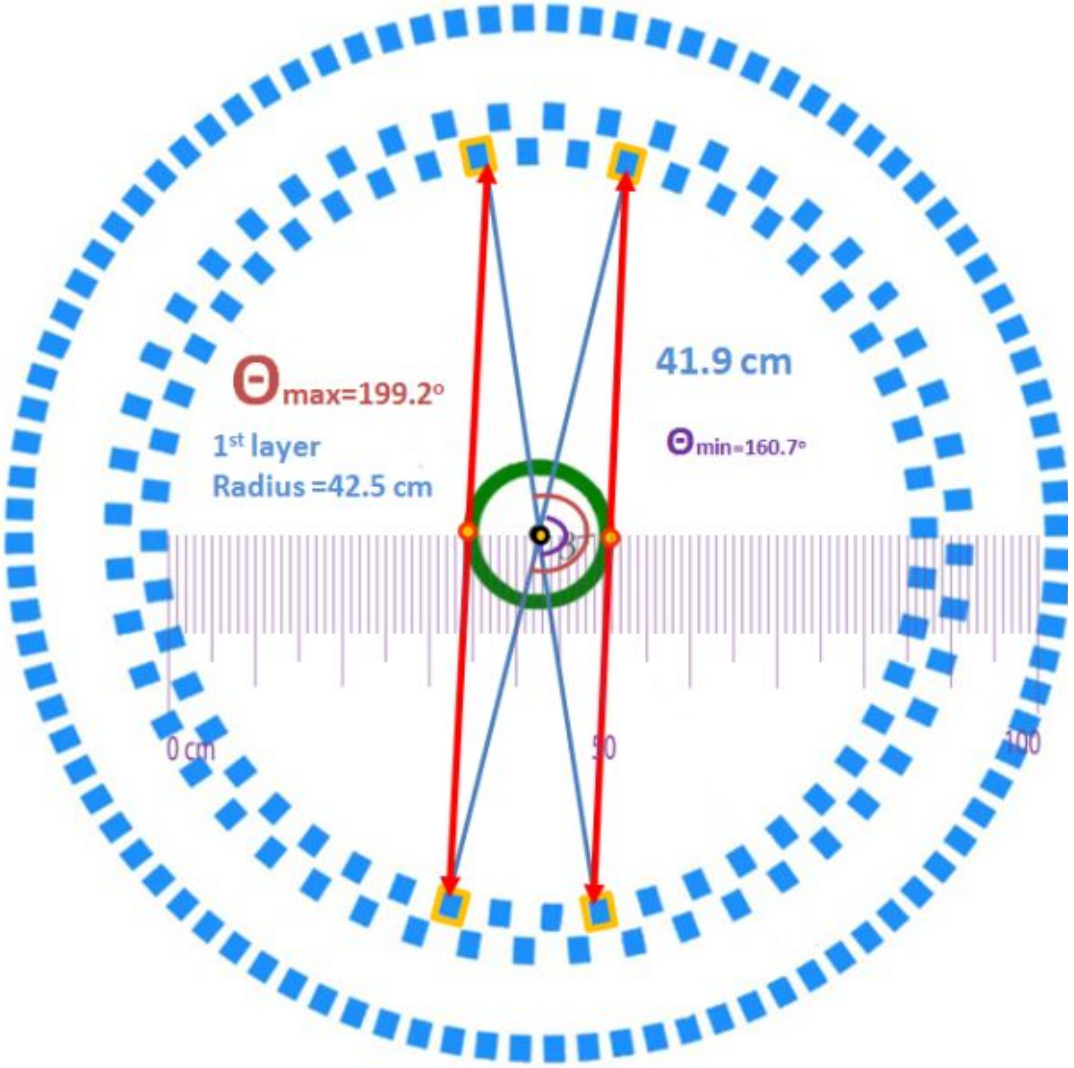
Θmax=199.2°
1st layer
Radius =42.5 cm
41.9 cm
Θmin=160.7°
0 cm
50
100

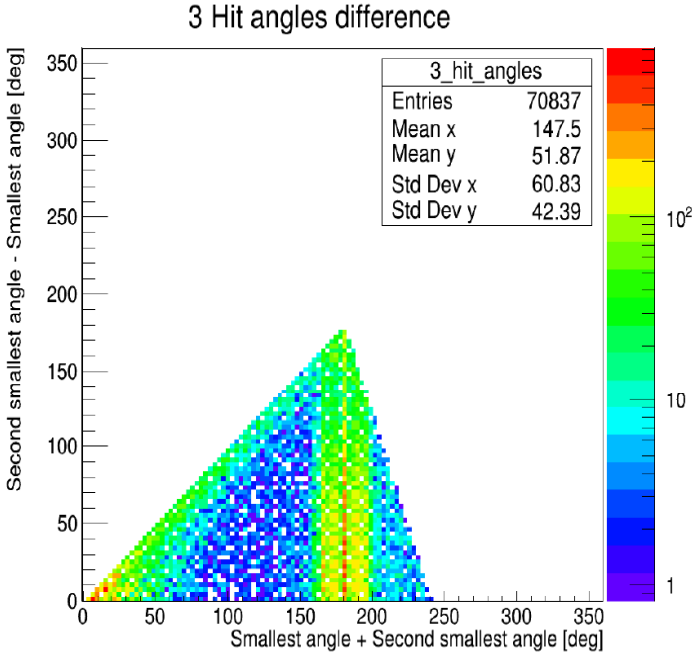
3 Hit angles difference
3_hit_angles
Entries 70837
Mean x 147.5
Mean y 51.87
Std Dev x 60.83
Std Dev y 42.39
Second smallest angle - Smallest angle [deg]
Smallest angle + Second smallest angle [deg]
0
50
100
150
200
250
300
350
10^2
10
1

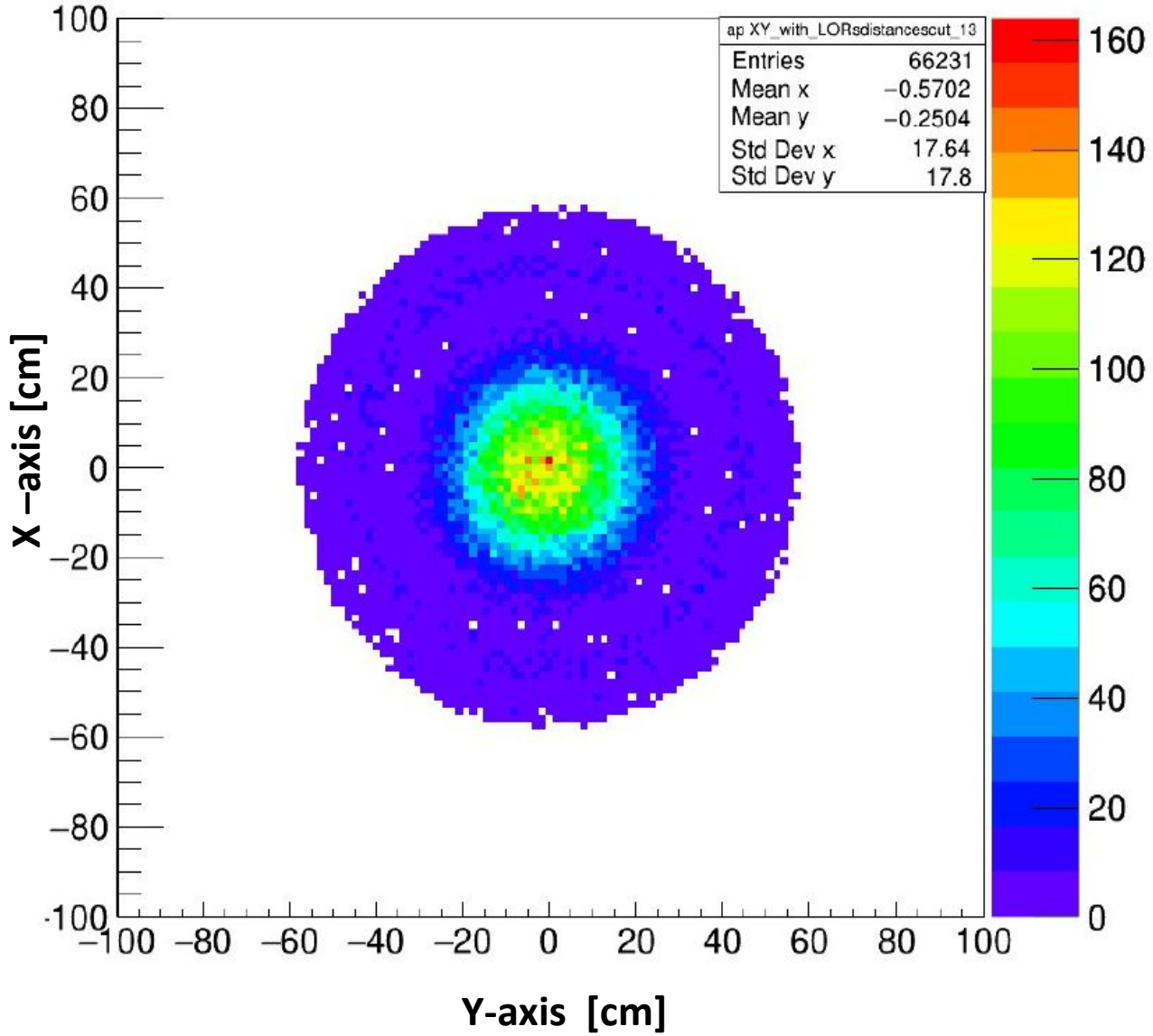

Figure : The tomographic image of of all the annihilation points .

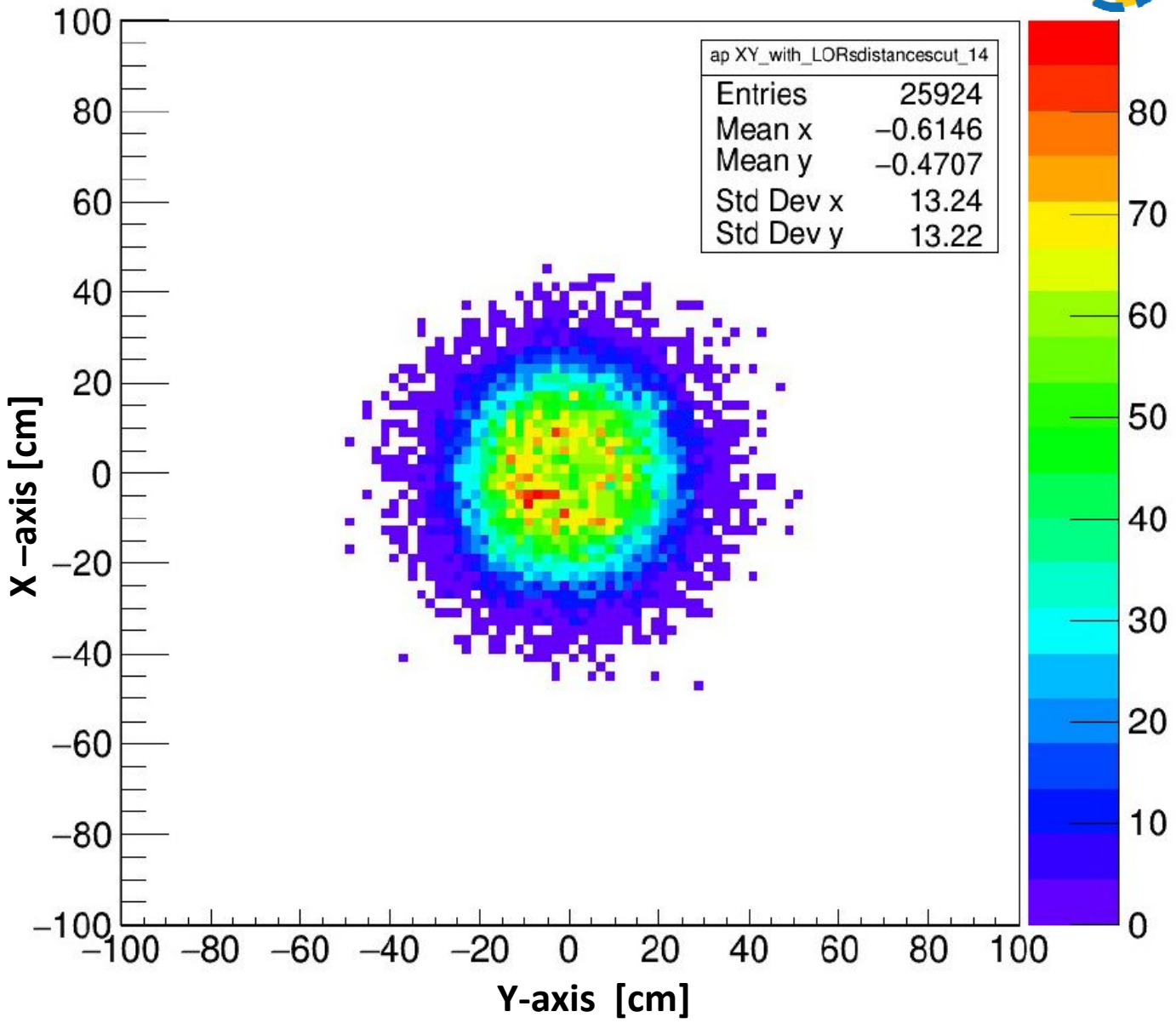

Figure : The decay points of the small chamber after applied the scatter test.

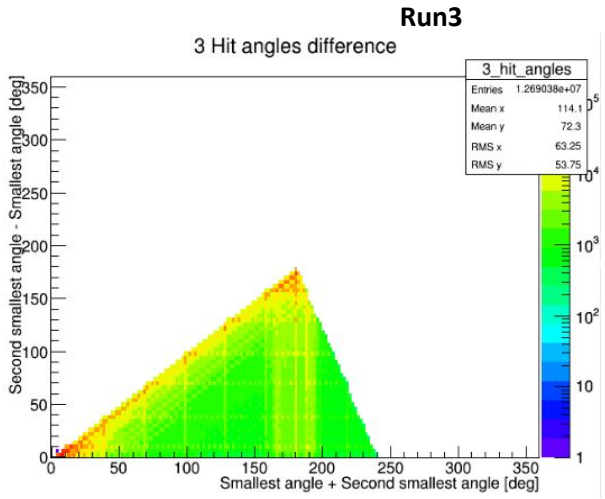

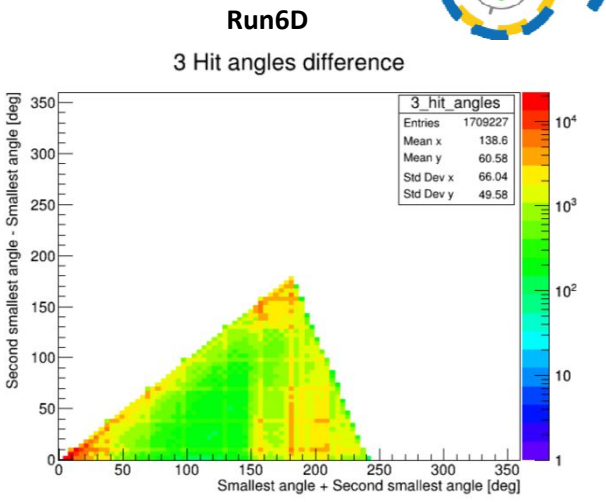

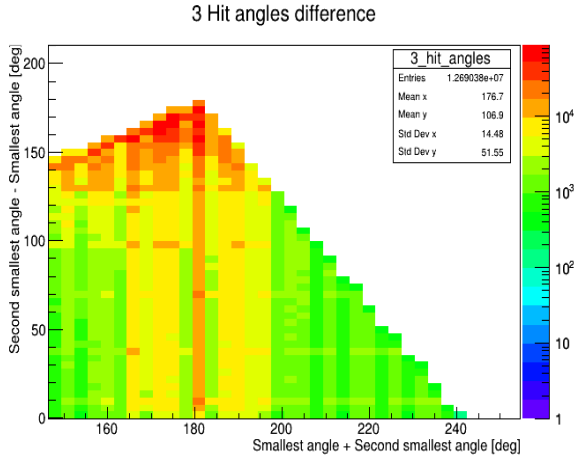

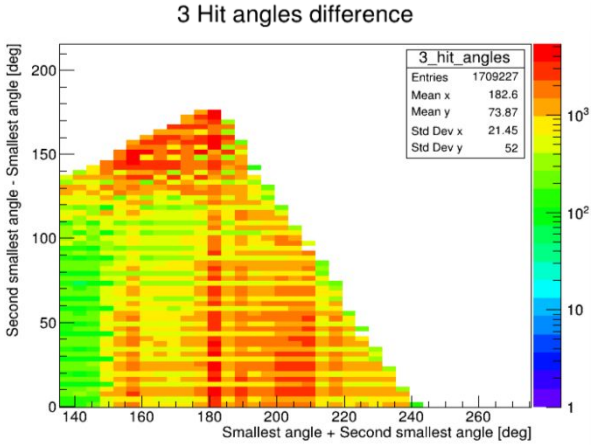

Figure : The plot of sum of the two smallest angles Vs the difference between them respect to the geometrical center of the detector for Run.3, Run.6D .

The annihilation points of 2-gamma decay

Run-3

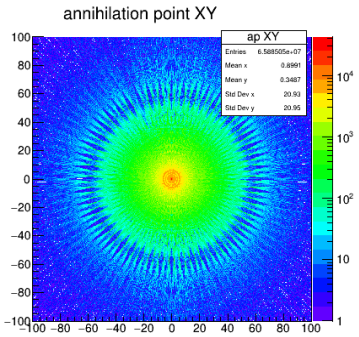

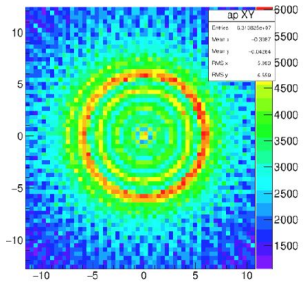

Run-6D

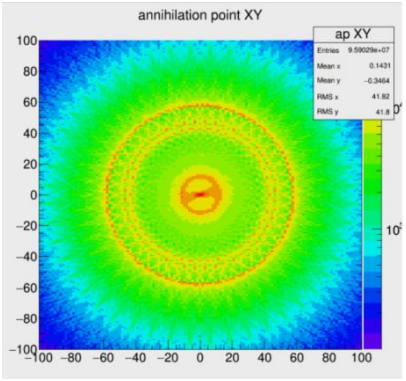

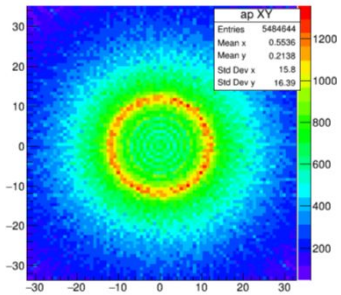

Run-7

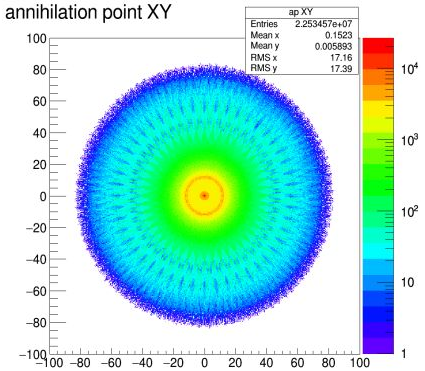

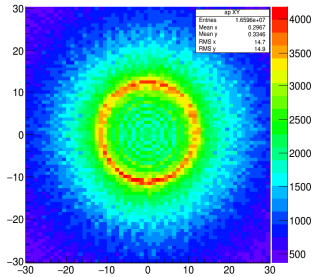

The annihilation points of 3-gamma decay

Run-3

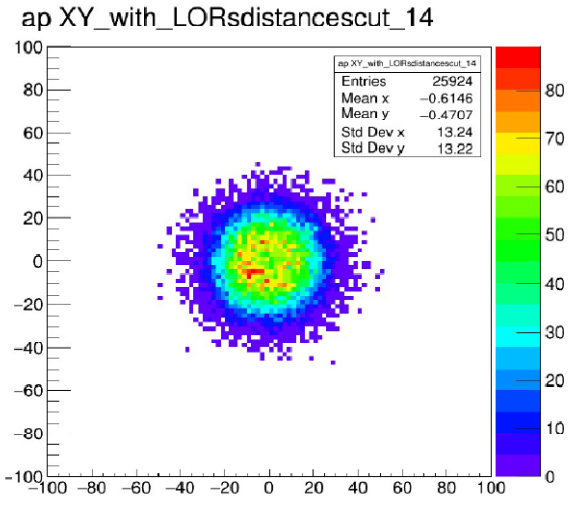

Run-6D

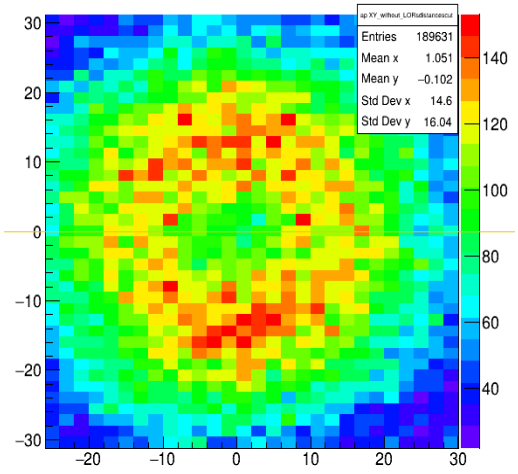

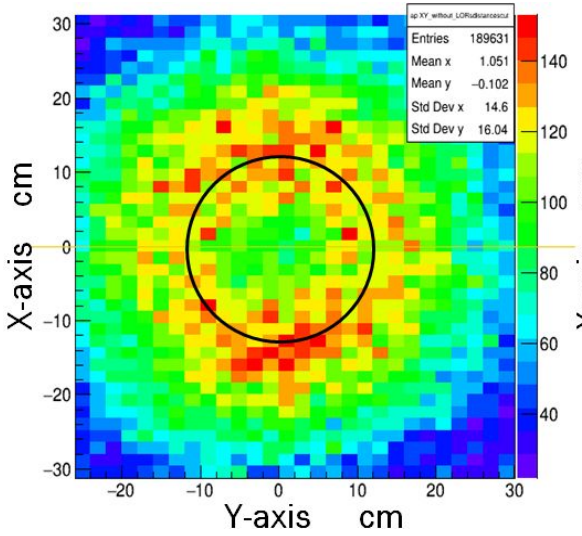

Run-7

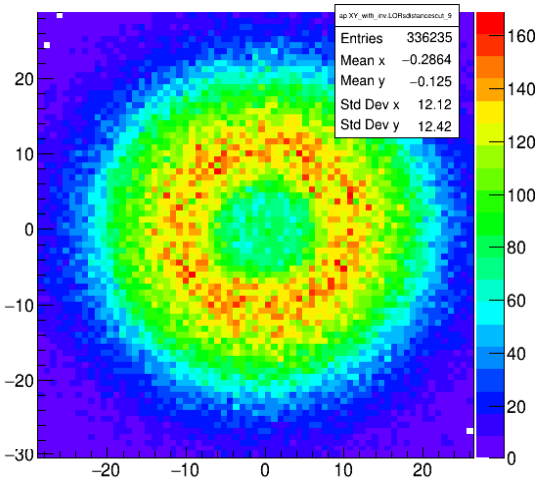

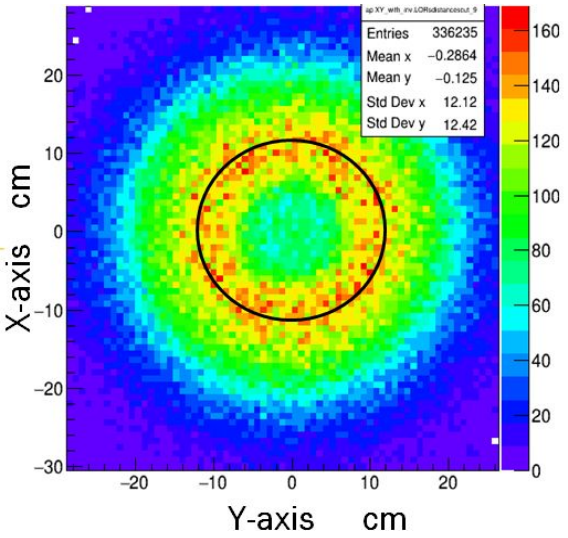

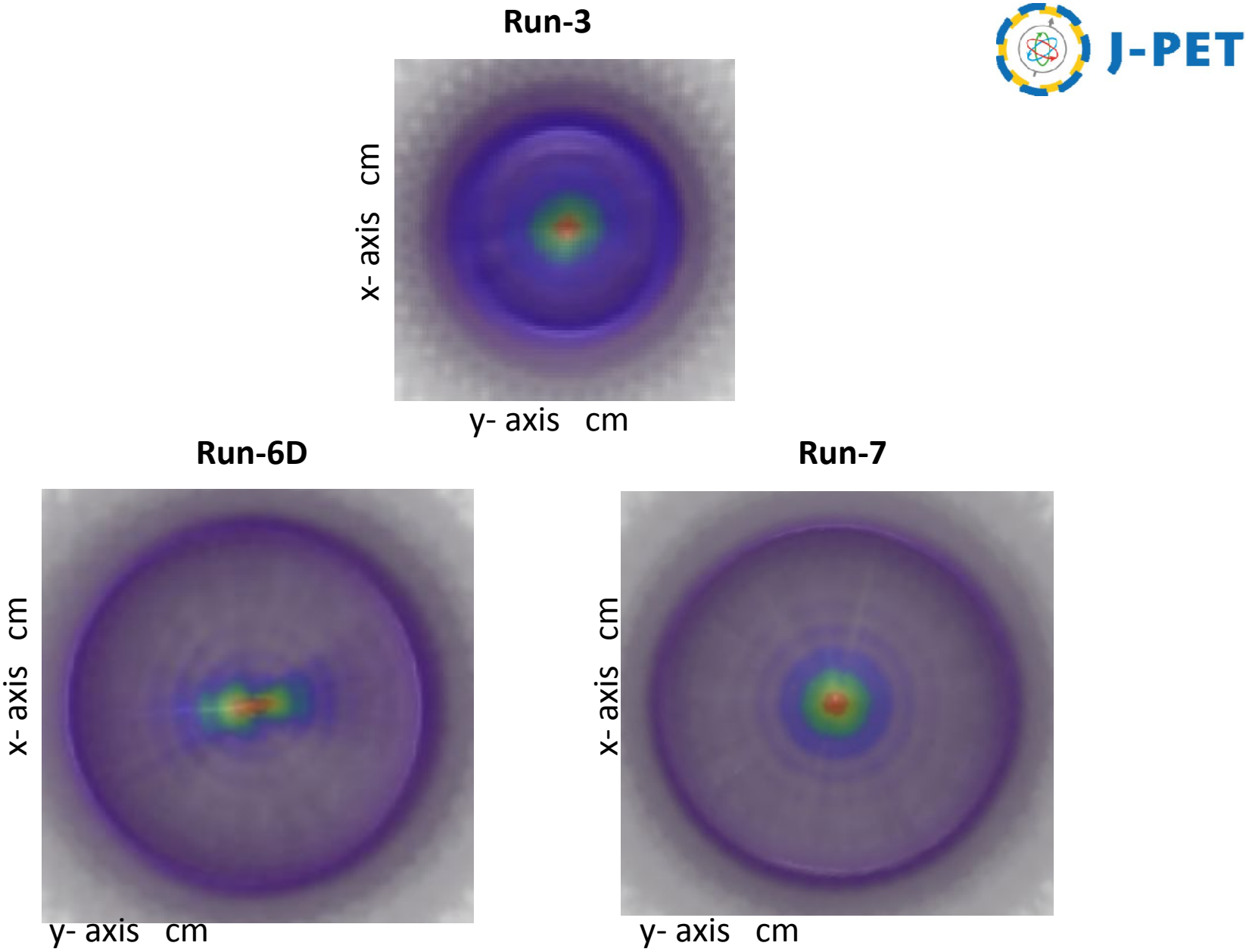

The tomographic image of the annihilation points based on 2-gamma decay

Distribution of the shortest distance between the o-Ps decay plane and the geometrical center of the J-PET

$$\left\|proj_{\vec{n}}\,\overrightarrow{PC}\right\| = \left\|\left(\frac{\overrightarrow{PC}\cdot\vec{n}}{\|\vec{n}\|^2}\right)\cdot\vec{n}\right\|$$

$$Distance = \left\|proj_{\vec{n}}\,\overrightarrow{PC}\right\| = \frac{\left\|\overrightarrow{PC}\cdot\vec{n}\right\|}{\|\vec{n}\|^2}.\|\vec{n}\|$$

$$Distance = \left\|proj_{\vec{n}}\,\overrightarrow{PC}\right\| = \frac{\left\|\overrightarrow{PC}\cdot\vec{n}\right\|}{\|\vec{n}\|} = \vec{d}.\hat{n}$$

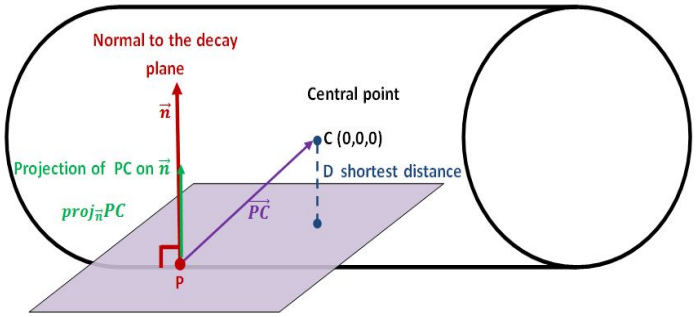

, Where

$$\overrightarrow{PC} = \vec{d}$$

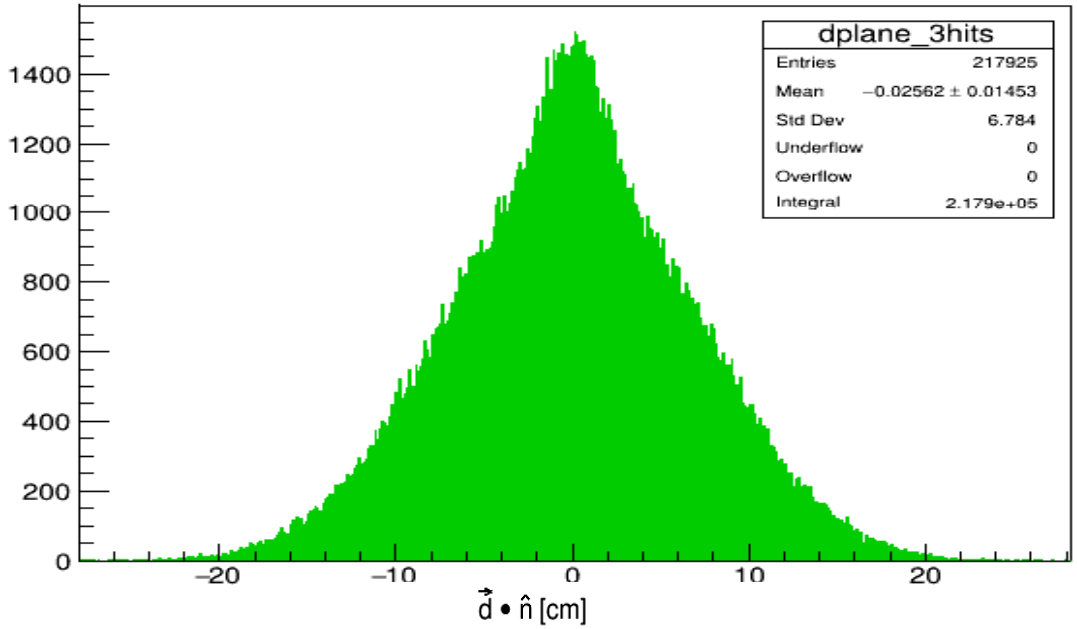

Figure : Distribution of the shortest distance (d) between the o-Ps decay plane and the geometrical center of the J-PET detector, calculated as a projection to the normal of the decay plane (). Extreme values allow for rejection of artificial decay planes obtained for accidental 3γ scintillation coincidences.

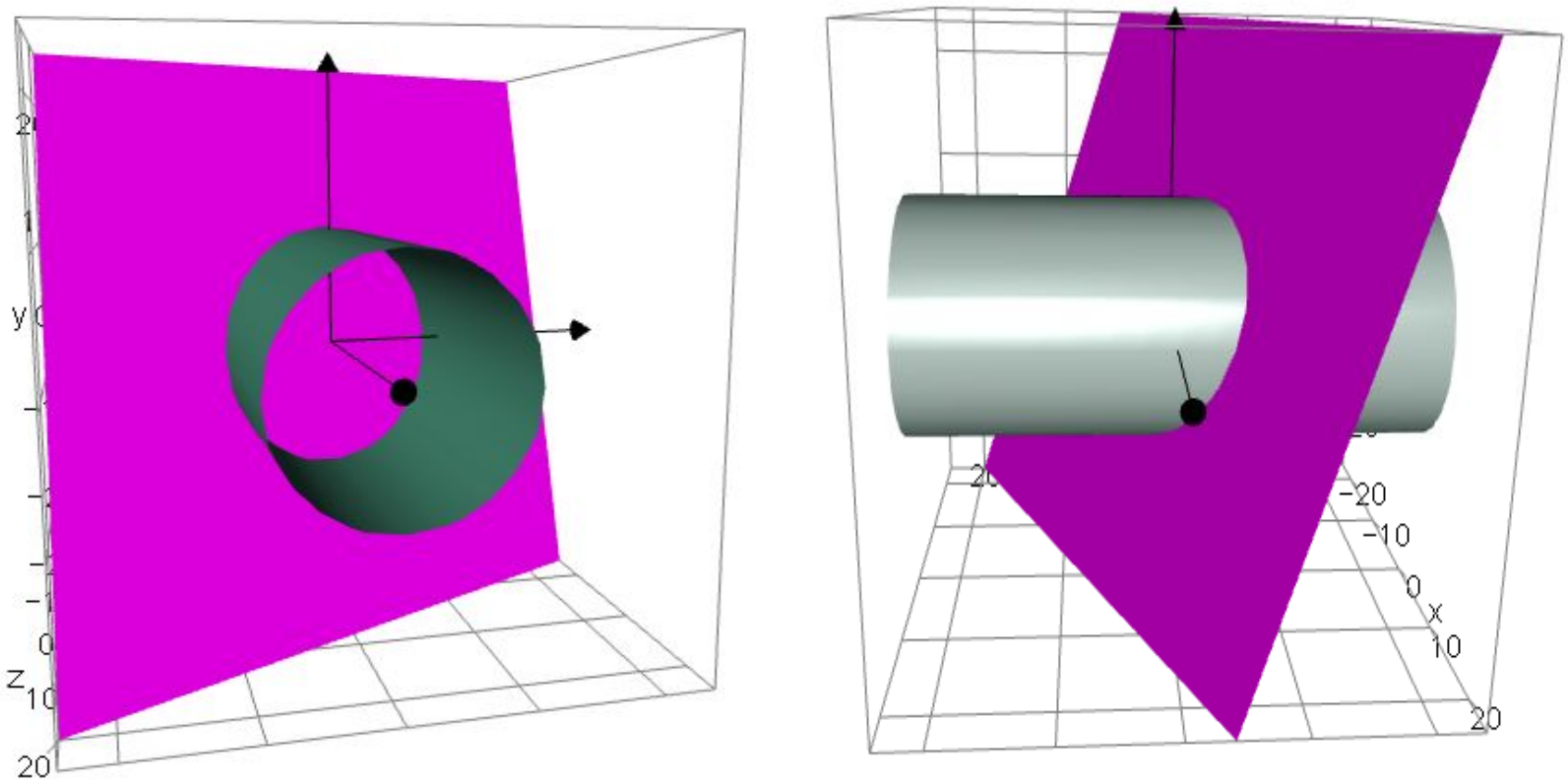

Figure : The annihilation plane for o-Ps decay point at the wall of the annihilation chamber. left (xy view) and Right (zx view).

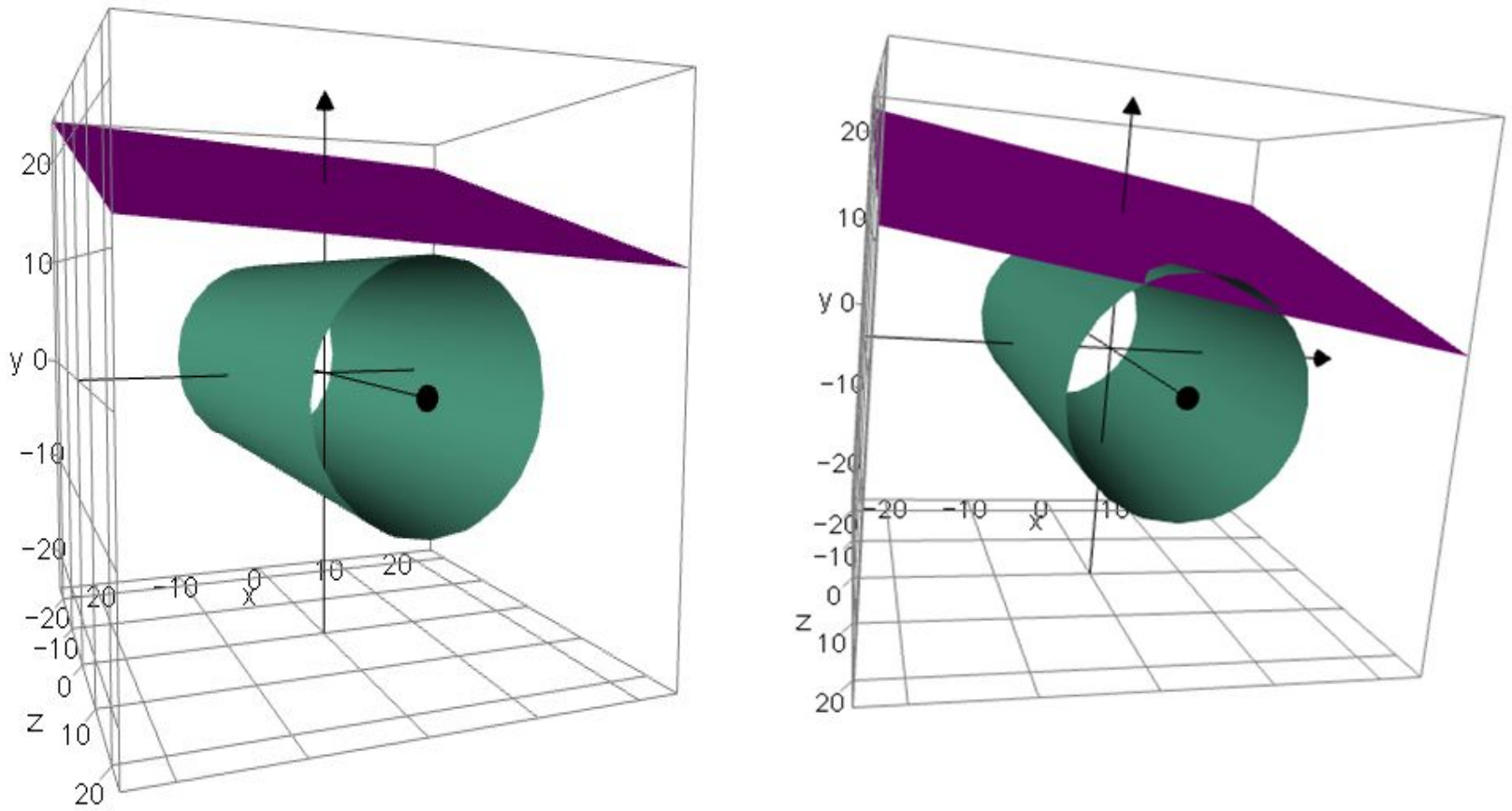

Figure : The annihilation planes for two different accidental coincidences.

The discrete symmetry tests operators

Operator	C	P	T	CP	CPT
$\vec{S}\cdot\vec{k}_1$	+	−	+	−	−
$\vec{S}\cdot\left(\vec{k}_1\times\vec{k}_2\right)$	+	+	−	+	−
$\left(\vec{S}\cdot\vec{k}_1\right)\left(\vec{S}\cdot\left(\vec{k}_1\times\vec{k}_2\right)\right)$	+	−	−	−	+
$\vec{k}_1\cdot\vec{\epsilon}_2$	+	−	−	−	+
$\vec{S}\cdot\vec{\epsilon}_1$	+	+	−	+	−
$\vec{S}\cdot\left(\vec{k}_2\times\vec{\epsilon}_1\right)$	+	−	+	−	−

Energy photon calculation

$$E_1 = -2m_e \frac{-\cos\theta_{13} + \cos\theta_{12}\cos\theta_{23}}{(-1+\cos\theta_{12})(1+\cos\theta_{12}-\cos\theta_{13}-\cos\theta_{23})},$$

$$E_2 = -2m_e \frac{\cos\theta_{12}\cos\theta_{13} - \cos\theta_{23}}{(-1+\cos\theta_{12})(1+\cos\theta_{12}-\cos\theta_{13}-\cos\theta_{23})},$$

$$E_3 = 2m_e \frac{1+\cos\theta_{12}}{1+\cos\theta_{12}-\cos\theta_{13}-\cos\theta_{23}}.$$

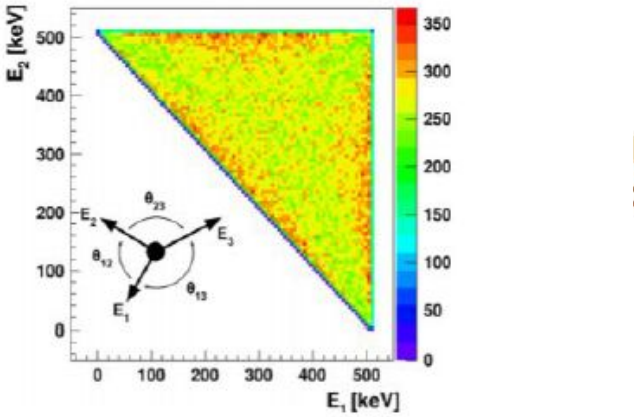

D. Kamińska, et al., **"A feasibility study of ortho-positronium decays measurement with the J-PET scanner based on plastic scintillators"**, Eur. Phys. J. C (2016) 76:445

```
E1 = -2*m_e*(-cos(Θ31)+cos(Θ12)*cos(Θ23))/((-1+cos(Θ12))*(1+cos(Θ12)-cos(Θ23)-cos(Θ31)))
E2 = -2*m_e*(-cos(Θ23)+cos(Θ12)*cos(Θ31))/((-1+cos(Θ12))*(1+cos(Θ12)-cos(Θ23)-cos(Θ31)))
E3 =  2*m_e*(1+cos(Θ12))/(1+cos(Θ12)-cos(Θ23)-cos(Θ31))
```

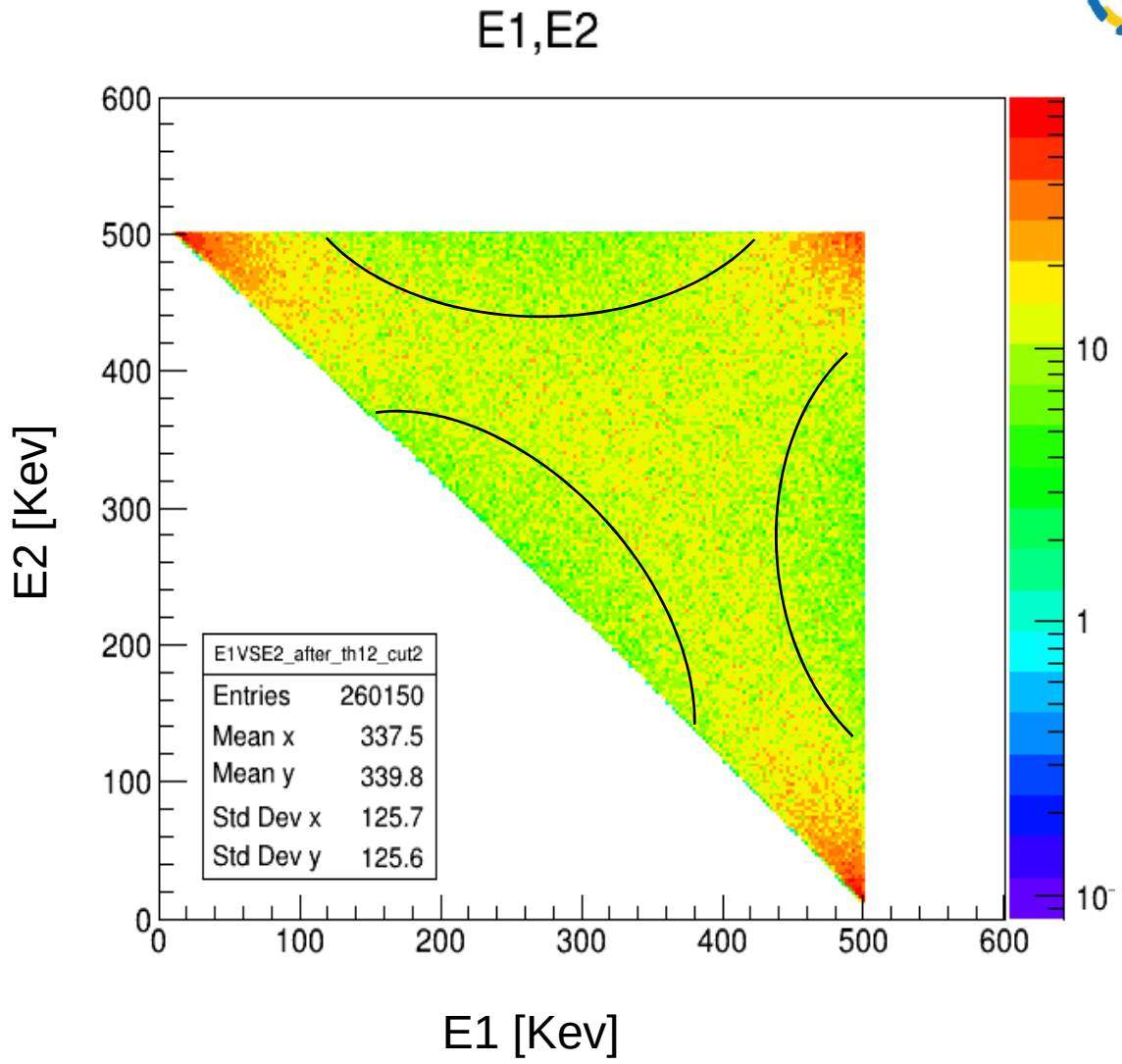
E1,E2
E2 [Kev]
E1 [Kev]
600
500
400
300
200
100
0
0
100
200
300
400
500
600
10
1
10⁻
E1VSE2_after_th12_cut2
Entries 260150
Mean x 337.5
Mean y 339.8
Std Dev x 125.7
Std Dev y 125.6

The calculation CPT Symmetry test(CPTST)

S.(k1xk2)

k1&k2 momenta of most and 2nd most energetic photons

x1=(firstHit.getPosX()-anh_point.X()) x-coordinate of the vector for the most energetic photon.
y1=(firstHit.getPosY()-anh_point.Y())
z1=(firstHit.getPosZ()-anh_point.Z())
x2=(thirdHit.getPosX()-anh_point.X())
y2=(thirdHit.getPosY()-anh_point.Y())
z2=(thirdHit.getPosZ()-anh_point.Z())
ax=y1*z2-y2*z1;
ay=x2*z1-x1*z2;
az=x1*y2-x2*y1;
CPTST=(anh_point.X()*ax+anh_point.Y()*ay+anh_point.Y()*az)

The tested operator (run-6D data)

Operator	C	P	T	CP	CPT
$S \cdot (k_1 \times k_2)$	+	+	−	+	−

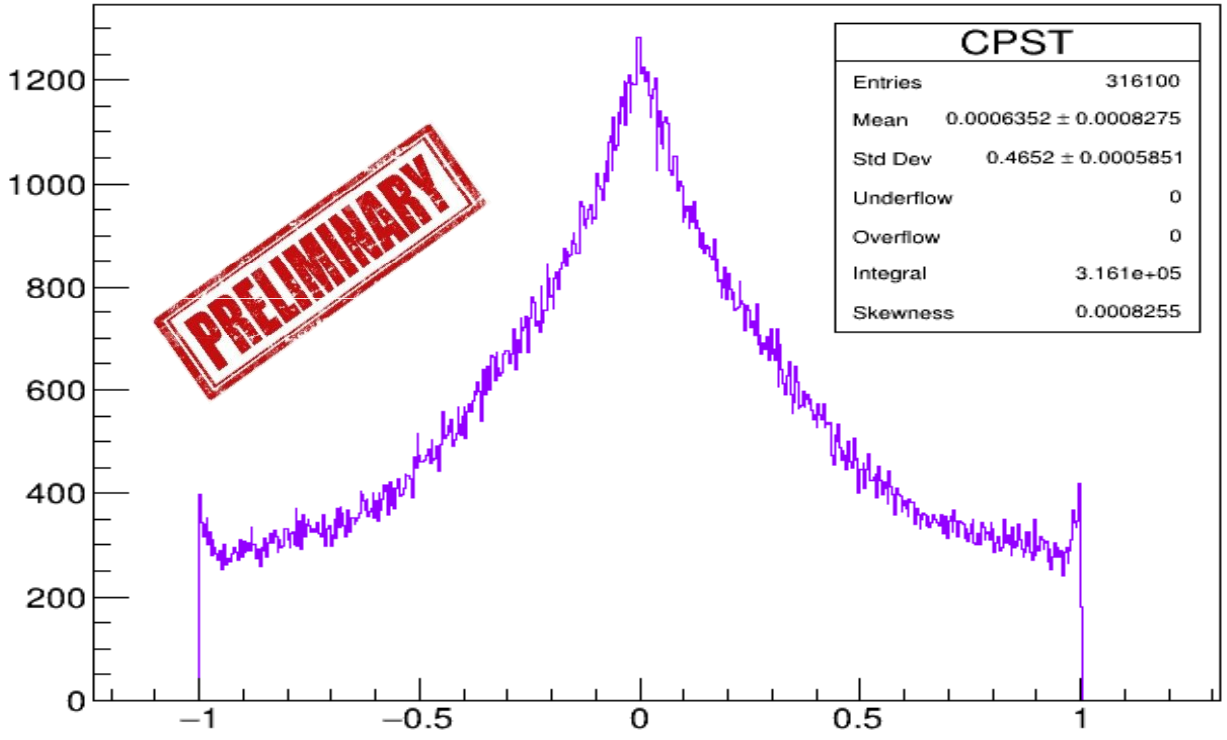

The tested operator (run-7 data)

Operator	C	P	T	CP	CPT
$S \cdot (k_1 \times k_2)$	+	+	−	+	−

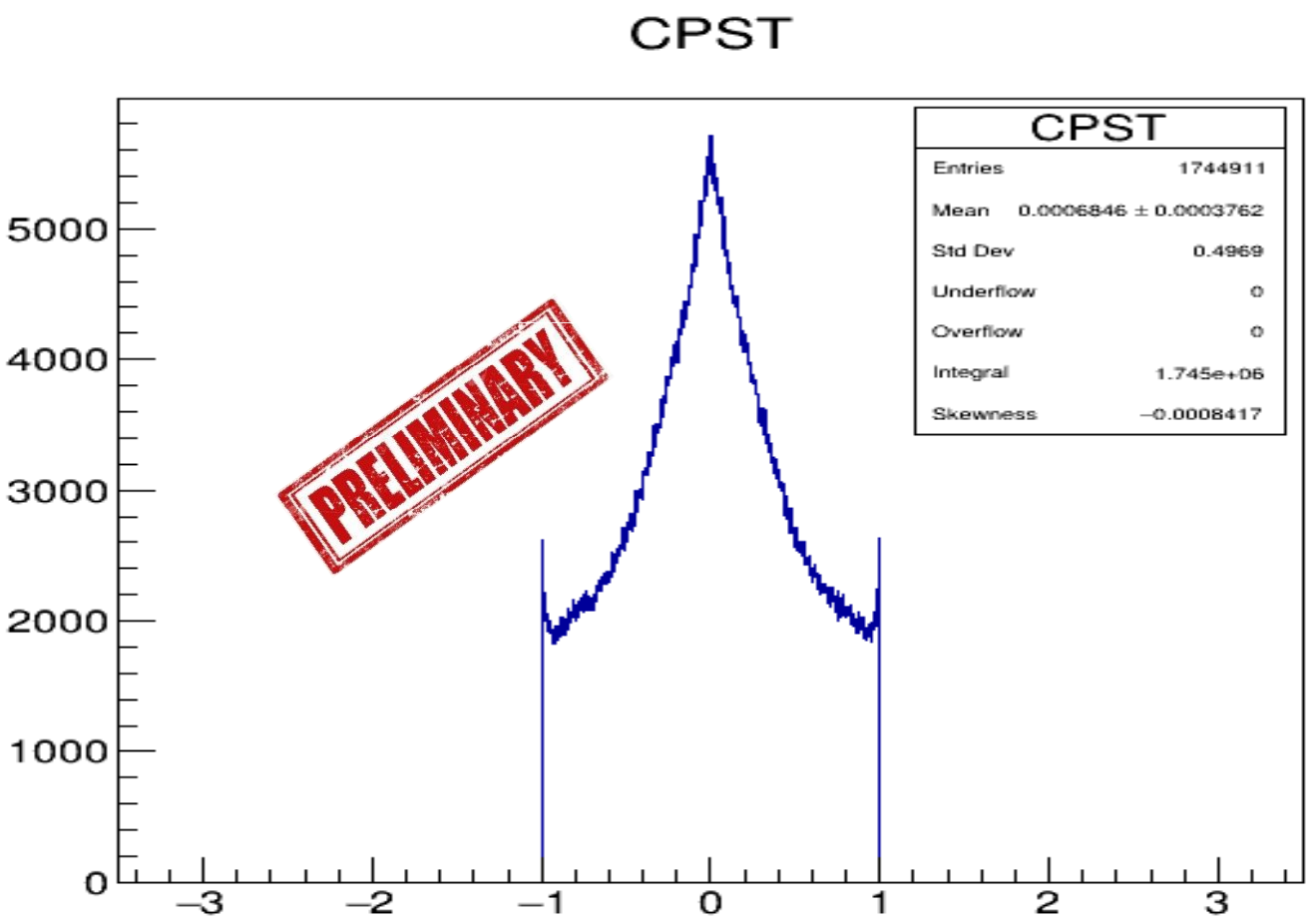

The tested operator (run-7 data)

Operator	C	P	T	CP	CPT
$(\vec{S}\cdot\vec{k}_1)\,(\vec{S}\cdot(\vec{k}_1\times\vec{k}_2))$	+	−	−	−	+

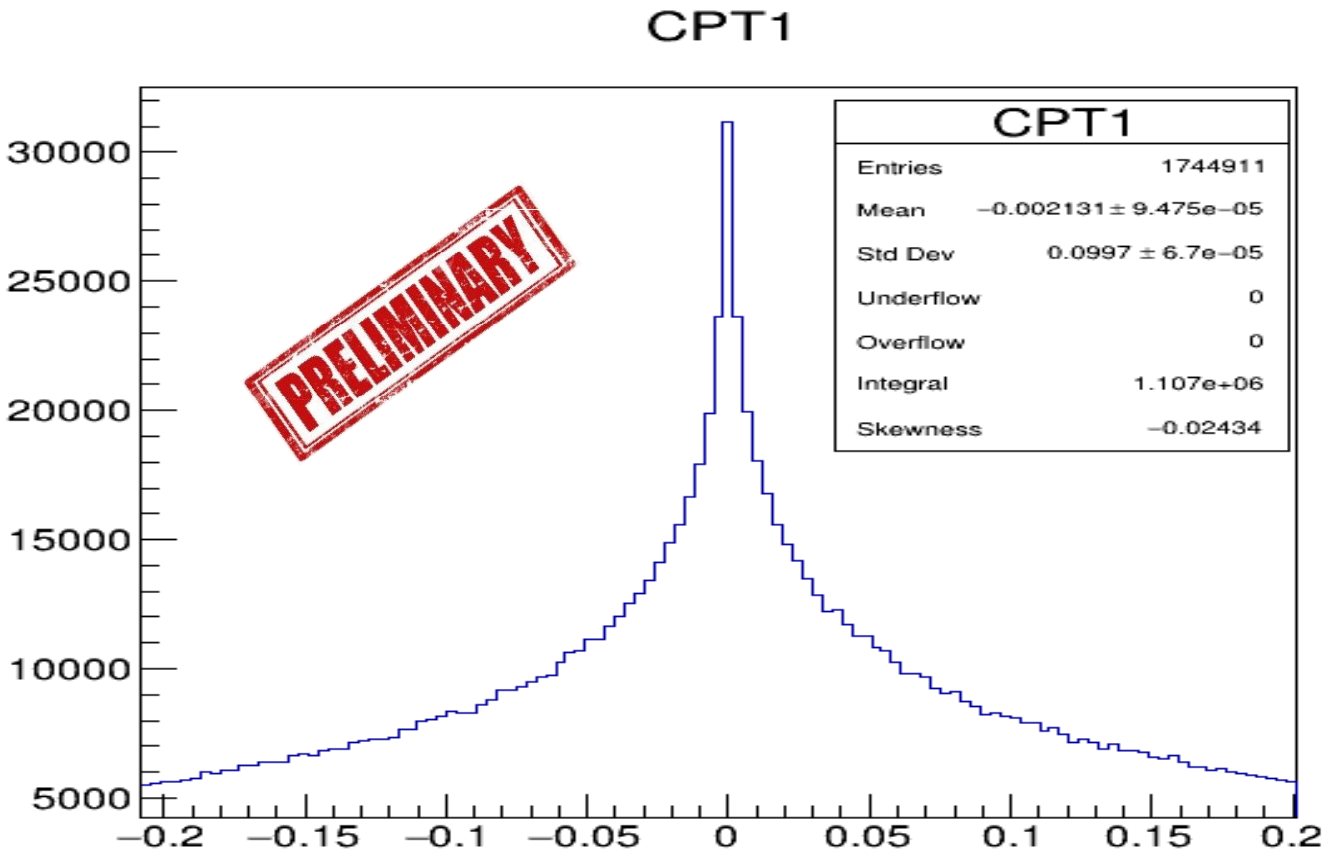

Summary:

1.J-PET is optimized for detection photons from Ps annihilation with high time and angular resolutions, thus providing new opportunities for Ps research in fundamental physics.

2.The precise experimental CP and CPT symmetry tests with J-PET are possible thanks to a dedicated reconstruction technique of 3γ o-Ps decays.

3.The positronium production chamber including a highly porous material target (R-60), whose setup allows for determining the o-Ps spin polarization without the use of external magnetic field.

4.This method of testing the CPT-violation by using J-PET detector achieved the sensitivity of 3.7×10^{-4} (statistical uncertainty), which is the result of analyzing 10% of the data, and after the full data analysis, we expected to achieve about 10^{-5} precision. This result is two orders of magnitude more precise than that of the previous experiments results which has been done so far.

Thank you for your attention